UNIVERSITA' DEGLI STUDI DI PADOVA

Sede Amministrativa: Università degli Studi di Padova

Dipartimento di Scienze Medico-Diagnostiche e Terapie Speciali

SCUOLA DI DOTTORATO DI RICERCA IN: SCIENZE MEDICHE, CLINICHE E SPERIMENTALI

INDIRIZZO: SCIENZE CARDIOVASCOLARI

CICLO 21° Ciclo

MAGNETIC RESONANCE IMAGING IN ACUTE MYOCARDIAL INFARCTION: AN INSIGHT INTO PATHOPHYSIOLOGY

Coordinatore: Ch.mo Prof. Gaetano Thiene

Supervisore : Ch.ma Prof. Ssa Cristina Basso

Dottorando : Dott.ssa Luisa Cacciavillani

INDEX

SUMMARY

Introduction: Recent clinical studies have shown that in acute myocardial infarction (AMI), delayed reperfusion results in less myocardial salvage and a higher mortality rate, irrespective of the reperfusion strategy chosen. In patients with ST-segment elevation myocardial infarction, myocardial salvage progressively declines as the time between symptoms and therapy increases. Recent clinical studies in patients with reperfused AMI have shown a close relation among microvasculature obstruction, myocardial viability, left ventricle (LV) function, and clinical outcome. However, although the entire spectrum of ischemic and reperfusion injury had been explored in experimental studies, the real mechanism *in vivo* in humans is not completely analyzed. Recently cardiac magnetic resonance (CMR) has been proposed as a comprehensive tool for AMI evaluation, since it provides data about regional myocardial wall motion, viability, perfusion and direct visualization of myocardial necrosis. In this respect, the aims of this study performed in AMI patients treated with primary angioplasty (PCI), were:

1. to clarify the impact of reperfusion time on pregression of myocardial damage;
2. to assess the predictive value of CMR features on ventricular post-AMI remodelling;
3. to investigate the pathological basis visualized by CMR of the persistence of ST-segment elevation after AMI;
4. to evaluate the effects of current therapy on CMR detection of necrosis and microvascular injury;
5. to evaluate the correlation between angiographic indexes of myocardial perfusion after primary PCI and anatomical features on CMR, in particular the correlation between the staining phenomenon and the presence of severe microvascular damage (SMD);
6. to investigate the possibility to detect intramyocardial hemorrhage after AMI by T2-weighted image on CMR, to establish its contribution to the delayed hypoenhanced core, traditionally referred only to microvascular obstruction. We also aimed to correlate radiological findings of myocardial hemorrhage with hystological features ex vivo in two died patients.

Methods: Consecutive patients with AMI treated by primary PCI from March 2003 and September 2008. All patients underwent CMR. For each patient we evaluated

the clinical profile, echocardiographic and ECG findings and the angiographic profile (Thrombolyis in Myocardial Infarction (TIMI) flow, and Myocardial Blush Grade (MBG). On CMR, the AMI was labeled as transmural if hyperenhancement was extended to ≥75% of the thickness of at least two contiguous ventricular segments. The total extent of necrosis was also expressed as Infarct Size Index (percentage of left ventricular involvement) obtained by adding the score of delayed hyperenhancement involvement in each segment divided by 68 (the whole extent of the left ventricle). We defined SMD as subendocardial areas of late low or absent signal surrounded by late enhanced tissue (14 and 15) in at least one ventricular segment. A clinical and echocardiographic follow-up was performed. During the follow-up were also collected data about died patients obtaining anatomical findings in two cases.

Results: In respect of proposed aims, we obtained the following results:

1. In the first group the patients enrolled were 64, the mean time to treatment was 190 $\pm$ 110 min, 45 (65%) patients had transmural necrosis (TN) and 23 (39%) had SMD. Mean pain to balloon time was 90 $\pm$ 40 min, 110 $\pm$ 107 min, and 137 $\pm$ 97 min in patients without TN and SMD, with TN but without SMD, or with both TN and SMD, respectively ($p = 0.001$). Multivariate analysis showed that time delay was significantly associated both with TN (odds ratio per 30 min, 1.37, $p = 0.032$), and SMD (odds ratio per 30 min, 1.21; $p = 0.021$).
2. In this subgroup of subjects remodeling was evaluated as a change in LV end-diastolic volume index by echocardiography at follow-up compared with baseline. At univariate analyses, TN, SMD, infarct size, and troponin level correlated directly with remodeling and inversely with LV function at follow-up ($p <0.001$). At multiple regression analysis, only TN and troponin level remained independent predictors of LV remodeling and function. With respect to troponin, TN improved the predictive power of LV remodeling (R2 for change = 0.19) and function (R2 for change = 0.16)
3. As far as ECG and CMR correlations are concerned, patients with persistent ST-segment elevation had higher Infarct Size Index ($p = 0.02$), also showed TN ($p = 0.03$) and persistent microvascular damage ($p = 0.003$) more often. Finally, LV aneurysm was seen more frequently in patients with ST-segment elevation ($p = 0.08$). In a multivariate model, persistent microvascular

damage was the only independent predictor of persistent ST-segment elevation (OR 3.13, CI 1.21 – 8.10, p = 0.01).

4. When we evaluated the impact of Abciximab administration on CMR findings, we observed that TN and SMD were present in 3.03 $\pm$ 2.8 versus 3.09 $\pm$ 2.9 (p = 0.9) and 1.05 $\pm$ 1.5 versus 1.06 $\pm$ 1.8 (p = 0.6) of LV segments, respectively, in the Abciximab group versus controls. At multivariate analysis, SMD was independently associated only with transmural necrosis (OR 1.5, p < 0.001) and age (OR 1.1, p = 0.02) but not with the use of Abciximab.
5. A total of 294 enrolled patients were classified into two groups on the basis of MBG (0/1 *versus* 2/3). According to the angiographic perfusion profile, 115 (39,1%) showed MBG 0/1, predominantly in anterior wall (72,2%). This group exhibited a larger enzymatic infarct size (p<0,001), a lower ejection fraction (p<0,001) and the CMR demonstrated both a greater transmural infarct size (p<0,001) and a worst microvascular impairment documented by presence of SMD on delayed post-contrast images (33,9%, p<0,001). In the MBG 0/1 group, a subgroup of 51 patients, characterized by presence of staining phenomenon (MBG-0-staining) showed the worst CMR outcome in term of both infarct size and SMD (p<0,001). On the contrary, subjects in the MBG 2/3 group showed a successful CMR perfusion index with lower infarct size, SMD and SMD index (p<0,001). Multivariate analysis confirmed the strong association between MBG 0/1 and mean number of TN segments (OR 1,62, 95% CI 1,17-2,24, p = 0,003), and the worst CMR perfusion pattern as demonstrated by SMD index (OR 3,13, 95% CI 1,185-8,286, p = 0,021).
6. The group of patients (108 patients) in which the entire CMR protocol including T2-weighted sequences was performed, was subdivided into two groups according to the presence of a dark area on T2 images, assumed to be indicative of intramyocardial haemorrhage. Thirty-two patients showed an hypointense stria within the high signal intensity zone on T2-images images; all these patients showed on delayed-enhanced (DE) midmural SMD according to the extent of hypointense signal on T2-weighted. In the remaining patients (76), only 14 (18,4%) subjects showed SMD, in the subendocardial region. Angiographic outcome was worst in patients with

hypointense signal on T2-weighted and SMD, since they had a lower TIMI 3 (65,6% vs 96%, p=0.017) and more frequently a MBG grade 0 (84,4% vs 13,1%, p<0.001) post-PCI. No difference was found on time delay for PCI. During the follow-up were collected pathologic data about two subjects who died for cardiogenic shock. By comparing in vivo and ex vivo CMR, the low-signal intensity areas observed by ex vivo T2 CMR strongly correlated with the hemorrhage quantified on histology (R = 0.93, p = 0.0007). Using ex vivo late gadolinium sequences, bright areas surrounded by thin dark rims, consistent with magnetic susceptibility effects, were detected, corresponding to hemorrhage. On in vivo CMR images, low-signal intensity and hyperintense areas with peripheral susceptibility artifacts were observed within the AMI core on T2 and late gadolinium sequences, respectively.

Conclusion: In AMI patients with impaired coronary perfusion undergoing PCI, the risk of TN and SMD seems to increase with the duration of the ischemic time. Also, the amount of TN results as a major determinant of LV remodeling and function, with significant additional predictive value to infarct size and SMD. The evaluation of effects of current therapy with Abciximab demonstrated that SMD seems related to TN without any influence of antiplatelet therapy. In addition, presence of SMD seems the most powerful determinant of persistent ST-segment elevation on ECG. In our experience the angiographic assessment of lack of myocardial perfusion correlates with microvascular damage and extent of infarct size detected on CMR. Inside MBG 0 the presence of staining phenomenon reflects a subgroup of patients with more SMD, as seen on CMR. Future study to evaluate prognostic value of staining will be able to define if MBG classification needs a revisitation. Finally, T2-weighted MRI in reperfused AMI allows identification of an hypointense dark stria related with SMD areas on DE after gadolinum: the absence of this radiological sign is associated with a better angiographic reperfusion as indicated by higher MBG. Looking at relationship with histological findings, CMR hypointense T2-image signal and susceptibility effects within the late gadolinium hypoenhanced areas are consistent with interstitial hemorrhage due to irreversible vascular injury: thus, on the basis of our results, the presence of both T2-hypoenhancement and delayed dark zones can be used as a marker of a worst microvascular damage possibly resulting in hemorrhage.

ABBREVIATIONS

AMI = acute myocardial infarction

CMR = contrast magnetic resonance

DE = delayed enhaced

LV = left ventricle

MBG = Myocardial Blush Grade

PCI = percutaneous coronary intervention

SMD = severe microvascular damage

STEMI = ST-segment Elevation Myocardial Infarction

TIMI = Thrombolysis In Myocardial Infarction

TN = transmural necrosis

BACKGROUND

Histopathology of acute myocardial infarction

Introduction

Acute coronary sydromes comprise all conditions caused by sudden impairment of blood flow in a coronary artery that leads to ischemia in the corresponding area of the myocardium. Before the thrombolytic era, clinicians typically divided AMI patients into those suffering a Q-wave or non-Q-wave infarct, based on the evolution of the pattern on the ECG over several days after AMI. The term "Q-wave infarction" was frequently considered to be virtually synonymous with "transmural infarction," whereas "non-Q-wave infarction" was often referred to as a "subendocardial infarction".

A more suitable framework is based on the pathophysiology of AMI, leading to a reorganization of clinical presentations into what is now referred to as the acute coronary syndrome. Acute coronary syndromes are now divided into two groups according with clinically pathologically features reaching the ECG presentation: persistent ST segment-elevation myocardial infarction (STEMI) and non-ST-segment elevation myocardial infarction (NSTEMI)(1,2).

The rupture of plaques is now considered to be the common pathophysiological substrate of the acute coronary syndromes (3). The dynamic process of plaque rupture may evolve to a completely occlusive thrombus, typically producing ST segment elevation on the ECG. Such completely occlusive thrombi lead to a large zone of necrosis involving the full or nearly full thickness of the ventricular wall in the myocardial bed subtended by the affected coronary artery. The infarction process alters the sequence of depolarization ultimately reflected as changes in the surface of the QRS. The most characteristic change in the QRS complex is the evolution of Q waves in the leads overlying the infarct zone, leading to the term "Q-wave infarction".

Less obstructive thrombi typically produce ST segment depression and/or T wave inversion on the ECG. Most patients with NSTEMI do not evolve a Q wave on the 12-lead ECG and are subsequently referred to as having sufferd a non-Q-wave MI (NQMI); only a minority of NSTEMI patients develop a Q-wave AMI and are later diagnosed as having a Q-wave AMI.

The acute coronary syndrome spectrum concept, organized around a common pathophysiological substrate, is a useful framework for developing therapeutic strategies. Patients presenting with persistent ST segment elevation are candidates for reperfusion therapy (either pharmacological or catheter-based) to restore flow in the occluded epicardial infarct–related artery. Patients presenting without ST segment elevation are not candidates for pharmacological reperfusion but should receive vigorous antiischemic therapy. (4,5)

Anatomy and Pathology

If a coronary occlusion persists for more than 30 minutes, irreversible damage to the myocardium occurs. Persistent coronary occlusion results in a progressive increase of the infarct size with a wave-front transmural extension from the endocardium towards the epicardium (6-7). Although reperfusion can occur spontaneously, thrombotic coronary artery occlusion persists in the majority of patients suffering an AMI. Thus, timely coronary artery recanalisation and myocardial reperfusion, either by thrombolytic therapy or primary angioplasty and/or stenting, represent the most effective way of restoring the balance between myocardial oxygen supply and demand. Prevention of myocardial cell necrosis by the restoration of blood flow depends on the severity and duration of pre-existing myocardial ischaemia.
Experimental and clinical data indicate that the recovery of systolic and diastolic function and the reduction in overall mortality are more favourably influenced by early coronary blood flow restoration. Collateral coronary vessels also appear to play an additional role, providing sufficient blood flow to the myocardium as to reduce the extent of myocyte irreversible injury (7).

The magnitude of coronary collateral flow is one of the principal determinants of infarct size. Indeed, it is rather common for patients with abundant collateral vessels to have totally occluded coronary arteries without evidence of infarction in the distribution of that artery; thus, the survival of the myocardium distal to such occlusions must depend on collateral blood flow. Even if collateral perfusion existing at the time of coronary occlusion is not successful in improving contractile function, it may still exert a beneficial effect by preventing the formation of a left ventricular aneurysm. Some collateral are seen in nearly 40 percent of patients with an acute total occlusion, and more begin to appear soon after the total occlusion occurs (8). It is likely that the presence of a high-grade stenosis (90

percent), possibly with periods of intermittent total occlusion, permits the development of collateral vessels that remain only as potential conduits until a total occlusion occurs or recurs. The latter event then brings these channels into full operation (9). The incidence of collateral vessels 1 to 2 weeks after AMI varies considerably and may be as high as 75 to 100 percent in patients with persistent occlusion of the infarct vessel or as low as 17 to 42 percent in patients with subtotal occlusion.

The location and extent of AMI can be assessed on pathological examination. On gross inspection, AMI may be divided into two major types: (i) transmural infarcts, in which myocardial necrosis involves the full thickness (or nearly full thickness) of the ventricular wall, and (ii) subendocardial (non-transmural) infarcts, in which the necrosis involves the subendocardium, the intramural myocardium, or both without extending all the way through the ventricular wall to the epicardium. An occlusive coronary thrombus appears to be far more common when the infarction is transmural and localized to the distribution of a single coronary artery. Non-transmural infarctions, however, frequently occur in the presence of severely narrowed but still patent coronary arteries (5). Patchy nontransmural infarction may arise from thrombolysis or PTCA of an originally occlusive thrombus with restoration of blood flow *before* the wave front of necrosis has extended from the subendocardium across the full thickness of the ventricular wall. The histological pattern of necrosis may differ, with contraction band injury occurring almost twice as often in non-transmural as in transmural infarction. Paradoxically, before their infarction, patients with nontransmural infarcts have, on average, a more severe stenosis in the infarct-related coronary artery than do patients suffering from transmural infarcts. This finding suggests that a more severe obstruction occurring before infarction protects against the development of transmural infarction, perhaps by fostering the development of collateral circulation. It also accords with the concept that less severely stenotic but lipid-laden plaques with a fragile cap are responsible for the abrupt presentation of ST segment elevation that may evolve into transmural infarctions.

The "Wavefront" of Necrosis

In the 1970s, Reimer and Jennings (6-7) performed a series of studies in dogs after acute coronary occlusion in which they examined the relation between duration of ischaemia, area at risk, collateral blood flow, and final infarct size. The results of their experiments were summarized by the concept of "*wavefront phenomenon of myocardial death*". In summary, this concept states that infarct size increases in a transmural wavefront extending from the endocardium to the epicardium with increasing duration of coronary occlusions and with increasing severity of ischaemia. Coronary occlusions lasting 6 hours result in subendocardial infarcts, in which infarct size is smaller than the ischaemic area at risk, because some epicardial rim of viable tissue is spared. When coronary occlusion exceeds 6 hours, infarcts become transmural with an infarct size encompassing the entire area at risk.

As already noted, within seconds of a coronary occlusion, blood begins to flow through preexisting collateral channels to the occluded segment of the artery. Collateral flow is lowest and myocardial oxygen consumption highest in the subendocardium, and therefore ischemia is most severe in this region. In the normal myocardium, thickening and shortening are greater in the subendocardium, as is wall stress, accounting for the higher subendocardial energy requirements (5, 10). Consistent with these findings, higher rates of metabolic activity, lower tissue oxygen tension, and greater oxygen extraction have been found in this region as a consequence, ischemia becomes most severe and myocardial cells undergo necrosis first in the subendocardium, beginning as early as 15 to 20 minutes after coronary artery occlusion. Necrosis progresses toward the epicardium, gradually involving the less severely ischemic outer layers. There is a rather sharp demarcation between ischemic and nonischemic myocardium at the lateral margins of the bed-at-risk. The onset of irreversible injury begins after about 20 to 30 min in the ischemic subendocardium, where the perfusion deficit is most severe compared with the subepicardium, which receives some collateral blood flow. Irreversible myocardial injury then progresses in a wavefront movement from the subendocardium into the subepicardium. Most myocardial infarcts are usually completed within about 3 to 4 hours of onset of severe ischemia. The major determinants of ultimate infarct size are the duration and severity of ischemia, the size of the myocardial bed-at-risk, and the amount of collateral blood flow available shortly after coronary occlusion. In response to myocardial infarction, progressive changes occur in viable myocardium

in an attempt to normalize increased stress on the ventricle. This process, known as remodeling, involves hypertrophy and apoptosis of myocytes, formation of new myocytes from stem cells, and connective tissue changes. Controlled remodeling can lead to the normalization of wall stress. With excessive wall stress, however, remodeling can lead to fixed structural dilatation of the ventricle and heart failure.The progression of the wavefront of necrosis is slowed by the presence of residual blood flow when the coronary occlusion is incomplete or when mature collaterals are present at the time of occlusion. The progression of the wavefront of necrosis is accelerated when myocardial ischemia is unusually severe, when collateral blood flow is low, in the presence of marked arterial hypotension and in the presence of elevated myocardial oxygen demand, as may be caused by inotropic stimulation, tachycardia, or fever.

The concept of Reimer and Jennings is fundamental to current revascularization therapy of STEMI. Indeed, modern treatment strategies of STEMI aim at opening the infarct-related artery as quickly as possible, in order to reduce the duration of ischaemia and to save viable myocardium in the risk area.

Reperfusion injury

Early after the onset of ischemia, contractile dysfunction is observed that is believed to be due in part to shortening of the action potential duration, reduced cytosolic free calcium levels, and intracellular acidosis. When reperfusion of myocardium undergoing the evolutionary changes from ischemia to infarction occurs sufficiently early (i.e., within 15 to 20 minutes), it may successfully prevent necrosis from developing. Beyond such a very early stage, the number of salvaged myocytes and therefore the amount of salvaged myocardial tissue (area of necrosis/area at risk) is directly related to the length of time the coronary artery has been totally occluded, the level of myocardial oxygen consumption, and the collateral blood flow. Typical pathological findings of reperfused infarcts include a histological mixture of necrosis, hemorrhage within zones of irreversibly injured myocytes, coagulative myocytolysis with contraction bands, and distorted architecture of the cells in the reperfused zone (11). After reperfusion, mitochondria in nonviable myocytes develop deposits of calcium phosphate and ultimately a large fraction of the cells may calcify. Reperfusion of infarcted myocardium also accelerates the washout of intracellular proteins (“serum cardiac markers”),

producing an exaggerated and early peak value of substances such as the MB isoenzyme of creatine kinase (CK-MB) and cardiac-specific troponin T and I. Prevention of cell death by restoration of blood flow depends on the severity and duration of pre-existing ischemia. Even after successful reperfusion and despite the absence of irreversible myocardial damage, a period of post-ischemic contractile dysfunction can occur, a phenomenon referred to as myocardial stunning.

The process of reperfusion, although beneficial in terms of myocardial salvage, may come at a cost owing a process known as "reperfusion injury"(12). With this term, we normally refer to causal events associated with reperfusion that had not occurred during the preceding ischaemic period. Although ischaemia/reperfusion injury is now a well accepted phenomenon in the research experimental setting, its clinical relevance remains to be proven (13). The main difficulty is in differentiating between the pre-existing ischaemic damage and any subsequent damage occurring during the reperfusion phase. As summarised by Kloner (14), four types of reperfusion injury have been observed in experimental animals and consist of: (i) the *myocyte lethal reperfusion injury*, a reperfusion-induced death of myocytes that are still viable at the time of restoration of coronary blood flow; (ii) the *vascular reperfusion injury*, a progressive microvasculature damage leading to the phenomenon of no-reflow and loss of coronary vasodilatatory reserve; (iii) the *stunned myocardium,* myocytes display a prolonged period of contractile dysfunction following coronary blood flow restoration due to abnormal intracellular metabolism leading to reduced energy production; (iiii) *reperfusion arrhythmias*, ventricular tachycardia or fibrillation that occurs within seconds of reperfusion.

Unlike the others, the concept of ''lethal'' reperfusion injury of potentially salvageable myocytes is still controversial (14). According to this theory, ischaemia is a necessary prerequisite for lethal reperfusion injury, but not in itself sufficient to cause cell death. Potential causes of injury that develop during reperfusion have been difficult to analyse as these must be clearly differentiated from ischaemic causes. From a practical point of view, it is obviously impossible to evaluate, in the same sample of myocardium, changes occurring both during ischaemia and during reperfusion (15). Moreover, in the reperfused myocardium it is difficult to establish whether cell death is caused by the period of ischaemia or by reperfusion. Thus, the only valid criterion to attribute cell damage to the reperfusion process, and not to

ischaemia, is by demonstrating that modifications of reperfusion conditions are able to prevent cell death or dysfunction (16).

Myocyte lethal reperfusion injury: CONTRACTION BAND NECROSIS

During the earliest phase (within minutes) of reperfusion, development of myocyte hypercontraction seems to precipitate cardiomyocyte necrosis and arrhythmias and this phenomenon (‘‘contraction band necrosis’’) has been ascribed to a rapid re-energisation of myocytes with calcium overload (17). Although ischaemic myocytes following reperfusion suddenly develop ultrastructural changes indicative of cell death, they are still apparently normal from a histological point of view; it is likely that most of the myocytes are already irreversibly injured by the time reperfusion occurs, due to loss of plasma membrane continuity, and reperfusion simply accelerates the phenomenon (18). The contraction band necrosis is a frequent finding at postmortem examination in sudden death victims caused by atherosclerotic coronary artery disease. It is caused by increased calcium ion (Ca^{2+}) influx into dying cells, resulting in the arrest of cells in the contracted state. It is seen in the periphery of large infarcts and is present to a greater extent in nontransmural than in transmural infarcts.

Vascular reperfusion injury: NO-REFLOW PHENOMENON

The “no-reflow phenomenon” refers to the absent distal myocardial reperfusion after a prolonged period of ischaemia, despite the culprit coronary artery’s successful recanalisation, and it appears to result from ischaemia-induced microvasculature damage (19-20). During the early phase of ischemia, functional and structural changes occur at the level of cardiac arterioles and capillaries and interaction between endothelial cells, leukocytes, and platelets ensue (21). These events underline slow flow or no-reflow phenomenon noted following relief of the epicardial obstruction. Concomitant with reperfusion, the sudden rush of leukocytes and various mediators as well as an occasional shower of atheroemboli add ‘‘insult’’ to the injury. Thus, the pathophysiology associated with no-reflow represents the outcome of a complex, interactive phenomenon. When canine myocardium was exposed to short periods of ischemia (<40 min of ischemia), no significant changes were noted in the small cardiac vessels. When ischemia was maintained for 90 min, a clear change was noted in the endothelium of the capillaries. Dignan et al. (22)

confirmed these observations in studies of ischemia in the porcine heart. Ischemia for less than 30 min did not have a significant effect on the small vessels. However, when arteries were exposed to ischemia of longer duration, capability for endothelium-mediated relaxation progressively decreased and was totally lost after 120 min of ischemia. With loss of normal endothelial function, the vascular system ceased to dilate in response to myocardial needs and was totally governed by external forces. In addition, intracellular edema and endothelial cell swelling occur during myocardial infarction (23), resulting in compression of capillaries and small arterioles, further decreasing flow through these dysfunctional vessels. Consequences of ischemia include development of local structural changes in the endothelial cells of small vessels, cellular, coupled with accumulation of activated platelets and leukocytes, which in turn, release various proinflammatory and vasoactive mediators (24). This seminal cascade of events converges to provide the pathogenic stimulus leading to microcirculatory dysfunction. Animal studies have shown that the area of no-reflow expands during the first few hours of reperfusion, suggesting that there is true reperfusion injury of the microcirculation (25). Determination of the area of no-reflow is dependent on duration of coronary occlusion, infarction size, and duration of reperfusion (26). Downstream atheroembolization may occur, further blocking the small vessels and worsening flow in the microcirculation. Unlike most animal models of mechanical coronary occlusion, the clinical setting probably involves microembolic events in a substantial number of cases. However, a prospective randomised controlled multicentre trial on distal microcirculatory protection during percutaneous coronary intervention in ST segment elevation acute myocardial infarction demonstrated that, although a distal balloon occlusion and aspiration system effectively retrieves embolic debris in most of the patients, this approach did not result in improved microvascular flow and in a better prognosis overall (27). These negative findings are not surprising, considering that the noreflow phenomenon does not appear to augment myocyte death and the myocardium of the no-reflow area is usually already necrotic at the time of reperfusion onset. The relevance of the microvascular obstruction caused by thromboembolic material in determining the no-reflow phenomenon should probably be re-evaluated in view of its therapeutic implications. In a recent postmortem investigation in patients who died in the acute phase of myocardial infarction, Basso et al. found that, despite a higher occurrence in treated versus

untreated patients, distal microembolisation was always confined to the necrotic myocardium and its spatial distribution was not widespread (28). In other words, while distal microcirculatory embolisation occurs during coronary recanalisation procedures and is preventable, such intervention may be ‘‘too little, too late’’ to achieve meaningful myocardial salvage in acute myocardial infarction, which is also characterised by systemic and local mediators of inflammation and endothelial dysfunction, capillary leakage, and interstitial edema. In fact, several studies in animal models and in man have shown thet the pathogenesis of no-reflow is multifactorial. Moreover, the role of platelets seems to be more important in the earlier stage of reperfusion while neutrophil infiltration might be more important at a latter stage (29.). Platelets may be implicated in no-reflow throught several mechanisms: microvascular obstruction by platelet aggregates and release of platelet-derived vasoactive and chemotactic mediators (30). In a recent study, Niccoli G et al (31) identified a possible central role in no-reflow pathophysiology of thromboxane A2 (TXA2), a mediator affecting platelet activation: TXA2 resulted as an independent indicator of no-reflow after primary PCI documented by both angiographic index and lack of ST-segment resolution.

Many techniques are utilized to diagnose or predict coronary no-reflow during acute coronary intervention. Although ECG ST-segment resolution is a readily available marker of tissue level reperfusion, persistence of ST-segment elevation in an AMI patient may reflect either epicardial artery occlusion or microvascular obstruction. Coronary flow velocity patterns utilizing Doppler wire are diagnostic tools (32,33). Recently, contrast echocardiography and transthoracic Doppler echocardiography have been used to assist in the diagnosis (34). Contrast-enhanced CMR has shown promising results in the diagnosis of no-reflow (35); tissue hypoenhancement on contrast-enhanced CMR reflects impaired myocardial perfusion and correlates with histological evidence of microvascular obstruction. Clinically, coronary angiography is the gold standard for diagnosis of no-reflow. The immediate recognition and diagnosis of no-reflow is very critical to prompt initiation of such therapy. On the basis of the large population clinical studies, angiographic parameters were established to define reperfusion and perfusion profile: TIMI score (36) and, preferably for myocardial perfusion, MBG (37). The TIMI score is a grading system to describe the rate of blood flow in the epicardial vessels and ranges between no flow at all (grade 0) to a normal flow rate (grade III). Tissue blush grade is described

as the tissue perfusion from grade 0, where there is no penetration of dye into the myocardial tissue to grade III where the dye passes through the microcirculation at normal rates. TIMI frame count is more accurate and less subjective, yet its value is mainly for research purposes because it is time-consuming. Following assessment of the success of the procedure on epicardial vessel residual stenosis, interventional cardiologists need to comment on coronary flow as a measure of success at the level of the microcirculation. At the conclusion of a successful coronary intervention, and in the absence of residual coronary stenosis, dissection, or formation of a thrombus, the artery should exhibit a TIMI 3 flow rate as well as a normal tissue blush. Normal tissue blush reaffirms normal blood flow through the microcirculation.

Multiple therapies for no reflow have been tested in animals and to a lesser degree in humans. Interventions for no reflow that were efficacious in preclinical research often have failed to translate into effective human therapies due to limitations of the available animal models.

Because loss of endothelial integrity as final stage of prolonged ischemia, finally, reperfused myocardial infarcts frequently appear reddish because of "intramyocardial haemorrhage" (38). Experimental models first showed myocardial haemorrhage in the setting of prolonged coronary occlusion and reperfusion. Then myocardial haemorrhage after reperfusion was also described in humans following cardiac surgery, percutaneous transluminal coronary angioplasty and fibrinolysis. Haemorrhagic infarcts are thought to be caused by vascular cell damage with leakage of blood out of the injured vessels.

It is well known that cell vascular damage occurs after myocardial cell necrosis and thus it represents a relatively late event in the course of acute myocardial infarction at the time of already irreversible myocyte damage. Moreover, haemorrhagic infarction occurs always within the area of necrosis and it is significantly related to the infarct size and to the period of coronary occlusion (39). As such, haemorrhage is not related to the type of recanalisation as was originally thought, when it was assumed that a lytic state associated with thrombolytic therapy could play a major role. In fact, haemorrhagic infarcts can develop after percutaneous coronary interventions without thrombolysis as well, and the major determinant is the time interval between coronary occlusion and reflow. Unfavourable mechanical consequences of intramyocardial haemorrhage could comprise increased myocardial stiffness, propensity to rupture, and a delayed healing process. However, at present

the clinical implications of haemorrhagic versus white infarcts remain undetermined, because of the absence of reliable and reproducible imaging modalities to detect its presence in vivo.

Stunned Myocardium

For four decades after Tennant and Wiggers's classic observation on the effects of coronary occlusion on myocardial contraction, it was believed that transient severe ischemia caused either irreversible cardiac injury or prompt recovery (40). However, in the 1970s Heyndrickx and colleagues reported that regional contraction remained depressed for more than 3 hours after a 5-minute coronary occlusion and for more than 6 hours after a 15-minute occlusion in conscious dogs (41). It became clear that after a brief episode of severe ischemia, prolonged myocardial dysfunction with gradual return of contractile activity occurs, a condition termed myocardial stunning. Subsequently, myocardial stunning was observed by other investigators under a variety of additional experimental conditions, including multiple, brief episodes of ischemia; prolonged ischemia resulting in an mixture of myocardial necrosis and stunning of adjacent, viable myocardium; global myocardial ischemia (e.g., cardioplegia arrest); and stunning after exercise-induced ischemia (42-44).

A number of factors converge in the pathogenesis of myocardial stunning. Probably, the three most important are: (i) generation of oxygen derived free radials, (ii) calcium overload, and (iii) reduced sensitivity of myofilaments to calcium and loss of myofilaments (42,43). These mechanisms interact synergistically in the pathophysiological process of stunning. Although antioxidants are effective, they do not prevent stunning completely. It has been postulated that stunning involves two components, one related to ischemia (not responsive to antioxidants) and a second larger component related to reperfusion (42).

Reperfusion arrhytmias

When present, rhythm disturbances may actually be a marker of successful restoration of coronary flow. However, although reperfusion arrhythmias have a high sensitivity for detecting successful reperfusion, the high incidence of identical rhythm disturbances in patients without successful coronary artery reperfusion limits their specificity for detection of restoration of coronary blood flow. In general, clinical features are poor markers of reperfusion, with no single clinical finding or constellation of findings being reliably predictive of angiographically demonstrated

coronary artery patency. Although reperfusion arrhythmias may show a temporal clustering at the time of restoration of coronary blood flow in patients with successful thrombolysis, the overall incidence of such arrhythmias appears to be similar in patients not receiving a thrombolytic agent who may develop these arrhythmias as a consequence of spontaneous coronary artery reperfusion or the evolution of the infarct process itself. Transient sinus bradycardia occurs in many patients with inferior infarcts at the time of acute reperfusion; it is most often accompanied by some degree of hypotension. This combination of hypotension and bradycardia with a sudden increase in coronary flow has been ascribed to the activation of the Bezold-Jarisch reflex. Premature ventricular contractions, accelerated idioventricular rhythm, and nonsustained ventricula tachycardia (VT) are also seen commonly after successful reperfusion. In experimental animals with AMI, ventricular fibrillation occurs shortly after reperfusion, but this arrhythmia is not as frequent in patients as in the experimental setting. Although some investigators have postulated that early afterdepolarizations participate in the genesis of reperfusion ventricular arrhythmias, Vera and colleagues have shown that early after depolarizations are present both during ischemia and during reperfusion and are therefore unlikely to be involved in the development of reperfusion VT or ventricular fibrillation (45,46).

Measurement of infarct size: old and new tools. The basis of current definition

Determination and quantification of infarct size offer the possibility to demonstrate the efficacy of a new therapy and is an attractive surrogate end point for the early assessment of new therapies with respect to early mortality and on long-term mortality. However, the measurement of infarct size has other several advantages as to permit early pilot studies to test the potential efficacy of new approaches, and it can serve as an end point for dose-ranging studies to select the most appropriate dose of a new drug for larger studies.

Traditional infarct size measurement was obtained by biochemical markers such as creatine kinase (CK) evolved to CK-MB fraction, Troponin T or I: the measurement of infarct size by serum markers has multiple theoretical and practical limitations (47). For example, the kinetics and release ratio of the troponins are not well defined. Notwithstanding the depletion of troponin T but not troponin I has been reported to correlate with pathologic infarct size in dogs, the release ratio is unclear

and could be different for the cytosolic and structural pools. Given its improved specificity, troponin should be a more accurate way to assess infarct size. Ideally, one would like to measure all the troponin released and then correct for clearance to determine release.

In order to avoid a more accurate determination of infarct size, recently several different lines of evidence provided clinical validation for the use of CMR using segmented inversion recovery, after gadolinium injection, for the measurement of its. Evaluating the data of Literature we could summarize that:

1. There is a close association between CMR infarct size and measurements that have been used clinically to assess infarct size, including ejection fraction, regional wall motion enzyme release, and positron emission tomography imaging (48-50).

2. The CMR infarct size predicts recovery of function after revascularization and after MI. The transmural extent of the infarct appears to delineate viable and nonviable myocardium and the recovery of function after revascularization. The extent of transmural enhancement also predicts recovery of function after MI (49).

3. In one small study of 44 patients (53), CMR infarct size was significantly associated with cardiovascular events generally is measured by computer-assisted planimetry of the hyperenhanced myocardium. The area of hyperenhanced myocardium is traced in each slice and multiplied by the slice thickness and the myocardial density of 1.05 g/ml to obtain the infarct mass. A second method to quantify infarct size determines the enhancement score (0 to 4) for each segment, sums these scores over all segments, and then divides this sum by the maximal possible score (total number of segments x 4).

It should be appreciated that over the years, current, more specific, and sensitive biomarkers and imaging methods to detect myocardial infarction are further refinements in this evolution and so the accuracy of detecting myocardial infarction has changed. Recently, European Guidelines Commettee (54) defined that the term “myocardial infarction” should not be used without further qualifications, whether in clinical practice, in the description of patient cohorts, or in population studies. Such qualifications should refer to the amount of myocardial cell loss (infarct size), to the circumstances leading to the infarct (e.g. spontaneous or procedure related), and to the timing of the myocardial necrosis relative to the time of the observation (evolving, healing, or healed myocardial infarction) This better definition of myocardial infarction will have a substantial impact on the identification,

prevention, and treatment of cardiovascular disease throughout the world. On this basis, regarding both myocardium loss and timing of necrosis, the use of CMR in specific subgroup of patients (i.e. diabetics population, patients with recent AMI) takes an important prognostic role for the possibility to quantify the real amount of necrosis. Regarding this point, recently, in the first international, multicenter trial of delayed enhancement imaging, Kim et al. (55) randomly allocated 282 patients with AMI and 284 patients with chronic myocardial infarction to different doses of gadolinium. They found the highest sensitivity (97%) for their highest dose of contrast (0.3mmol/kg), and the lowest sensitivity (76%) in patients with AMI in the lowest tertile of creatine kinase-myocardial band values, suggesting a lower limit for the detection of AMI by CMR delayed enhancement imaging.

Magnetic Resonance Imaging

Since from its discovery in 1946 and the real fruition only since the mid 1990s, magnetic resonance, because of its unique versatility and non-invasive nature, become an attracting diagnostic modality in cardiovascular medicine, allowing a noninvasive comprehensive and reproducible imaging modality to asses both function, morphology an tissue characterization.

Magnetic resonance imaging views the water and fat in the human body by observing the hydrogen nuclei in these molecules (56). Magnetic resonance is sensitive to any nucleus that possesses a net "spin". Nuclear spin is a fundamental property of atomic nuclei that depends on the numbers of neutrons and protons it contains, and so nuclei either have it. Nuclei possessing net spin will behave as tiny radiofrequency receivers and transmitters when placed in a strong magnetic field. Both the frequency and the strength of the transmitter increase with increasing magnetic field strength. One feature of magnetic resonance is that the frequency at which signals are received and re-emitted (known as the resonant frequency) is exquisitely sensitive to the exact magnetic field, for example hydrogen nuclei (lone protons) resonate at 42.575 Hz/Tesla. So, if we have two regions where the magnetic field is different by a small amount (e.g. at 1.000 Tesla and 1.001 Tesla), then the protons in one region will transmit at 42.575 MHz (the Larmor frequency for protons), and the protons from the other region will transmit at 42.575+0.042 MHz. If we sample this transmitted signal, it is possible to determine these two different frequencies. Numerically this transformation from a sampled signal to the component frequencies is known as a Fourier transform. By modifying the frequency of the RF pulse, and by playing out the gradient pulses on more than one axis simultaneously we can move the slice of interest freely. We are not limited to axial planes, since that we can acquire data with oblique or doubly oblique axes with complete flexibility too. The term "pulse sequence" or "imaging sequence" describes the way in which the scanner plays out RF pulse and gradient fields and how it acquires and reconstructs the resultant data to form an image.

The basic imaging sequences used in CMR are (57):

• FLASH (Fast Low Angle SHot). This plays out a small excitation RF pulse which is followed by a rapid read-out and then spoiling (or removing) of the residual signal to prevent it appearing as an artifact in subsequent acquisitions. The process is repeated, yielding a single phase-encode line per acquisition.

• TrueFISP (aka Balanced FFE (Balanced Fast Field Echo). This sequence is similar to FLASH but instead of spoiling the magnetization at the end of each acquisition it re-uses that signal. Compared to FLASH the benefit of this approach is that the images are of higher signal-to-noise ratio, with natural contrast between cavity and myocardium; the disadvantages being increased sensitivity to artifacts, increased RF power deposition, and contrast that is more complex to interpret.
• FSE (Fast Spin Echo, TSE (Turbo Spin Echo). This sequence acquires a number of phase-encode lines per acquisition by playing out a series of refocusing pulses after the initial excitation pulse. These refocusing pulses are a phenomenon of MR, which allow us to hold into the signal created by the excitation pulse for longer so that we can sample it multiple times.The optimum excitation pulse can be used, which maximises the available signal, and it is possible with this sequence to obtain T2 contrast without the undesirable effects of T2*. It is possible to acquire all the phase encodes in FSE in a single acquisition, which has some advantages, although this is likely to result in low temporal resolution.
Additional modules can be included with the above sequences to modify the image contrast, for example:
• Black-blood pulses can be applied to effectively remove all the signal from material that moves quickly (i.e. blood). This is usually performed using double inversion, which requires a delay prior to acquisition so is most compatible with FSE-based sequences.
• Inversion recovery is a prepulse method that allows to introduce T1 contrast into an image. An inversion time that completely removes the signal from materials with a certain T1 can be choosen. In practice this is often used to better define small changes in T1 in late enhancement type sequences.
• Fat suppression (or water suppression) can be used to remove all the signal from either of these tissues, which may improve the delineation of the structures of interest.

For our aims the sequences to characterize myocardial necrosis are the segmented inversion recovery fast gradient echo (seg IR-GE) sequence for differentiating irreversible injured from normal myocardium with signal intensity differences of nearly 500% (58).

Contrast agent: Gadolinium

Addition of even small amounts of certain molecules, called CMR contrast agents, can massively change relaxation rates (i.e. T1, T2 and T2*) within the patient, which results in major changes in the appearance of an CMR image (59). Fundamentally, there are two types of contrast agents:

• T1 contrast agents, which by interaction with the nuclear spins, shorten the T1 of the sample. For this to operate there needs to be intimate contact between the agent and the protons.

• T2 and T2* contrast agents. In this case the contrast agents will shorten the T2 and T2* of the sample. These effects do not need close interactions between the nuclei and the agent as they occur over much larger distances.

In each case the contrast agents are based upon molecules or ions that are magnetically active. Paramagnetic moieties (typically, Fe, Dy, Gd but also O2) are used because these demonstrate the greatest effects. The most commonly used nucleus is gadolinium, chelated with diethylenetriaminepentaacetate (DTPA) so as to render it non-toxic and safe for injection. Gadolinium compounds act predominantly as T1 contrast agents in the blood and myocardium, although where the contrast cannot freely mix with the observed water (i.e. in the brain because of the blood-brain barrier), their small T2 and T2* effects can also be observed. Iron-oxide particles predominantly affect the T2 and T2* of the sample. In CMR images the regions where these particles accumulate will decrease the signals in T2-weighted images. For both types of contrast agent the effects are regionally specific, i.e. compounds affect the contrast at the site of the contrast agent and by an amount that increases with contrast agent concentration. This can be used, for example, when looking at myocardial infarction when contrast agent (~10–20 min after its administration) remains within infarcted tissue at higher concentration than in surrounding normal tissue. By adding CMR contrast agents to compounds that can adhere to specific molecules (e.g. Fibrin) we can create “targeted contrast agents”. This type of molecular imaging provides a promising approach for the future. Contrast agents that remain within the vascular system can be produced, and are thus termed “intravascular”. With an agent that decreases the T1 it is possible to boost the signal in angiographic examinations, and hence improve the image quality. Presently Gd-DPTA is used in such angiographic examinations, but as it is not an “intravascular” agent the acquisition needs to occur when the Gd-DTPA is

undergoing its first pass through the vascular tree. “Intravascular” contrast agents would remove this restriction, enabling longer, and hence higher quality, imaging. Presently no agents of this kind are approved for clinical use.

About the safety of CMR as an emerging problem, numerous reports describing the development of nephrogenic systemic sclerosis have been reported. This is a systemic disease involving fibrosis of multiple organs, particularly the skin, that has been linked to gadolinium exposure in patients with renal insufficiency (60.). There have been numerous reports describing the development of nephrogenic systemic sclerosis in small numbers of patients with renal failure exposed to CMR contrast agents. The prevailing theory is that gadolinium dissociates from its carrier molecule and accumulates in the tissue of patients with renal failure because it is not cleared. Singh et al. (61), Swaminathan et al. (62.), and Schroeder et al. (63.) reported cases in which gadolinium deposits were detected in the skin and other organs in a total of 5 patients with nephrogenic systemic sclerosis. The European Society of Urogenital Radiology released guidelines regarding the use of gadolinium-containing CMR contrast agents (64.), suggesting that these agents are contraindicated for patients with a glomerular filtration rate <30 ml/min and recommending caution for patients with a glomerular filtration rate of 30 to 60 ml/min.

Magnetic Resonance and Myocardial Infarction

Ischemic heart disease and in particolar myocardial infarction is caused by a regional acute reduction of blood flow to the myocardium with an imbalance between oxygen supplì and demand. This progressive reduction of blood flow leads to the so-called “ischemic cascade” where the acute myocardial infarction is located on the top (65). CMR allows a comprehensive study including: assessment of myocardial perfusion and function (at rest and under stress), delayed contrast enhancement (for viability imaging) and also the delayed hypoenhacement to visualize the major microvascular damage after reperfusion. So far, the CMR represents the unique, noninvasive in vivo imaging modality to study the entire ischemic cascade as “one-stop-shop”.

Perfusion impairment

Firstly, atherosclerosis can cause reduction of blood flow that may result in a perfusion defect. Generally, perfusion imaging relies on a sequence to create images that enhance the myocardium compared with precontrast images with passage of a contrast agent. The perfusion defect is identified by attenuation or absence of this brightening in the myocardium and can demonstrate the transmural extent. Resting coronary blood flow is not reduced until the stenosis exceeds 90% of the normal vessel diameter (66). However, when using a stress agent, blood flow is already reduced at a stenosis of 50% of the vessel diameter. Therefore, perfusion imaging should be performed in conjunction with pharmacological vasodilatation to identify subcritical coronary stenosis. The ability to combine first-pass perfusion (at rest and with adenosine) to delayed contrast images compared to conventional coronary angiograms has been succesfully performed in patients with acute coronary syndromes to predict the presence of coronary stenosis (67). However, in the setting of AMI, in the subacute phase after percutaneous intervention, performing first pass sequences CMR identifies perfusion defects often characterized by severe microvascular damage on delayed contrast imaging. In fact, in the first experiences in the literature, microvascular obstruction has usually been assessed within 1 to 3 minutes after contrast injection (53,68-70) However, several investigators have also recently reported the finding of microvascular obstruction as areas of hypoenhancement in late delayed-enhancement imaging (71).
To understand the mechanins inside perfusion defects on first pass in acute

myocardial infarction, a recent paper by Lund GK and co-workers (72) clarify the role of microvascular obstruction about first pass defects. They showed an high concordance between microvascular obstruction on firts pass images and persistent hypoenhancement on delayed enhancement images. However, the sensitivity of delayed enhancement images was only 74% for the detection of microvascular obstruction with first pass images used as the reference standard. In 26% of patients with microvascular obstruction, no persistent hypoenhancement was present on delayed enhancement images. This finding was related to areas of microvascular damage on first pass images: the larger the first pass defects, more often an area of persistent hypoenhancement on delayed enhancement images was found. The reduction in size of the hypoenhanced zone indicates that the edges of the perfusion defect are filled in over time by contrast material, through collateral flow or slow diffusion. Thus, first pass imaging preferably should be used, in their experience for visualization of microvascular obstruction.

Finally, perfusion defects at rest in AMI setting may represent a more severe microvascular impairment than the hypoperfusion in the pre-infarctual patients, and so the integration with delayed enhancement is useful to understand the underlying mechanism.

Myocardial Edema: "Area at Risk"

The pathophysiological processe that occuring after AMI are complex. CMR provides noninvasive in vivo myocardial tissue characterization, including myocardial edema. Without intervention or collateral flow from other arteries, the "wavefront phenomenon" ends in a complete necrosis of the myocardial tissue within the perfusion bed. The latter has been referred to as the area at risk. Early reopening of the infarct-related artery, however, interrupts this process and salvages tissue within the area at risk. Although salvaged, the myocardium within this zone is altered by the recent severe ischemia. Induced by inflammation, edema is one of the features of the salvageable area at risk. In contrast to chronic coronary artery occlusion, myocardial edema occurs early after even brief episodes of myocardial ischemia. Increased myocardial signal intensity depicted by T2-weighted imaging identifies areas of increased water content with active myocardial inflammation and edema, which are distinctive aspects of acute myocardial infarction. T2- weighted sequences are very sensitive to water-bound protons indicating tissue edema and

recent results indicate its clinical applicability for differentiating acute from chronic infarctions. Abdel-Aty et al. demonstrated in seventy-three pts that the Signal to Noise Ratio (SNR) of AMI was higher than that of the remote myocardium (11.8±2.9 versus 6.5±2.2; P<0.0001). In chronic infarcts, there was no significant difference between the SNR of infarcted and remote myocardium (7.4±1.9 versus 6.9±2.0; P=NS). The CMR of acute infarcts was significantly higher than that of chronic myocardial infarction (5.3±1.6 versus 1.1±2.6; P<0.0001). There was no significant difference between the CMR of acute reperfused and nonreperfused infarcts (5.5±1.9 versus 4.9±0.8; P=NS) (73).

Detection of edema of risk area offers the capability to evaluate the real myocardial salvage after reperfusion therapy. After initial experimental study (74), a recent clinical experience by Friedrich et al (75) reveals the possibility for further investigation starting from their observations regarding the CMR visualization of both reversible and irreversible injury. Their preliminary observation allows for quantifyng the extent of the salvaged area after revascularization as an important parameter for clinical decision-making and research.

Yet, T2-weighted sequences are sensitive not only to edema related signal changes, but also to a variety of pathological phenomena taking place during infarct healing, as fibrosis. Although brightness of edema on T2-weighted, in the same sequences is possible to recognize an hypointense area. This signal void has been explained by haemoglobin degradation products, such as methaemoglobin and hemosiderin, having strong magnetic susceptibility effects. This radiological findings are currently applied to study intracranial haemorrhage; on the opposite side, intramyocardial haemorrhage is not well established with this imaging modalities. A recent experimental study by van de Bos (76) demonstrated the corrispondence by hystology between signal void on T2- weighted inmages in experimental infarction after injection of iron oxide-labelled human cells and hemorrhagic infarcts core. Some report also in humans suggest that the application of these sequences allow identification, in the high signal intensity of edema, a hypoenhanced core identify with microvascular damage.

Myocardial necrosis: delayed enhancement

Beyond the possible reversible events (ischemia and edema) of the ischemic cascade, CMR can be used for assessment of the extent of a AMI using delayed contrast-hyperenhaced images. After administration of a contrast agent, normal myocardium will show increased signal intensity during the first pass, followed by wash-out from the tissue. In infarcted myocardium, contrast agent follows different wash-out kinetics than in normal myocardial tissue. This tissue is termed "hyperenhanced" or "delayed hyperenhanced". Detection of myocardial necrosis as delayed hyperenhanced area by CMR has three major clinical scenarios. The first situation is about the recognization of ischemic scar in peculiar subgroup of patients with major cardiovascular risk factors: this observation has an important clinical prognostic role in silent ischemia, for example, in diabetics subjects, as recently demonstrated (75-76). A second possibility is represented by detection of myocardial viability since delayed hyperenhanced could be used to distinguish between reversible myocardial ischemic injury and myocardial necrosis. The final third scenario occurs in the acute setting of myocardial infarction where infarct size, as the total amount and location, reveals on the follow up relevant clinical prognostic impact both for mechanical remodelling and arrhythmic risk profile. For our aim the second and third conditions are the more important.

In the assessment of reversible versus irreversible ischemic myocardial injury, CMR presents several advantages over the other imaging modalities. The major advantage is its ability to image tissue with millimeter resolution, providing with the administration of a gadolinium-based contrast agent, an assessment of the transmural extent of viable versus nonviable myocardium within a segment of the LV wall. The contrast agent applied in CMR imaging is a gadolinium-chelate, such as gadolinium-diethylenetriamine pentaacetic acid (Gd-DTPA). This metabolically inert molecule has an extracellular distribution and accentuates the difference in tissue relaxation characteristics (shortening of both T1 and T2 relaxation times, with the former predominating) between infarcted and normal myocardium. Because the duration of the cardiac cycle is ~ 800 msec, corresponding to myocardial T1, the resulting images are T1-weighted. Following intravenous administration, the contrast agent diffuses rapidly from the intravascular to the extracellular compartment, and over several minutes, concentrates into regions with irreversible injury. The increased image intensity is the result of the shortening of myocardial T1

caused by Gd-DTPA. In the setting of an acute infarction, the contrast agent enters the intracellular space through damaged cell membranes. As a result, the contrast agent accumulates to a greater concentration when compared to normal myocardium over a timeframe of 10 to 15 minutes. Similarly, the volume of distribution of the contrast agent also increases in chronic infarcts, probably due to an increased extracellular space from collagenous scar tissue (77). In both cases, CMR identifies the presence of nonviable from viable tissue by exploiting the relative differences in contrast concentrations (78). In addition, areas of edema and inflammation that result during acute myocardial infarction have greater accumulation and slower clearance of Gd-DTPA because of the increased capillary permeability and expansion of the interstitial space (79). Saeed et al (80) have suggested that CMR contrast hyperenhancement does not occur exclusively in regions with myocardial necrosis but also in the border zones of injured but viable myocardium surrounding acute infarcts. The mechanisms by which Gd-DTPA concentrates in infarcted myocardium is still not completely elucidated, but it is likely related to its expanding volume of distribution due to rupture of myocyte cell membranes in the acute setting and to the increased intracellular space between collagen fibers in the chronic setting (78). In normal regions, contrast wash-in and wash-out are rapid, reaching steady state within 2 to 3 minutes. The time of imaging after contrast injection is crucial. In fact, as Kim et al (52) have described, a region that is hypoenhanced or hyperenhanced at one time point may become isoenhanced at another time point and no longer be distinguishable from normal (81) Accordingly, allowing 15 to 20 minutes after contrast injection has been determined to be the ideal time interval in which to obtain optimal contrast-enhanced CMR images.

Imaging time after Gd-DTPA injection is critical for accurate determination of infarct size. Oshinski et al (82) using a rat model of acute myocardial infarction, demonstrated that, immediately after contrast injection, the enhanced region overestimates the true infarct size, as determined by TTC, by 20 to 40%. Moreover, the initial overestimation of infarct size gradually decreased over time.

Recently Ingkanisorn et al (83) tested the hypothesis that gadolinium delayed enhancement assessment of infarct size correlated with clinical indices of myocardial infarction in humans; they found that acute CMR infarct size was strictly related to acute and chronic indices of infarct size, as peak of troponin I and follow-

up left ventricle ejection fraction. However, CMR infarct size appeared to diminish in size on follow-up from 16 ± 12% to 11 ± 9% (p<0,003).

The same reduction on infarct size was noted by Hombach and collagues (71) in a large population studied by CMR after a reperfused myocardial infarction. They found a reduction of infarct size on follow-up on both groups of patients divided into two groups according with the presence of microvascular damage on the same sequences. The reduction on infarct size detected by CMR can be hypotized as a part of the normal myocardial repairing phenomenon with scar development and progressive reuction of edema, an important factor fo gadolinium depositition.

After acute phase, the accurate delineation of irreversibly damaged versus viable myocardium by CMR, even in regions with severe contractile dysfunction, provides the basis for CMR to identify dysfunctional myocardium that has the potential for recovery of function after revascularization or medical interventions. Hillenbrand et al (84) demonstrated the potential of contrast-enhanced CMR to predict myocardial salvage and recovery of regional myocardial dysfunction using a dog model of acute coronary occlusion. This study confirmed that hyperenhancement does not occur in regions with severe but reversible ischemic injury and that there is an inverse relationship between the transmural extent of necrosis and recovery of function. Kim et al (52) applied contrast-enhanced CMR prospectively in a series of patients with chronic CAD and LV dysfunction undergoing myocardial revascularization (with either CABG or percutaneous intervention) to determine the accuracy of CMR in predicting recovery of regional and contrast-enhanced CMR is a valuable tool for identifying those patients with the greatest potential for improvement in LV function after revascularization The findings of Selvanayagam et al (85) who confirmed the role of contrast-enhanced CMR as a viability tool in patients undergoing CABG.

Reperfusion injury: delayed hypoenhancement

The no-reflow phenomenon, as previously described, leads a final development of microvascular obstruction, traditionally identified in contrast CMR studies as areas of hypoenhancement (called “dark zones”), due to poor contrast penetration, within the area of hyperenhancement, as validated by histological studies (86). In the literature, microvascular obstruction has usually been assessed within 1 to 3 minutes after contrast injection (53, 68, 87). Several investigators have also recently reported the finding of microvascular obstruction as areas of hypoenhancement in late

delayed-enhancement imaging.(71). At present there are no conclusive data regarding the ideal time after contrast injection for evaluation of the presence and extent of microvascular obstruction.

The preliminary description of no-reflow using CMR compare with traditional methods was reported by Rochitte et al (69), who described that microvascular obstruction, assessed by both CMR and microspheres, were increased in size in the first 48 hours after reperfused myocardial infarction. Moreover, such areas of hypoenhancement correlated well with thioflavin-negative regions at postmortem examination. Thioflavin S is a fluorescent dye used to demonstrate the distribution and patency of the microvasculature by means of endothelial staining (87). The same group of investigators (88) demonstrated later in a dog model of reperfused myocardial infarction that myocardial sodium accumulation caused by ischemia-reperfusion injury is delayed in regions with microvascular obstruction (assessed by radioactive microsphere myocardial blood flow), thus suggesting that this process is governed by microvascular integrity. These investigators also observed that myocardial regions with sodium accumulation, measured by CMR 8 to 9 hours after reperfusion, correlate well with infarct size defined by TTC-negative regions ($r=0.95$) as well as with regions of myocardial hyperenhancement ($r=0.98$).

In addition to the extent of infarcted myocardium, the magnitude of microvascular obstruction sustained during acute myocardial infarction and reperfusion has been described as a predictor of complications and LV remodeling (69, 88, 89). These investigators reported that 45% of patients with microvascular obstruction experienced a post-infarction complication, such as cardiac death, reinfarction, congestive heart failure, or stroke, in comparison to only 9% of the patients without microvascular obstruction ($P < 0.01$). In addition, long-term prognosis was also related to infarct size by CMR, and the risk of complications increased with infarct size ($P < 0.05$). Thus, in this study population, events occurred in 30% of patients with small infarcts, in 43% with medium infarcts, and in 71% with large infarcts. Wu et al (90) also observed that microvascular obstruction in the acute post-infarction period was associated with greater LV remodeling, in terms of both increased end-diastolic and end-systolic volumes and LV mass. The mechanisms by which microvascular obstruction may influence LV remodeling are still poorly understood. Some authors hypotized that microvascular obstruction alters the mechanical properties of infarcted myocardium, as demonstrated by the reduction in

circumferential and longitudinal stretching in infarcted myocardium with extensive areas of microvascular obstruction (70). The same authors suggested another possible explanation of this phenomenon an increase in myocardial stiffness resulting from intramyocardial edema or even from the intramyocardial hemorrhage, which has been described in infarcted tissue with microvascular obstruction (38). Gerber et al (70) observed that the extent of microvascular obstruction correlated better with subsequent LV end-diastolic volumes than did infarct size ($r = 0.84$ versus $r = 0.74$).

Analyzing the possible mechanism underlying delayed hypoenhancement, an elegant study performed by Amado et al. (91,92) recently demonstrated that intra-aortic balloon counterpulsation performed after reperfused myocardial infarction improves myocardial perfusion and reduces the extent of microvascular obstruction with a concomitant reduction in infarct area expansion. These findings encourage additional investigation of future strategies to further limit LV damage beyond epicardial reperfusion.

AIM

In order to investigate the following aims of my PhD thesis, were prospectively enrolled patients with acute myocardial infarction with persistent ST-segment elevation admitted to our Cardiology Department, treated with primary PCI and eligible to CMR. The examination was performed in the subacute phase, during the same hospitalization. The purposes were:

1. To assess the relationship between duration of ischemia and both myocardial TN and SMD. We aimed also to estimate the risk of transmurality and severe microvascular obstruction with the duration of ischemia.
2. To assess the predictive value of myocardial/microvascular injury assessed by DE CMR on LV remodeling and LV ejection fraction after primary PCI compared to peak troponin levels, an established index of myocardial infarct size.
3. To investigate the pathological basis of persistence of ST-segment elevation after AMI, traditionally ascribed to LV aneurysm development, using DE CMR.
4. To investigate the role of current antiplatelet therapy during AMI: we evaluated the impact of periprocedural (before primary PCI) Abciximab administration on microvascular obstruction in patients with occluded infarct-related artery.
5. To evaluate the correlation between angiographic index of myocardial perfusion after primary PCI, MBG, and the anatomical features on CMR, in particular the correlation between staining phenomenon and SMD.
6. To investigate the possibility to detect intramyocardial hemorrage after AMI, assessed by T2-weighted image on CMR, and define its real contribution to the delayed hypoenhanced core traditionally referred, so far, only to microvascular obstruction. For this aim we also correlated these CMR findings with in vivo histological data of two patient died for cardiogenic shock.

METHODS

Between March 2003 and September 2008, we prospectively enrolled a total of 310 patients that referred to our Intensive Cardiological Care Unit for acute myocardial infarction with persistent ST-segment elevation (STEMI) treated with primary angioplasty, including rescue and facilitated procedure. They were admitted to our department within 12 hours of the onset of AMI and underwent successful primary PCI. The AMI was defined by prolonged chest pain with ST-segment elevation on the electrocardiogram > 0.1 mV in two or more contiguous leads, or with new left bundle branch block, or with anterior ST-segment depression caused by posterior infarction at the echocardiogram. All patients received aspirin 250 mg and heparin (70 IU/kg) intravenously before the procedure. Primary PCI with stent was systematically attempted and accomplished with standard techniques. Intravenous Abciximab was administered in the cardiac catheterization laboratory at discretion of the interventional cardiologist. Enzymatic infarct size was calculated by the peak release of troponin I obtained by determinations systematically performed on the admission and every 6 hours for the subsequent 24 hours, and every 12 hours for the following 2 days. All patients underwent CMR during the same hospitalization period.

Electrocardiographic analysis

For each patient a standard twelve-leads ECG was recorded at admission, 30 to 60 minutes after the PCI procedure, and daily thereafter up to discharge. The sum of ST-segment elevation (STE) was measured manually 60 msec after the end of the QRS complex. Patients were prospectively classified in two groups, according to the results of pre-discharge ECG analysis: (i) patients exhibiting STE of at least 2 mm in two or more contiguous leads on pre-discharge ECG were classified as STE persistence group, and (ii) patients who did not as STE resolution group. The sum of STE at baseline ECG has been used to define the extent of the risk area. To evaluate the electrocardiographic extent of necrosis, the presence and the number of leads showing Q-wave, defined by ≥ 0.04 sec in duration and/or by ≥ 25% of corresponding R wave in amplitude, were analyzed. All measurements were done by two experienced observers, blinded to both clinical and cardiac imaging data.

Angiographic data analysis.

In all cases PCI and postprocedural angiographic control were performed according to the standard procedure. The control angiogram after PCI was obtained in the right anterior oblique -30°/cranial 30° projections for the assessment of the left descending anterior coronary artery (LAD), right anterior oblique -40°/ caudal 30° projections for the left circumflex artery (LCX) and left anterior oblique 30°/ cranial 15° or right anterior 30°/ cranial 0° projections for the right coronary artery (RCA); furthermore the length of the angiographic run was kept long enough to evaluate the venous phase of the contrast medium passage. A final left ventriculogram in a 30° right anterior oblique projection was obtained in all cases, with the exclusion of patients with renal failure or on dialysis.

Coronary flow in the infarct-related artery before and after revascularization was graded according to the TIMI study group classification (36). Collateral flow before direct angiography was graded using the classification of Rentrop et al (93,94). A successful procedure was defined when both TIMI grade ≥ 2 and residual stenosis was < 30% were obtained. Unsuccessful angiographic PCI was defined when TIMI flow was scored 0 or 1 at any level of residual stenosis. The effectiveness of myocardial reperfusion was assessed angiographically immediately after PCI by MBG and graded, as previously described (37, 95, 96), as: 0 = no myocardial blush or contrast density; 1 = minimal myocardial blush or contrast density; 2 = moderate myocardial blush or contrast density, which appears to be less than that observed during angiography of a controlateral or ipsilateral non-infarct-related coronary artery; 3 = normal myocardial blush or contrast density, comparable to that obtained during angiography of a controlateral or ipsilateral non-infarct-related coronary artery.

The presence of persistent myocardial blush (staining) (97) was assesed by a single operator with longstanding experience on the post procedural angiograms as well as on the final left ventriculogram; the persistence of contrast medium from previous injections within myocardial walls was also assessed and referred as MBG 0 with staining as previously defined (37-96).

Two different observers evaluated all coronary angiograms, first in a blinded fashion, then together to reach a consensus regarding Thrombolysis In Myocardial Infarction (TIMI) flow grade, collateral flow, and blush grade, as previously described (98). A successful angioplasty was defined as a combination of

postprocedural TIMI flow grade 3 and residual restenosis <30%. Time to treatment was calculated as the interval from the symptom onset to the first balloon inflation. Time to treatment was calculated as the interval from symptom onset to the first balloon inflation.

Cardiac Magnetic Resonance data analysis.

Patients were examined in a supine position on a clinical 1.0-T scanner (Harmony, Siemens, Erlangen, Germany) using cardiologic software by Siemens with system MRease SYNGO 2002B. All images were acquired using a four-channel phased-array receiver coil during repeated breath holds of varying duration depending on heart rate and patient compliance (12 to 15 sec.). Images were acquired using a steady-state free precession sequence (true FISP) in three short-axis views (at the level of the mitral valve, papillary muscles, and apex) and three long-axis views (two, three, and four chambers). A breath-hold, black-blood T2-weighted fat saturation turbo spin-echo sequences (repetition time 2 to 3 RR intervals, echo time 92 ms, mean voxel size 1,6x 1,4x7 mm) was performed in three short-axis slices and a long axis view. Contrast-enhanced images were acquired in the same views 10 min after intravenous administration of a gadolinium-based contrast agent (gadobenate dimeglumine, Multihance, Bracco, 0.2 mmol/kg of body weight). We excluded patients with creatinine clearance rate < 60 ml/min. Using a 17-segment model (99), the images were analyzed independently by two observers blinded to clinical and procedural characteristics. To evaluate areas of late enhancement and to differentiate infarcted from non-infarcted myocardium, a segmented gradient echo inversion recovery turbo FLASH sequence was used with the following characteristics: inversion time optimized for each patient, 17 to 21 K-space lines acquisition every 1 or 2 R-R interval (depending on heart frequency), TE 6 ms, flip angle 30°, BW 150 hz/pixel, resolution 134 x 256, typical voxel size of approximately 1.8 x 1.3 x 8 mm depending on the field of view (300 to 360 mm in relation to the patient's size), and slice thickness of 8 mm. Considering the T1 relaxation times of the tissues on the magnetic resonance imaging unit (1.0-T) and the wash-in and washout kinetics of extracellular interstitial contrast agents (81), the optimized T1 nullifies the signal from normal myocardium in the images acquired 10 min after contrast medium injection, allowing a clear visualization of the late enhanced infarcted areas, characterized, by definition (60), as a signal intensity at least 400% higher than the

signal from normal (remote) myocardium. Areas of gadolinium enhancement were assessed by visual approach with a scheme based on the spatial extent of delayed enhancement tissue within each segment as reported by others (48).

Cardiac Magnetic Resonance Definitions

The AMI was labeled as transmural if hyperenhancement was extended to ≥75% of the thickness of at least two contiguous ventricular segments. Distribution of DE was made following semi-quantitative scale: 0% no DE; 1%–25% of myocardial thickness enhanced; 26%–50% of myocardial thickness enhanced; 51–75% of myocardial thickness enhanced; 76%–100% of myocardial thickness enhanced. We defined SMD as subendocardial areas of late low or absent signal surrounded by late enhanced tissue (100, 101) in at least one ventricular segment.

Infarct size was expressed as an infarct size index (percent LV involvement) obtained by adding the percentages of delayed enhancement of every segment divided by 17 (number of LV segments). A myocardial segment was judged as nonquantifiable if delayed enhancement could not be clearly differentiated from the healthy myocardium (i.e., because of breathing artifacts or erroneous electrocardiographic triggering). All CMR measurements were performed independently by 2 observers who were blinded to clinical and procedural characteristics and by a single observer 1 week later. Correlation indexes (r) of transmural necrosis/microvascular obstruction and infarct size index measurements were 0.94 and 0.94 for interobserver variability and 0.96 and 0.96 for intraobserver variability, respectively.

Left ventricular aneurysm was defined by the presence of ≥ 2 akinetic or dyskinetic segments with dilatation in end-diastole; diskynetic areas was defined as regions of the left ventricle with normal dimension in end-diastole and outward systolic movement (102).

To investigate the role of CMR in detection of haemorrhagic AMI (see aim 5. and 6.), we defined severe microvascular damage in the infarct core (SMD) as areas of low or absent signal surrounded by late enhanced tissue (19, 103). To make SMD assessment more reliable and avoid potential mismatch due to equivocal cases or thin subendocardial thrombosis (53), only SMD extended in two adjacent ventricular segments was considered. As for infarct size, we also calculated the SMD score

index obtained by adding the percentages of SMD of every segment divided by 17 (number of LV segments).

As previously described (19), the high signal intensity on T2-weighted were identify as myocardial edema and related to risk area. T2 weighted images were considered abnormal if increased signal was observed within the myocardium; increased signal was defined as a signal intensity greater than the mean signal intensity plus 2SD of normal myocardium. Care was taken to not include the LV cavity, particularly toward the apex and apical level of the LV, where slow flow can lead to increase signal within the LV cavity. Hemorrhagic myocardial infarction was defined by the presence of midmural dark area on T2-weighted images (38, 53,), sourrounded by high signal intesity (15), as showed in our histological findings in humans, extended at least two adjacent ventricular segments.

Echocardiography

Complete M-mode and 2-dimensional echocardiographies were performed with commercially available imaging systems (Sequoia-512, Acuson, Mountain View, California; Sonos 5500, Philips, Andover, Massachusetts). Images were digitally stored onto magnetooptical disks for off-line analysis of LV cavity volumes at end-diastole and end-systole. LV volumes and ejection fraction were measured at baseline and follow-up by echocardiography according to standardized methods (104). LV ejection fraction was calculated as end-diastolic volume minus endsystolic volume divided by end-diastolic volume. LV volumes were expressed as indexes by dividing by body surface area at each time point. LV remodeling was evaluated as change in LV volume and calculated as the difference between end-diastolic volume index at follow-up and at baseline. All echocardiographic measurements were performed independently by 2 observers who were blinded to clinical and procedural characteristics and by a single observer 1 week later. Correlation indexes (r) of LV volume and LV ejection fraction measurements were 0.95 and 0.96 for interobserver variability and 0.96 and 0.97 for intraobserver variability, respectively.

Left ventricular aneurysm was defined by the presence of ≥ 2 akinetic or dyskinetic segments with dilatation in end-diastole; diskynetic areas was defined as regions of the left ventricle with normal dimension in end-diastole and outward systolic movement (105).

Statistical analysis

Data are expressed as mean value ± standard deviation for continuous variables, and as frequency with percentage for categorical variables. Differences between means of continuous variables were tested by the one-way analysis of variance. Frequencies were compared using the chi-square or Fisher exact test analysis when the expected value of cells was <5.

- **Statistical analysis for CMR and influence of duration of ischemia.**
  A logistic regression analysis was used to evaluate the relationship between time to treatment and (patient) CE-MR evidence of TN or SMD and to calculate odds ratios (for each 30-min delay) after adjustment for characteristics related to the ischemic time. The relationships between ischemic time and patient probability of SMD and/or TN at CE-MR were reported as a continuous function. An interobserver and intraobserver concordance of 98% and 99%, respectively, was found in evaluation of TN. In this case, discrepancies were resolved by consensus. By contrast, full agreement was reported for SMD. Comparison of proportions was performed using the chi-square test.
- **Statistical analysis for CMR predictors of remodelling:** Paired Student's *t* test was applied to evaluate differences in end-diastolic volume index and LV ejection fraction between baseline and follow-up. Linear regression analyses were applied to evaluate the relation between the separate prediction variables and end-diastolic volume index, LV ejection fraction at time 0, and/or follow-up. Multiple regression analysis was carried out to quantify the additional value of infarct size index, TN, and SMD to troponin level in the prediction of LV remodeling and LV function at follow-up. The linearity assumption was assessed by examining scatterplots of standardized residuals against standardized predicted values. A normal distribution of the residuals was found (P-P plots of regression standardized residuals) and the mean value of the residuals was 0. We report regression coefficients (B) ± SEs, standardized regression coefficients (β), p values, and model R2 values (percent variance in outcome variable explained by prediction variable). Linear regression analysis was used to determine intra- and interobserver variabilities. Logistic regression analysis was used to find independent

predictors of adverse remodeling (>20% increase in end-diastolic volume index from baseline to follow-up).7,8 Receiver-operating characteristic curve analysis was performed to establish the diagnostic accuracy of the number of LV segments with transmural necrosis as a predictor of ≥ 20% remodeling. All significance was accepted at $p < 0.05$.

- **Statistical analysis for CMR and use of** A**bciximab**. Both univariate and multivariate logistic regression analyses were used to identify potential predictors of SMD. Relationships between the number of left ventricular (LV) segments with transmural necrosis and patient probability of severe microvascular obstruction at DE CMR, according to whether abciximab was used or not are reported as a continuous function.
- **Statistical analysis for ECG-CMR correlations.** The association between persistent STE and the potential independent predictors at ce-CMR analysis was assessed using logistic regression analysis. Variables appearing statistically significant at univariate analysis were included in the multivariate analysis. In particular, the following variables have been included: infarct size index; presence of transmural necrosis; presence of microvascular damage; pain-to-balloon time; sum of ST-elevation at baseline; sum of ST-elevation post-PCI; final myocardial blush grade.
- **Statistical analysis for CMR and relationship with angiographic parameters.**

  Reproducibility of the MBG grading and staining assessment was evaluated by rewieving a random sample of patients a second time. For this purpose 50 coronary angiograms and ventriculograms were rewieved by an experienced independent observer without access to clinical data, and the intraobserver and interobserver percentages of agreement in MBG grading and stain detection were recorded. An interobserver and intraobserver concordance of 95% and 90%, respectively, was found in evaluation of MBG. Moreover, reproducibility of visual assessment of staining was good, with high interobserver and intraobserver agreement, 88% and 95% respectively. In both cases, discrepancies were resolved by consensus. An interobserver and intraobserver concordance of 98% and 99%, respectively, was found in evaluation of TN. In this cases, discrepancies were resolved by consensus. By contrast, full agreement was reported for SMD.

- **Statistical analysis for CMR and haemorrhagic AMI evaluation.** About T2 scans, an interobserver and intraobserver concordance of 88% and 92% respectively, was found in evaluation of hypoenhanced midmural dark area suggesting hemorrhage in the myocardial infarct. In this case, discrepancies were resolved by consensus. Evaluating post-contrast images, an interobserver and intraobserver concordance of 98% and 99% respectively, was found in evaluation of transmurality. In this case, discrepancies were resolved by consensus. By contrast, full agreement was reported for SMD. For hystological correlation, analysis was performed independently for the histopathologic and CMR studies, with the researchers for histopathology blinded to the CMR results and vice versa. Linear regression was used to compare the extent of MI and hemorrhage on T2 ex vivo CMR and pathology.

Comparison of proportions were performed using the chi-square test. Data were analysed by SPSS 13 for Windows (SPSS Inc., Chicago, Illinois).

RESULTS

The Results are here explained to avoid the indications of pre-specified aims for subgroups of patients.

1. The relationship between duration of ischemia and both myocardial transmural necrosis and severe microvascular obstruction. Estimation of the risk of transmurality and severe microvascular obstruction with the duration of ischemia.

For this aim we evaluated the first 77 patients enrolled, without previous infarction: clinical and procedural characteristics are summarized in Table 1. The mean time to treatment was 190 ± 111 min. Thirteen (17%) patients already had a TIMI flow grade 3 at the index angiography before the primary PCI. Myocardial blush grade (MBG) 2 or 3 was observed in 55 subjects (70%). Collateral circulation (Rentrop 2 or 3) was present only in two patients. Fifty patients (65%) had CMR evidence of TN, and 25 (32%) of SMD.

The presence of MBG 0/1, TN, and SMD in patients with or without TIMI flow grade 3 is summarized in Table 2. Despite a similar delay in time to treatment between the two groups, the percentages of patients with TN and SMD, as well as the levels of troponin I release, were significantly higher in patients with TIMI flow grade < 3. A similar trend, although not yet statistically significant, was observed for MBG 0/1. When only patients with TIMI flow grade < 3 were considered, pain to balloon time (reasonably the expression of the ischemic time in these patients) and peak troponin I levels were positively correlated with the presence of TN and SMD. In fact, the pain to balloon time was progressively longer and troponin I release was progressively greater in patients with both TN and SMD compared with those with TN but not SMD, and those with neither TN nor SMD (Table 3). Three typical examples of TN and/or SMD detected by CE-MR are shown in Figure 1. Among demographic, clinical, and angiographic characteristics of these patients (Table 4), the only variables significantly related to the ischemic time were abciximab use (abciximab, 136 ± 41 min vs. no abciximab, 205± 120 min, p = 0.03) and MBG 2/3 (MBG 2/3, 160 ± 93 min vs. no MBG 0/1, 233 ± 116 min, p = 0.01). By contrast, age was not related to the ischemic time, even when analyzed as a continuous variable (p = 0.8). After adjustment for these confounders, patients with TIMI flow

grade < 3 showed, for each 30-min delay in reperfusion, the increase of both TN (odds ratio per 30 min,1.37; 95% confidence interval, 1.03 to 1.8; p = 0.032), and SMD (odds ratio per 30 min, 1.21; 95% confidence interval, 1.03 to 1.4; p = 0.021). Figure 2 illustrates the relation among time to reperfusion and (patient) probability of TN and/or SMD as continuous functions. Total ischemic time was closely correlated with CE-MR evidence of TN and SMD. In addition, a close correlation was observed between the presence of SMD and the evidence of TN at CMR (chi-square = 6.2, p = 0.01), with SMD always detected in association with TN.

Table 1. Patients characteristics

Characteristics	Value
Age (years)	60 ± 11.5
Men, n (%)	65 (84)
Current Smoker, n (%)	41 (53)
Hypertension, n (%)	38 (49)
Diabetes mellitus, n (%)	7 (9)
Previous angina pectoris, n (%)	19 (25)
Previous coronary angioplasty, n (%)	4 (5)
Previous coronary bypass, n (%)	0
Location of myocardial infarction:	
Anterior n (%)	39 (51)
Inferior, n (%)	35 (46)
Pain to balloon time, minutes	190 ± 111
Pre TIMI 3 flow, n (%)	13 (17)
MBG 2-3, n (%)	55 (71)
Abciximab, n (%)	16 (20)
Stent, n (%)	72 (95)
Troponin I, μg/L	91 ± 90
Left ventricular ejection fraction (%)	59 ± 14
CE-MR image of TN, n (%)	50 (65)
CE-MR image of SMD, n (%)	25 (32)

Data are presented as mean value ± SD or number (%) of patients in group.
TN= transmural necrosis. SMD= Severe microvascular damage.

Table 2. Percentage of myocardial blush grade 2/3, transmural necrosis and severe microvascular obstruction in patients according to TIMI flow grade at index angiography.

	TIMI <3	TIMI 3	p Value
Patients, n	64	13	
Time to treatment, minutes	190 ± 110	189 ± 110	0.97
MBG 0/1, n (%)	20 (31)	2 (15)	0.1
TN, n (%)	45 (65)	5 (38)	0.036
SMD, n (%)	23 (39)	2 (15)	0.045
Peak of Troponin I, ug/L	101 ± 96	41 ± 60	0.042

Data are presented as mean value ± SD, or number (%) of patients in group. MBG= myocardial blush grade.

Table 3. Ischemic time and enzymatic data according to the CE-MR evidence of TN and /or SMD in patients without TIMI 3 of infarct related artery at index angiography.

	TN-/SMD-	TN+/SMD-	TN+/SMD+
Patients, n (%)	19 (29.7)	22 (34.4)	23 (35.9)
Time to treatment, minutes*	90 ± 40	177 ± 101	255 ± 145
Peak of Troponin I, ug/L†	53 ± 50	110 ± 107	137 ± 97

Data are presented as mean value ± SD, or number (%) of patients in group. + means presence; - means absence. TN= transmural necrosis. SMD= Severe microvascular damage. Univariate P values among subgroups; * p=0.001, †p=0.01.

Table 4. Patients characteristics and ischemic time

Variables	Yes	No	p Value
Age >70 years	163 ± 78	198 ± 118	0.3
Male gender	189 ± 117	198 ± 83	0.8
Diabetes	177 ± 99	192 ± 114	0.7
Hypertension	203 ± 120	179 ± 102	0.3
Current smoker	207 ± 133	172 ± 78	0.2
Anterior infarction	201 ± 124	98 ± 16	0.5
Abciximab	136 ± 41	205 ± 120	0.03
MBG 2/3	160 ± 93	233 ± 116	0.01

Data are presented as mean value ± SD.

Figure 1. Typical examples of the different myocardial alterations detected by CE-MR in patients undergoing primary PCI at increasing time delay from the onset of the chest pain.

Patient A Patient B Patient C Patient D

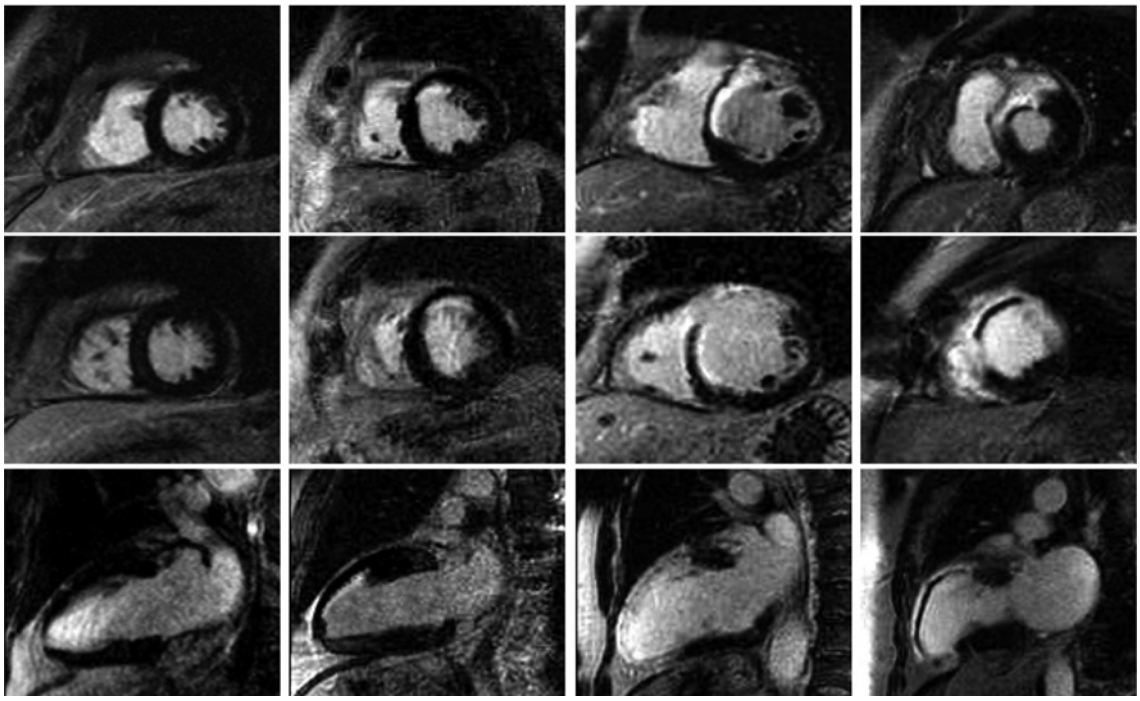

Upper, middle and lower panels respectively show CE-MR images obtained at 2 different short axis levels and in long axis two-chamber plane.

-Patient A: male, aged 76; hypertension, history of smoke, dislipidemia, familiarity of coronary artery disease; ECG evidence of anterior ST elevation myocardial infarct; pain to balloon time: 70 minutes; Troponin I peak: 11.7 ng/ml. After 6 days from acute event, no signs of necrosis are shown at the late contrast enhancement CMR ("aborted" infarct).

-Patient B: male, aged 49, hypertension, familiarity of coronary artery disease; ECG evidence of anterior AMI; pain to balloon time: 170 minutes; Troponin I peak: 38.6 ng/ml. After 6 days from acute event, CMR shows a non transmural necrosis in the middle and apical segments of the anterior wall.

-Patient C: male, aged 78, hypertension; ECG evidence of antero-septal AMI; pain to balloon time: 240 minutes; Troponin I peak: 199 ng/ml. After 8 days from acute event, CMR shows a transmural necrosis of the entire anterior wall and of the apical segment of the inferior wall.

-Patient D: female, aged 73; no cardiovascular risk factor; ECG evidence of septal, anterior and inferior AMI; pain to balloon time: 310 minutes; Troponin I peak: 258 ng/ml. After 7 days from acute event, CMR shows a transmural necrosis of the antero-lateral, anterior and septal wall. In the same area of the infarct, there is evidence of a sub-endocardial dark zone referred as to severe microvascular obstruction.

Figure 2 Relationship between ischemic time and in hospital (patient) probability of TN or SMD assessed with logistic regression model. The coefficients of both the equations have been computed for 30 minutes intervals. Black dots represent observed TN rate expressed in number (percent). White dots represent observed SMD rate expressed in number (percent).

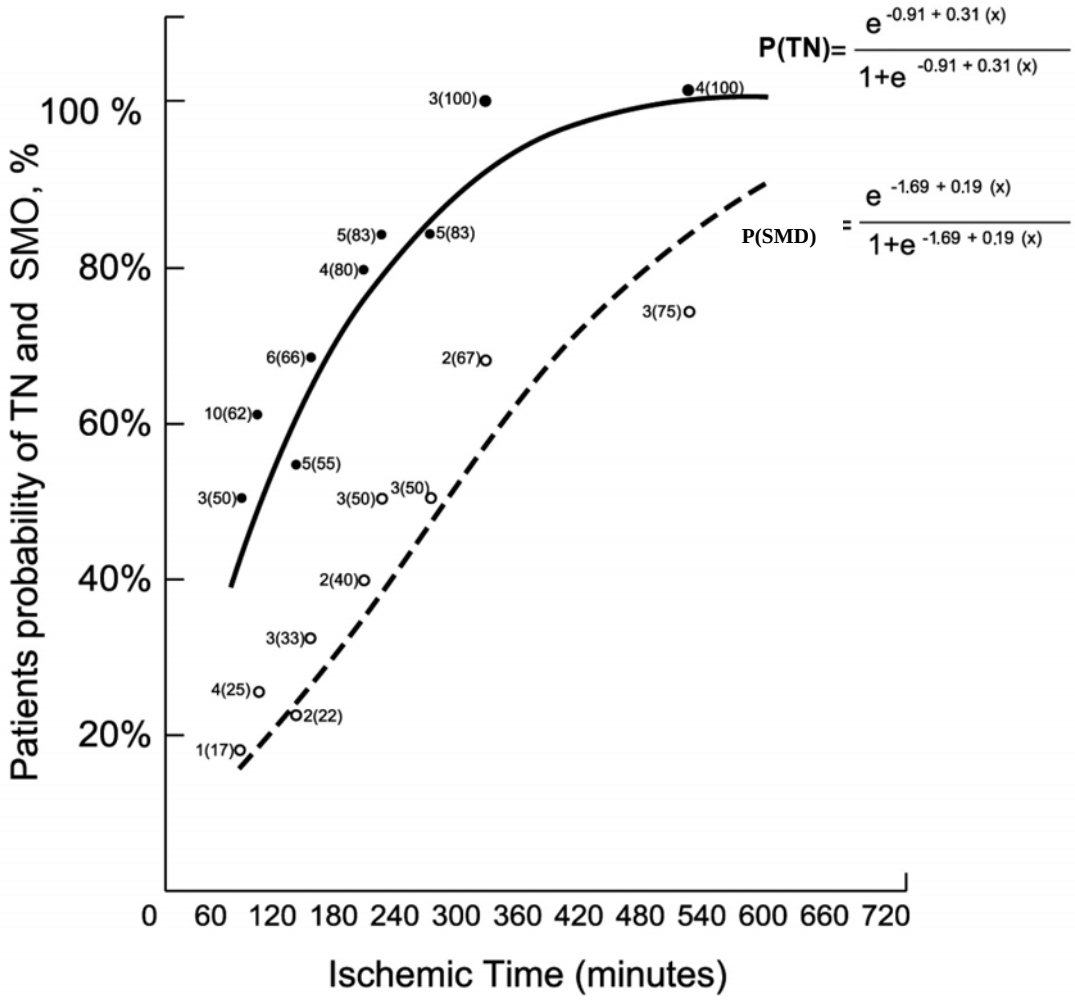

2. The assessment of the predictive value of myocardial/microvascular injury by delayed-enhanced CMR on LV remodeling and LV ejection fraction after PCI compared to peak troponin level (an established index of myocardial infarct size)

For this aim we excluded previous AMI, infarct-related artery stenosis < 50% with Thrombolysis In Myocardial Infarction grade 3 flow at index angiography, clinical signs of cardiogenic shock during the first week after infarction, significant other cardiac and/or lifelimiting noncardiac diseases. Of the 85 patients, 3 died in the hospital, 1 was excluded because of inadequate echocardiographic image quality, and 2 refused the CMR study. Final population included 76 patients. Patients' clinical and procedural characteristics are presented in Table 5. Mean time to treatment was 200 ± 120 minutes. Collateral circulation (Rentrop class 2/3) was present in only 3 patients. Transmural extent of delayed enhancement was evaluated in 1,257 LV segments. Thirty-five segments (2.8%) were not assessable due to poor image quality. Severe microvascular obstruction was always detected within LV segments with transmural extent of delayed enhancement. Transmural necrosis and severe microvascular obstruction were present in 2.9 ± 2.6 and 1.15 ± 1.9 of LV segments, respectively. Fifty-four patients (71%) had CMR evidence of transmural necrosis in ≥ 1 LV segment, whereas 28 (36%) showed severe microvascular obstruction. The average calculated infarct size index was 24 ± 14%. The end-diastolic volume index increased from 64 ± 15 to 75 ± 24 ml/m^2 at follow up (p = 0.001). LV ejection fraction remained unchanged from 51 ± 7% to 50 ± 11% at follow up (p = 0.6). The end-systolic volume index increased from 32 ± 8 to 38 ± 8 (p = 0.001). During follow-up, there was no significant variation in dosage and type of medication; only 2 patients discontinued β-blocker therapy due to severe bradycardia and 1 decreased the dosage of the angiotensin-converting enzyme inhibitor because of hypotension. At univariate regression analysis, the number (per patients calculated) of LV segments with transmural necrosis was significantly related to changes and absolute value of the end-diastolic volume index at follow-up (R2 = 0.37 and 0.51, respectively). Similar relations were observed for the calculated number of LV segments with severe microvascular obstruction (R2 = 0.22 and 0.34); for the infarct size index, the R2 values were 0.26 and 0.42, respectively, and for troponin peak level, the R2 values were 0.25 and 0.36,

respectively (Figure 3). Transmural necrosis, severe microvascular obstruction, infarct size index, and troponin I peak level were also significantly related to changes in LV ejection fraction and LV ejection fraction absolute value at follow-up; the number of LV segments with transmural necrosis produced R2 values of 0.37 and 0.47, respectively, and the number of LV segments with severe microvascular obstruction produced R2 values of 0.24 and 0.19, respectively. The R2 values for the infarct size index were 0.32 and 0.49, and those for troponin I peak level were 0.28 and 0.48, respectively (Figure 4). Peak troponin I concentrations were significantly correlated with the calculated infarct size index ($r = 0.74$, $p < 0.001$). Results of hierarchical multiple regression analyses are listed in Tables 6 and 7). With all prediction variables in the model, only transmural necrosis and troponin peak level were independent predictors of changes (compared with baseline) and absolute values at follow-up of the end-diastolic volume index and LV ejection fraction. With respect to troponin peak level, however, the number of LV segments with transmural necrosis added to predicting LV remodeling. The number of LV segments with transmural necrosis improved the prediction of end-diastolic volume index changes and end-diastolic volume index absolute value at follow-up (R2 for change = 0.19 and 0.22, respectively) and, to a lesser extent, the prediction ofthe LV ejection fraction changes and LV ejection fraction absolute value at follow-up (R2 for change = 0.16 and 0.15, respectively). Twenty-eight patients (37%) showed an adverse remodelling at follow-up, which was defined as a ≥ 20% increase in end-diastolic volume index from baseline. Beta blockers were equally distributed in patients with and without remodeling. In those subjects, only the number of LV segments with transmural necrosis remained an independent predictor of LV remodeling (odds ratio 1.7, 95% confidence interval 1.3 to 2.3, $p < 0.0001$), whereas troponine I peak level lost its predictive power ($p = 0.4$). By receiver-operating characteristic curve analysis, 4 LV segments with transmural necrosis at CMR showed better sensitivity (0.70) and specificity (0.82) for major adverse LV remodeling. The area under the receiver-operating characteristic curve was 0.80 (95% confidence interval 0.70 to 0.92). Extent of coronary artery disease was not related to LV remodeling. Ten patients (13%) with spontaneous Thrombolysis In Myocardial Infarction grade 3 flow before PCI had fewer LV segments with transmural necrosis (1.2 ± 1.4 vs 3.5 ± 2.6, $p = 0.028$), smaller infarcts (troponin I peak level 42 ± 42 vs 88 ± 70 ng/ml, $p = 0.03$; infarct size index 11 ± 9% vs 26 ±

14%, p = 0.01), better LV remodeling (enddiastolic volume index changes -6 ± 13 vs 15 ± 23, p = 0. 02) and LV global function (LV ejection fraction changes 9 ± 5% vs 2 ± 7%, p = 0.004), and decreased major adverse remodeling (end-diastolic volume index changes ≥ 20% vs 10% vs 40%, p = 0.05).

Table 5. Patients characteristics

Characteristics	Value
Age (years)	60 ± 11.5
Men, n (%)	62 (81)
Current Smoker, n (%)	43 (57)
Hypertension, n (%)	38 (49)
Diabetes mellitus, n (%)	6 (8)
Previous angina pectoris, n (%)	11 (14)
Previous coronary angioplasty, n (%)	4 (5)
Previous coronary bypass, n (%)	0
Location of myocardial infarction:	
Anterior n (%)	46 (60)
Pain to balloon time, minutes	200 ± 120
Multivessel coronary artery disease	28 (37)
TIMI grade 3 flow before procedure	10 (13)
Myocardial blush grade 2-3	60 (78)
Abciximab, n (%)	16 (21)
Stent, n (%)	76 (100)
Troponin I, µg/L	75 ± 79
ACE inhibitors	70 (92)
B-blockers	55 (72)
Clopidogrel	76 (100)
Statin	76 (100)
Aspirin	76 (100)

Data are presented as mean value ± SD or number (%) of patients in group.
TN= transmural necrosis. SMO= Severe microvascular obstruction.

Figure 3. Univariate regression analysis showing correlations between (A to D) changes (compared with baseline) or (E to H) absolute value at follow-up of end-diastolic volume index and (A, E) number of LV segments with transmural necrosis, (B, F) infarct size index, (C, G) number of LV segments with SMD, and (D, H) troponin peak level. ΔEnd-diastolic volume index = changes (compared with baseline) in end-diastolic volume index.

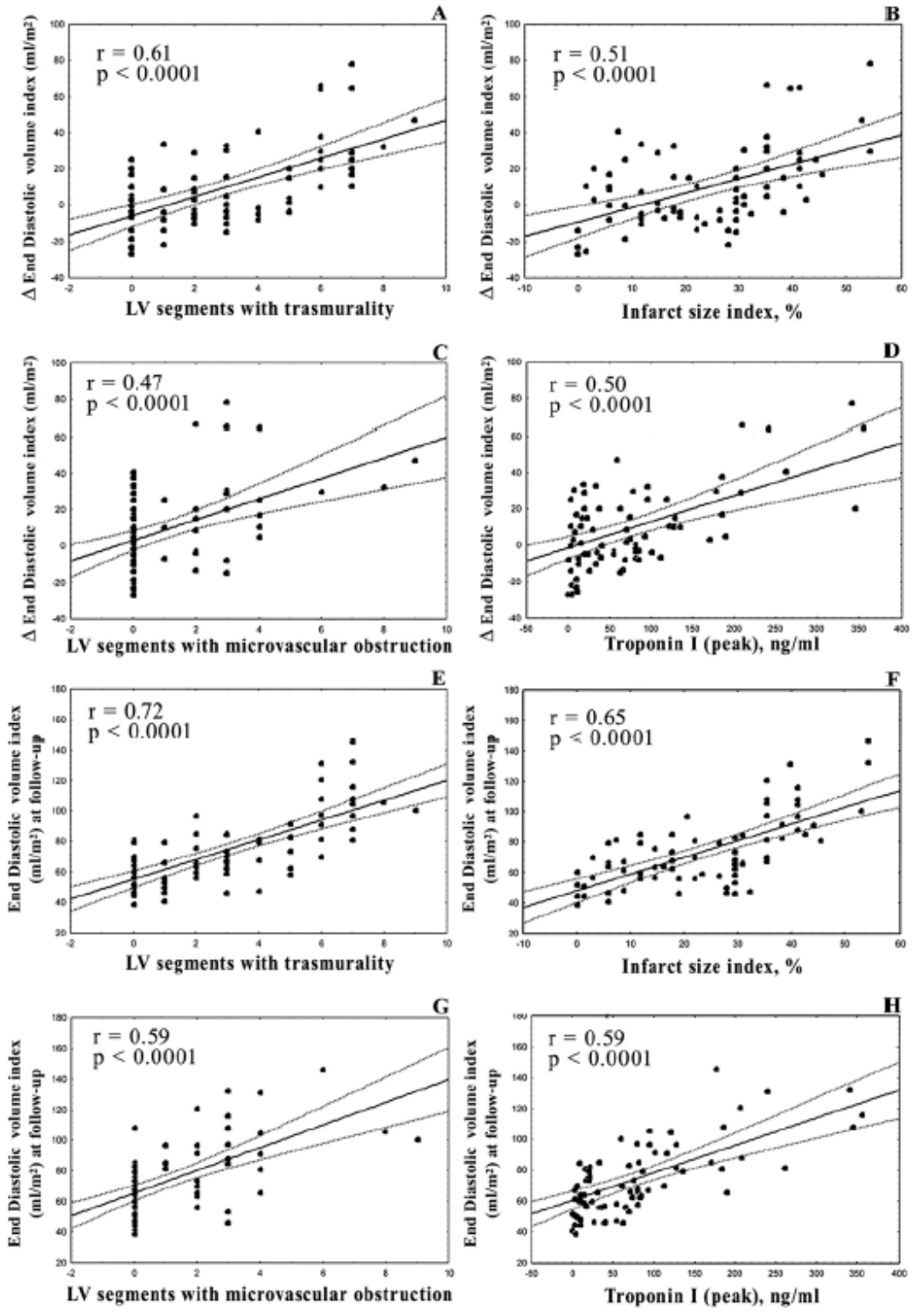

Figure 4. Univariate regression analysis showing correlations between (A to D) changes (compared with baseline) or (E to H) absolute value at follow-up of LV ejection fraction and (A, E) number of LV segments with transmural necrosis, (B, F) infarct size index, (C, G) number of LV segments with SMD, and (D, H) troponin peak level. ΔLVEF = changes (compared with baseline) in LV ejection fraction.

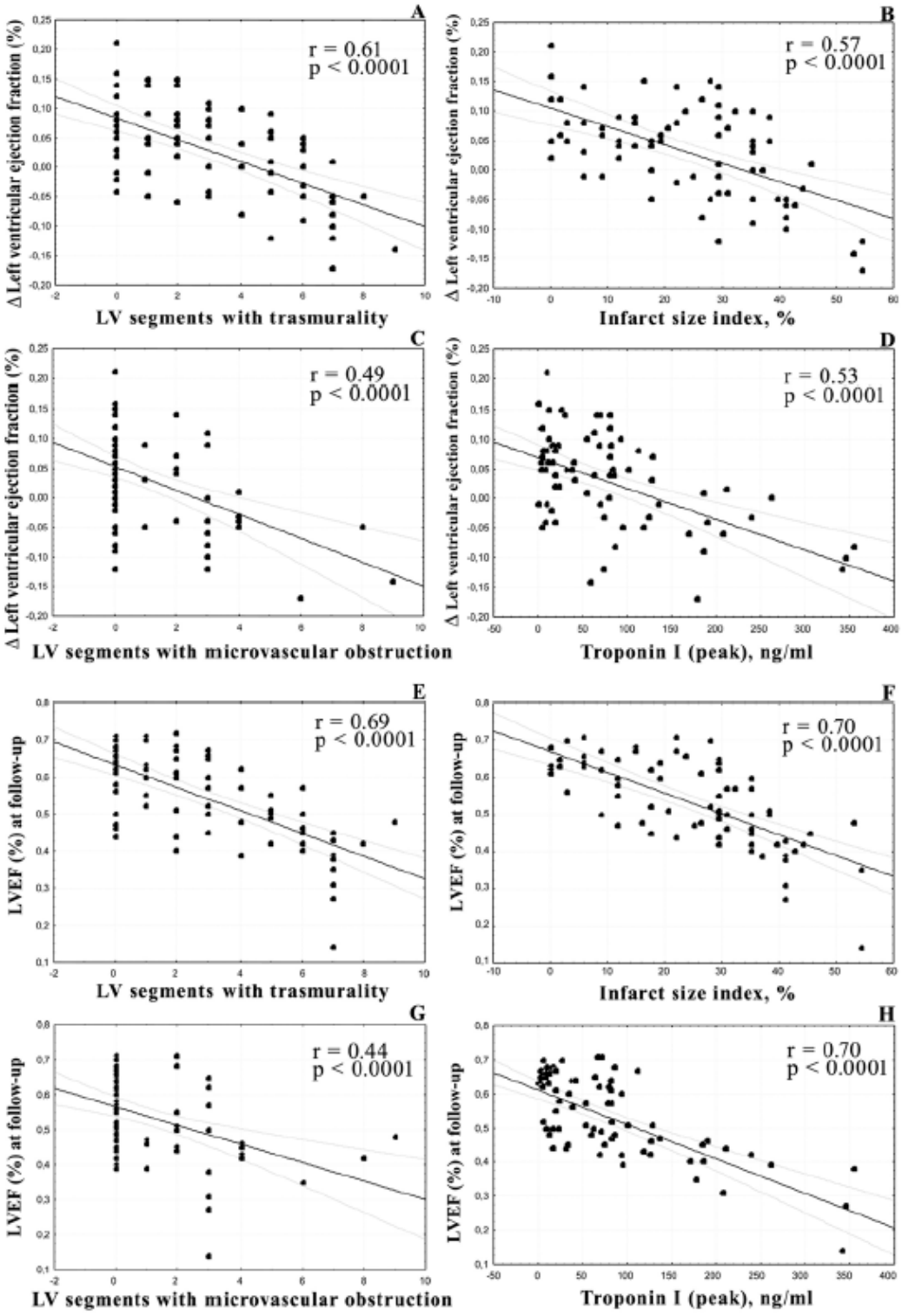

Table 6. Multiple linear regression analysis according to different models of correlations between changes or absolute value at follow-up of end-diastolic volume index with transmural necrosis, severe microvascular obstruction, and infarct size.

	ΔEnd-Diastolic Volume Index				End-Diastolic Volume Index at Follow up			
	B ± SE	β	p Value	R^2	B ± SE	β	p Value	R^2
Model 1								
Troponin I (peak)	0.09 ± 0.03	0.30	0.01	0.34	0.09 ± 0.03	0.32	0.0001	0.54
LV segments with severe microvascular obstruction	2.80 ± 1.5	0.23	0.06		3.30 ± 1.26	0.26	0.01	
Infarct size index	0.29 ± 0.22	0.18	0.16		0.53 ± 0.18	0.32	0.007	
Model 2								
Troponin I (peak)	0.06 ± 0.03	0.22	0.04	0.44	0.08 ± 0.03	0.28	0.002	0.64
LV segments with severe microvascular obstruction	1.5 ± 1.39	0.13	0.27		2.64 ± 1.26	0.21	0.04	
LV segments with transmural necrosis	3.50 ± 1	0.41	0.002		3.92 ± 0.18	0.44	<0.0001	
Model 3								
Troponin I (peak)	0.07 ± 0.03	0.24	0.03	0.44	0.08 ± 0.027	0.26	0.006	0.64
LV segments with severe microvascular obstruction	1.79 ± 1.45	0.15	0.22		2.42 ± 1.24	0.19	0.055	
Infarct size index	--0.16 ± 0.26	--0.1	0.54		0.14 ± 0.22	0.40	0.58	
LV segments with transmural necrosis	4.00 ± 1.39	0.46	0.005		3.47 ± 1.19	0.08	0.004	

Table 7. Multiple linear regression analysis according to different models of correlations between changes or absolute value at follow-up of left ventricular ejection fraction with transmural necrosis, severe microvascular obstruction, and infarct size index

	Δ LV Ejection Fraction				LV Ejection Fraction at Follow up			
	B ± SE	β	p Value	R^2	B ± SE	B	p Value	R^2
Model 1								
Troponin I (peak)	0.0001 ± 0.0001	--0.26	0.03	0.41	--0.001 ± 0.0001	--0.41	<0.001	0.59
LV segments with severe microvascular obstruction	--0.01 ± 0.005	--0.20	0.08		0.0001 ± 0.006	--0.006	0.95	
Infarct size index	0.002 ± 0.001	--0.29	0.05		--0.004 ± 0.0001	--0.44	<0.001	
Model 2								
Troponin I (peak)	0.0001 ± 0.0001	--0.26	0.04	0.44	--0.001 ± 0.0001	--0.45	<0.001	0.62
LV segments with severe microvascular obstruction	--0.006 ± 0.005	--0.15	0.27		0.002 ± 0.006	--0.02	0.78	
LV segments with transmural necrosis	--0.01 ± 0.004	--0.38	0.002		--0.02 ± 0.006	--0.45	<0.001	
Model 3								
Troponin I (peak)	0.0001 ± 0.0001	--0.25	0.037	0.44	--0.001 ± 0.0001	--0.39	<0.001	0.63
LV segments with severe microvascular obstruction	--0.006 ± 0.005	--0.14	0.25		0.004 ± 0.006	--0.06	0.52	
Infarct size index	0.0001 ± 0.001	--0.06	0.71		--0.002 ± 0.0001	--0.22	0.18	
LV segments with transmural necrosis	--0.01 ± 0.005	--0.35	0.034		--0.01 ± 0.006	--0.01	0.01	

3. The evaluation of pathological basis of persistence of ST-segment elevation after myocardial infarction, traditionally ascribed to left ventricular aneurysm development: we studied the myocardial structural abnormalities underlying persistent ST-segment elevation, using contrast enhanced-magnetic resonance imaging.

Persistent STE was observed in 11 of 40 patients (27.5%). The last ECG was recorded at 8.6 ± 2.1 days after the revascularization in the STE persistence group and at 7.2 ± 2.5 days in the STE resolution group (p = 0.8).

No differences about cardiovascular risk factors have been proven between the two groups (Table 8).Patients with persistent STE showed a trend toward a longer pain-to-balloon time (361.4 ± 241.6 vs 229.9 ± 179.1, p=0.06) (Table 8), larger sum of STE and higher number of leads showing STE at baseline ECG, than

Table 8. Baseline characteristics

	STE persistence n = 11 (27.5%)	STE resolution n = 29 (72.5%)	p Value
Age (years)*	58.3 ± 10.7	58.6 ± 12.7	0.94
Male	9 (81.8%)	14 (86.2%)	1.0
Hypertension	4 (36.4%)	14 (48.3%)	0.72
Hypercolesterolemia	3 (27.3%)	13 (44.8)	0.47
Diabetes	2 (18.2%)	3 (10.3%)	0.60
Current smokers	7 (63.6%)	16 (55.2%)	0.73
LVEF (%)*	54.1 ± 13.9	53.8 ± 15.6	0.84
LVEDVI, ml/m^2*	63.5 ± 9.0	74.2 ± 24.3	0.18
Baseline TIMI flow 0/1	8 (72.7%)	22 (75.8%)	0.49
Pain-to-balloon time (min)*	361.4 ± 241.6	229.9 ± 179.1	0.06
Stent	9 (81.8%)	27 (93.1%)	0.30
Final TIMI flow 2/3	9 (81.8%)	27 (96.4%)	0.19
Final MBG 2/3	5 (45.4%)	22 (75.8%)	0.02
Abciximab	5 (45.4%)	12 (41.4%)	0.10
TnI (mcg/L)*	146.5 ± 114.4	107.4 ± 103.0	0.30

data are expressed as number (%) of patients or *means ± standard deviation
LVEDVI = left ventricular end-diastolic volume index at baseline angiography. LVEF = left ventricular ejection fraction at baseline angiography. MBG = myocardial blush grade. STE = ST-segment elevation. TIMI = Thrombolysis In Myocardial Infarction. TnI = Troponin I.

patients in STE resolution group (Table 9). Interestingly, at the end of the revascularization procedure, patients in the STE persistence group showed worse Myocardial Blush and lower reduction in ST-segment than patients in the STE resolution group (Table 8 and Table 9, respectively). Moreover, at ECG, both the presence of Q-waves and number of leads exhibiting Q-waves were significantly greater in the STE persistence group than in the STE resolution group, either at admission or at pre-discharge ECG (Table 9). Patients in the persistent STE group showed an higher peak of TnI (146.5 ± 114.4 vs 107.4 ± 103.0), although the difference did not result statistically significant (p=0.30). No differences about use of Abciximab or stent positioning have been highlighted, the same for left ventricle function valued at pre-discharge echocardiography (Table 8).

Table 9. Electrocardiographic findings

	STE persistence n = 11 (27.5%)	STE resolution n = 29 (72.5%)	P Value
Admission ECG			
ST sum, mm*	21.2 ± 12.4	10.0 ± 9.8	0.005
ST leads, number*	5.4 ± 1.1	3.6 ± 1.7	0.003
Q waves†	9 (81.8%)	12 (41.4%)	0.02
Q waves, number of leads*	2.5 ± 1.8	0.8 ± 1.1	0.001
Post-PCI ECG			
ST sum, mm*	11.2 ± 10.2	2.2 ± 3.3	0.001
ST leads, number*	4.0 ± 1.6	1.5 ± 1.8	< 0.0001
Pre-discharge ECG			
ST sum, mm*	8.4 ± 4.9	1.1 ± 1.4	<0.0001
ST leads number*	4.2 ± 1.4	1.0 ± 1.3	<0.0001
Q-waves discharge†	10 (90.9%)	14 (48.3%)	0.03
Q-waves number of leads*	3.1 ± 1.6	1.5 ± 1.5	0.04

*data are expressed as mean ± sd; †data are expressed as number (frequency value). ECG = elettrocardiogram; PCI = Percutaneous Coronary Intervention; STE = ST-segment elevation.

At CMR, performed at 6.6 ± 2.1 and at 6.2 ± 2.5 days after revascularization in the STE persistence group and STE resolution group, respectively, the patients in STE persistence group had greater Infarct Size Index and more often Transmural Necrosis than those in the STE resolution group (Figure 5: Panel A and B). Furthermore, the number of myocardial segments showing transmural necrosis was higher in the STE persistence than in the STE resolution group: 5.4 ± 2.4 vs 3.06 ± 2.87 respectively; p = 0.02 (Figure 6). Persistent microvascular damage was detected in 81.8% patients in the STE persistence group and in 27.6% of patients without STE (Figure 5: Panel C). Likewise, the number of myocardial segments exhibiting persistent microvascular damage was significantly higher in the STE persistence group: 3.45 ± 2.80 vs 0.93 ± 1.51; p < 0.001. Interestingly, left ventricular aneurysm was seen more often in patients with STE, even tough this difference was not statistically significant (Figure 5: Panel D); the presence of dyskinesia in one or more segments of the left ventricular wall was not statistically different between the two groups (60.0% vs 35.7%, p = 0.27).

Figure 5. Differences in Infarct Size Index (Panel A) and presence of Transmural Necrosis (Panel B), Persistent Microvascular Damage (Panel C) and Left Ventricular Aneurysm (Panel D),between STE persistence group (solid bar) and STE resolution group (open bar).STE = ST-segment elevation

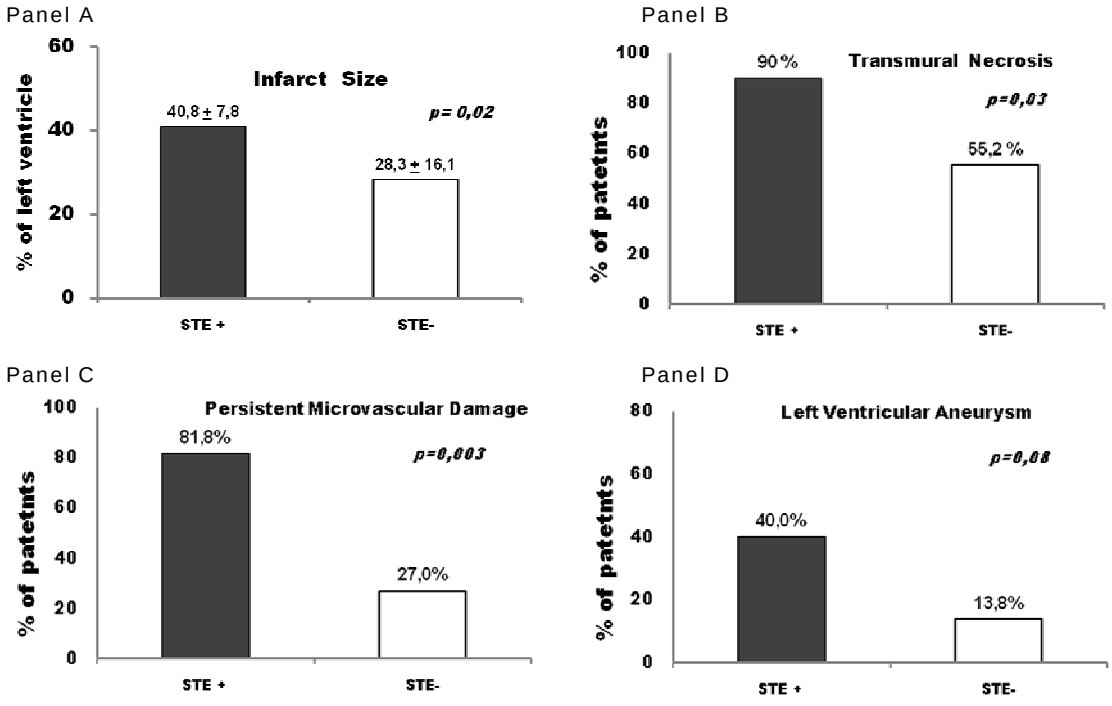

Figure 6. Extent of Infarct Size Index (Panel A), Transmural Necrosis (Panel B), and Persistent Microvascular Damage (Panel C) in STE persistence group (STE +) (solid bar) and STE resolution group (STE -) (open bar), according to the presence of LVA. § p = 0.01 versus STE+/LVA+ and STE+/LVA- group;* p = 0.05 versus STE+/LVA+ and STE+/LVA- group; ‡ p = 0.05 versus STE+/LVA+ and p = 0.02 versus ST+/LVA- group. All others comparisons were not statistically significant. LVA = left ventricular aneurysm; STE = ST-segment elevation.

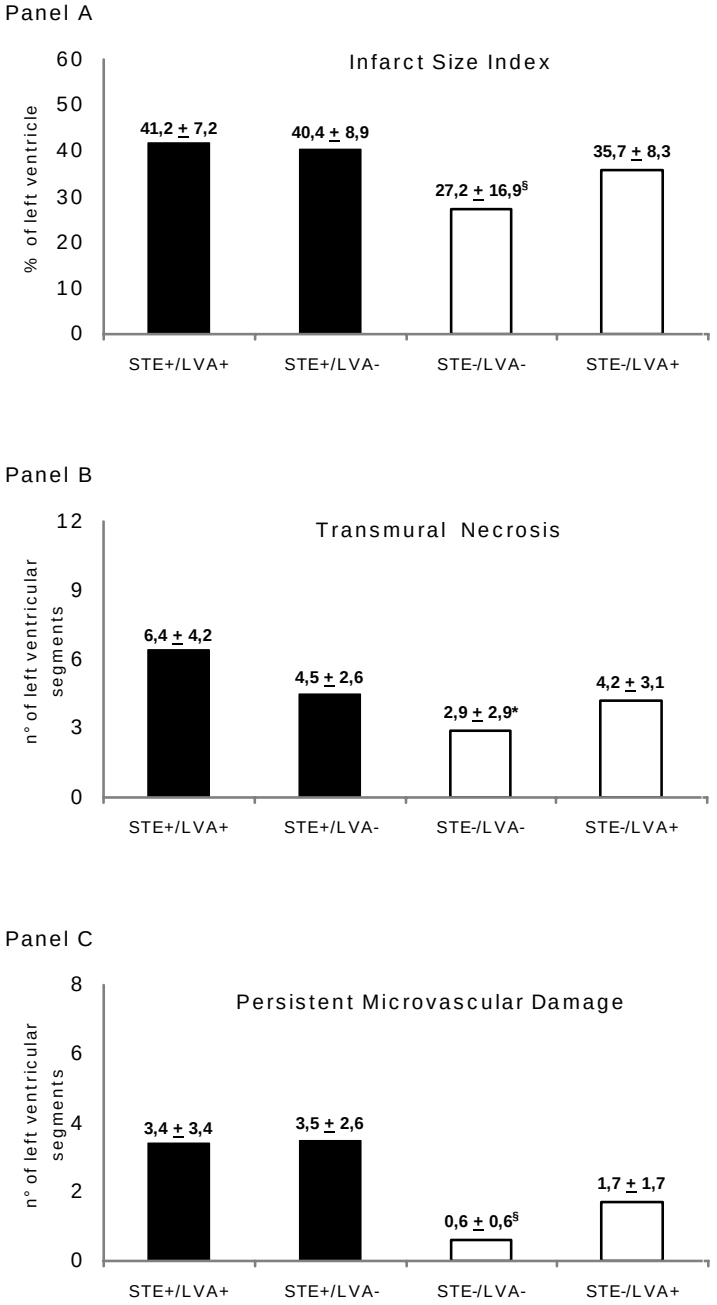

Logistic regression analysis (Table 10) identified the presence of persistent microvascular damage and the sum of STE on admission ECG as independent predictors of STE persistence: OR 3.13, CI 1.21-8.10, p = 0.01; OR 1.13, CI 1.02 – 1.25, p = 0.02, respectively.

Table 10. Logistic Regression Analysis. Determinants of persistence of ST-segment elevation

	OR	CI	P Value
Infarct size index	1.14	0.96-1.36	0.128
TN presence	0.013	0.00-0.02	0.99
PMD presence	3.13	1.21 – 8.10	0.01
Pain-to-balloon time	0.99	0.98-1	0.45
ST-segment sum at baseline	1.13	1.02 – 1.25	0.02
ST-segment sum post-PCI	1.4	1.06-1.86	0.06
Myocardial Blush Grade	0.25	0.69 – 0.88	0.68

TN = transmural necrosis
PMD = persistent microvascular damage.

An example of different patterns of myocardial abnormalities detected by ce- CMR and corresponding ECG before discharge is shown in Figure 7.

Figure 7. Different patterns of myocardial abnormalities detected by DE CMR and corresponding 12-leads ECG before discharge are shown.
Panel A: pre-discharge electrocardiogram shows pathological q-waves in leads V1-V2; the corresponding DE CMR shows transmural necrosis (white arrows) of the septum, anterolateral wall (mid-apical segments) and apex, without evidence of persistent microvascular damage in the setting of necrotic core and without left ventricular aneurysm.
Panel B: ECG shows pathological q-waves in leads V1 through V4, and STE in leads V1 through V4; the corresponding DE CMR shows the presence of transmural necrosis (white arrows) of the septum and anterior wall (mid-apical segments) and of the apical segments of inferior wall, with evidence of persistent microvascular damage (black arrows), without left ventricular aneurysm.
Panel C: ECG shows q-waves in leads V1 through V3, and STE in leads V1 through V5; the corresponding DE CMR shows a large transmural necrosis (white arrows) in the septum and anterolateral wall (mid-apical segments), and of the apical segments of inferior wall, with evidence of persistent microvascular damage in the necrotic core (black arrows), with a large left ventricular aneurysm.

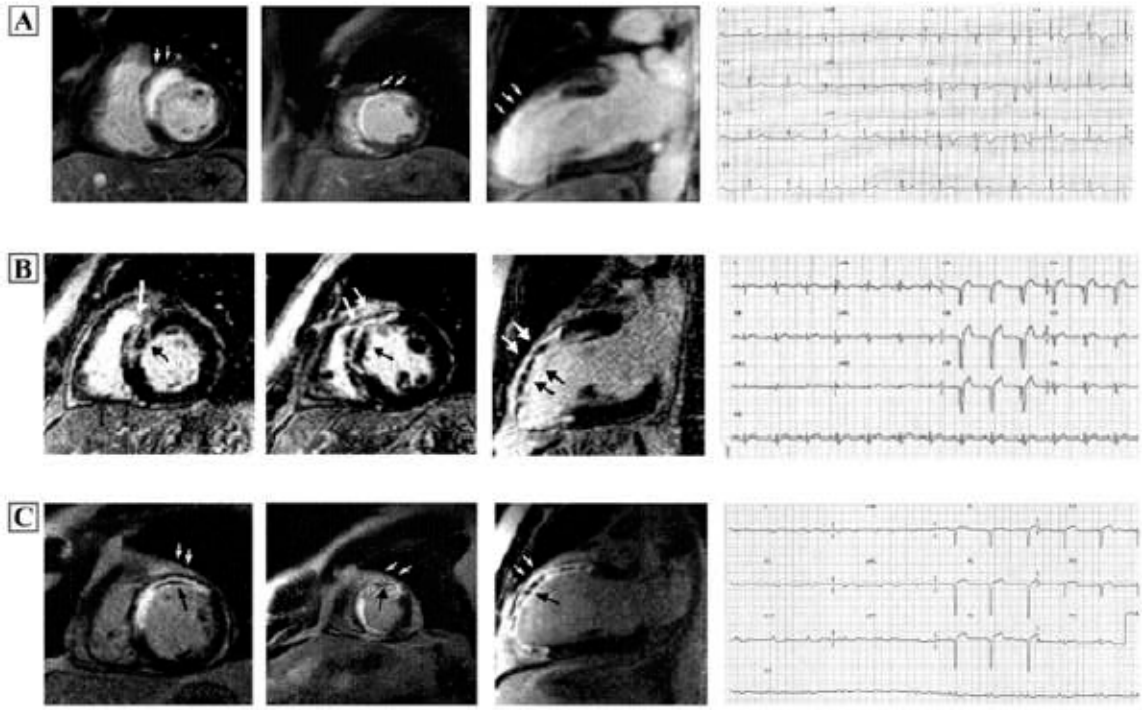

Occurrence of death, non-fatal reinfarction, stroke, target vessel revascularization, and severe bleeding during the hospitalization was not statistically different between the two groups (Table 11). One patient in the STE persistence group died because of cardiac free wall rupture, and one patient in the STE resolution group died because of refractory pump failure after re-infarction due to stent thrombosis. Non-fatal re-infarction occurred in one patients in the STE persistence group because of non-IRA

occlusion. In-hospital heart failure tended to occur more often in patients in the STE persistence group (63.6% vs 27.6%, p= 0.06).

Table 11. Adverse In-hospital Events

	STE persistence n = 11 (27.5%)	STE resolution n = 29 (72.5%)	P Value
Death	1 (9.1%)	1 (3.4%)	0.48
Reinfarction	1 (9.1%)	1 (3.4%)	0.48
Stroke	0	0	-
Congestive Heart Failure	7 (63.6%)	8 (27.6%)	0.06
Target Lesion Revascularization	0	1 (3.4%)	0.27
Major bleeding	0	1 (3.4%)	1.0

STE = ST-segment elevation.

4. The investigation of the role of current antiplatelet therapy during AMI; the impact of periprocedural (before primary PCI) Abciximab administration on microvascular damage in patients with occluded infarct-related artery.

Also for this aim we excluded previous AMI, infarct-related artery stenosis with Thrombolysis In Myocardial Infarction grade $\geq$ 1 flow at index angiography, presence of collateral circulation (Rentrop $\geq$ 1), use of protection devices or thrombus aspiration devices, clinical signs of cardiogenic shock during the first week after infarction.

From the pool of the patients who underwent primary PCI and CMR in our institution in the same period, we identified 95 subjects who met the same inclusion criteria and who did not receive Abciximab. Of them, those patients with the same gender, age, time to treatment, and number of vessels involved in coronary artery disease as the sample population were considered as controls. Subjects in whom one or more of these variables did not match those of the abciximab group were excluded. The process was blinded, computerized, and resulted in a total of 49 patients in the comparison group.

The clinical, angiographic characteristics of the patients are summarized in table 12. Time to treatment was comparable between patients treated or not treated with abciximab (166 ± 84 vs. 170 ± 99 min, p = 0.7). Similarly, the other baseline clinical and angiographic characteristics did not differ between the two groups. After primary PCI, final TIMI 3 flow was observed in 94% of patients in both groups. Myocardial blush grade was not statistically different between patients treated with abciximab in comparison with the control group. The extent of myocardial and microvascular damage assessed by DE-MR was not different between the two groups (table 12), neither when the percentage of patients nor the number of LV segments were considered. At univariate analysis, predictors of severe microvascular obstruction were age (OR 1.2/1 year, 95% CI 1.05– 1.3, p = 0.01), time to treatment (OR 1.4/1 h, 95% CI 1.1– 2.1, p = 0.46), and number of LV segments with transmural necrosis (OR/1 LV segment 6.5, 95% CI 2.2–20, p !

0.001). By contrast, Abciximab was not related to severe microvascular obstruction (OR 1.2, 95% CI 0.5–2.9, p = 0.6). At multivariate analysis, only the number of LV segments with transmural necrosis (OR 1.5/1 LV segment, 95% CI 1.2–1.8, p =

0.001) and age (OR 1.1/1 year, 95% CI 1.01–1.12, p = 0.02) turned out to be independent predictors of severe microvascular obstruction. When presence/absence of transmural necrosis was considered, it remained an independent predictor of severe microvascular obstruction (OR 7, 95% CI 3.3–23, p = 0.001). The relationship between the adjusted patients' probability of severe microvascular obstruction and the number of LV segments with transmural necrosis in patients treated with abciximab and controls is illustrated in figure 8.

Table 12. Baseline characteristics

	Abciximab	Control	p Value
Patients, n	**36**	**49**	
Age (y)	56.9 ± 10.7	58.9 ± 11.9	0.5
Gender, male	31 (86%)	40 (82%)	0.6
Hypertension	18 (50%)	25 (51%)	1
Hypercholesterolemia	20 (56%)	24 (49%)	0.6
Current smoker	22 (61%)	28 (57%)	0.6
Diabetes Mellitus	5 (14%)	7 (14%)	1
Prior PCI	2 (6%)	0	0.2
Pre (<24h) infarction angina, n (%)	11 (31%)	17 (35%)	0.6
Prior angor	4 (11%)	9 (18%)	0.4
Time to treatment, minutes	166 ± 84	170 ± 99	0.7
Left ventricular ejection fraction, (%)	60.5 ± 9.6	58.87 ± 15.3	0.4
End diastolic volume, ml/m2	70.5 ± 14.7	70.4 ± 22.3	0.4
End systolic volume, ml/m2	26.4 ± 10.3	26.24 ± 15.6	0.4
Distribution of coronary artery disease, n (%)			0.9
Single-vessel	24 (66%)	31 (63%)	
Double-vessel	10 (27%)	14 (28%)	
Triple-vessel	2 (6%)	4 (8%)	
Number of treated vessels, n (%)			0.4
Single-vessel	34 (94%)	48 (98%)	
Double-vessel	2 (6%)	1 (2%)	
Myocardial blush grade 2/3, n (%)	24 (67%)	32 (65%)	0.8
Peak of Troponin I, μg/L	80 ± 55	74.95 ± 46.7	0.4
LV segments with transmurality	3.03 ± 2.8	3.09 ± 2.9	0.9
LV segments with SMD	1.05 ± 1.5	1,06 ± 1,8	0.7
Patients with trasmurality, n (%)	22 (61%)	30 (61%)	0.932
Patients with SMD, n (%)	15 (41%)	18 (37%)	0.66

LV= left ventricle

Figure 8. Relationship between number of LV segments with TN and in hospital (patient) probability of SMD assessed with logistic regression model. The coefficients of the equation have been computed for increment of one LV segment with TN. Early abciximab (i.e from four to two hours from symptom onset) may increase the probability of TIMI 3 flow of the IRA before PPCI [1], and consequently to reduce the "true" ischemic time and the "wavefront" phenomenon of trasmural necrosis. In this case, the benefit in term of reduction of TN and SMD probability might be described by a shift from point A to point B (TN and SMD likelihood according to time to treatment has been extrapolated from ref. 6).

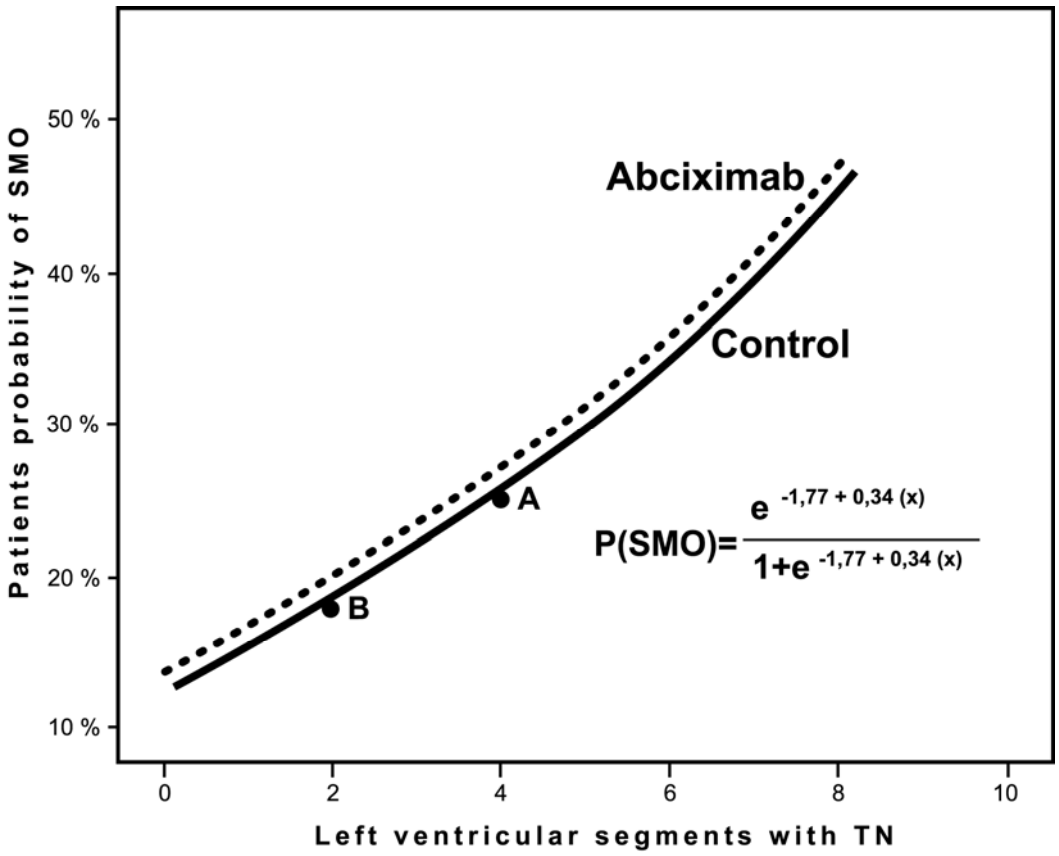

5. The evaluation between angiographic index of myocardial perfusion after primary PCI, MBG, and anatomical features on CMR (the correlation between staining phenomenon and SMD).

In 9/320 patients MBG couldn't be assessed because of renal failure (5 pts), poor quality of the postprocedural angiogram/ventriculogram (4 pts). In 17 additional patients CMR data were non available because of claustrophobia (8 pts), recurrent ischemia after reperfusion preventing CMR examination (2 pts) and poor quality of CMR images (7 pts). So 294 pts were available for the final evaluation.

Baseline Clinical Characteristics

Patients were divided into two groups according with the final MBG. One hundred fifteen patients (39%) had MBG 0/1, the remaining 179 (61%) showed a good myocardial perfusion pattern with MBG 2/3. Demographic characteristics of the two group of patients are summarized in Table 13.

No difference between different MB grades as far as the other demographic variables was concerned (pre-infarction angina and history of previous myocardial infarction, previous coronary by-pass) and also about pain-to-ballon-time. In comparison with MBG 2/3 group, MBG 0/1 infarcts were associated with a significantly greater TnI release (159 ± 136,4 ug/L vs 74,9 ± 81,9 ug/L; p = 0,000).

Relationship between Myocardial Blush Grades and Other Angiographic Characteristics.

In patients with MBG 0/1 LAD was the most frequently involved infarct-related artery (Table 14). Left ventricular ejection fraction on angiography was lower in patients with lower grades of MBG. Values of pre and post PCI TIMI flow in patients with MBG 0/1 and MBG 2/3 are detailed in Table 14. As shown, patients who exhibited a final good perfusion pattern also had a significantly higher pre PCI TIMI flow (TIMI 3 19% vs 8,7%, p=0,016). On the other hand, patients with MBG 0/1 showed more frequently the culprit vessel occluded as showed by pre-procedural TIMI 0 (73,9% in MBG 0/1 group vs 59,2% in MBG 2/3 group, p=0,010). Collateral circulation (Rentrop 2 or 3) was present in only seven patients. No difference was found in abciximab administration among two groups.

CMR and MBG findings

All patients underwent CMR 7±3 days after PCI. Transmural necrosis, per patient, was shown in 86,1% of patients with MBG 0/1 and in only 45,8% of those with successful myocardial reperfusion (p<0,001) (see Table 15). The evaluation of the other parameters of infarction extent (mean number of TN segments and Infarct Size Idex), confirmed the relationship between myocardial damage and lower MBG. The anterior and septal location of infarct was significantly related to a worse myocardial perfusion pattern (p=0,000, p=0,001, respectively); on the contrary the inferior involvement was most frequently related to MBG 2/3 (46,6% vs 27%, p=0,001).
On delayed contrast imaging the presence of persistent SMD was detected only in transmural infarcts and occurred in 47 patients (16%). When compared to patients with MBG 2/3 (Table 15), patients with MBG 0-1 had more frequently SMD (33,9% vs 4,5%, p= 0,000), and also a greater extent of microvascular damage, expressed as SMD index (0,62 ± 0,8 vs 0,12 ± 0,34; p= 0,000).

CMR findings and Staining Phenomenon.
In our series staining phenomenon was detected in 44,3% of patients with MBG 0/1 (Table 16). Among the patients with MBG 0 (103 pts), 51 patients had staining (MBG 0 staining) while 52 did not (MBG 0-no staining). At CMR patients with MBG-0-staining, if compared to those with MBG 0 without staining, had worst myocardial damage as demonstrated by the extent of necrosis in terms of the higher mean number of TN segments (6,2 ± 2,3 vs 4,7 ± 3,1, p=0,008), and Infarct Size Index (1,63 ± 0,49 vs 1,28 ± 0,64, p=0,008) and TN (96,1% vs 78,8, p=0,008). Presence of staining was also related to microvascular damage as assessed by CMR and identified with SMD (Fig 9,10); in fact, patient with MBG 0 staining had an overall higher occurrence of SMD per patient (52,9% vs 21,2%, p=0,002) and a greater extent of the damage as SMD index (0,52 ± 0,5 vs 0,21 ± 0,41, p=0,001).
At multiple linear regression analysis, variables independently and directly correlated with MBG 0/1 were mean number of TN segments (OR 1,62, 95% CI 1,17-2,24, p = 0,003), and the worst CMR perfusion pattern as demonstrated by SMD index (OR 3,13, 95% CI 1,185-8,286, p = 0,021).

Table 13. Relationship Between Clinical Characteristics and MBG.

Demographic and Clinical Characteristics	MBG 2/3 (n=179)	MBG 0/1 (n=115)	p Value
Age (years)	58 ± 12	60 ± 11	0,376
Men, n (%)	158 (88,3)	89 (77,4)	0,013
Current Smoker, n (%)	96 (53,4)	65 (56,5)	0,664
Dyslipidemia, n (%)	80 (44,9)	51 (44,3)	0,920
Hypertension, n (%)	95 (53,1)	59 (51,3)	0,767
Diabetes mellitus, n (%)	22 (12,4)	19 (16,5)	0,316
Previous AMI, n (%)	15 (8,5)	7 (6,1)	0,450
Angina pre-AMI, n (%)	53 (29,8)	29 (25,2)	0,396
Angina during stress	34 (18,9)	19 (16,5)	0,599
Previous coronary angioplasty, n (%)	10 (5,6)	4 (3,5)	0,402
Previous coronary bypass, n (%)	1 (0,6)	0	0,421
Pain to balloon time, minutes	248,3 ± 224,3	273,3 ± 184,32	0,340
Troponin I, µg/L	74,9 ± 81,9	159 ± 136,4	0,000

Data are presented as mean value ± SD, or number (%) of patients in group. SMD= Severe microvascular damage.

Table 14. Angiographic Characteristics by Perfusion Pattern (MBG).

Characteristics	**MBG 2/3 (n=179)**	**MBG 0/1 (n=115)**	**p Value**
Infarct-related artery, n (%)			
Left anterior descending	89 (49,7)	83 (72,2)	0,000
Left circumflex	27 (15,1)	13 (11,4)	0,371
Right coronary artery	74 (41,3)	26 (22,6)	0,001
Ejection fraction (FE)	60 ± 12	54 ± 12	0,000
EDV (ml/mq)	72 ±18	66 ± 19	0,040
ESV (ml/mq)	29 ± 14	30 ± 14	0,381
TIMI pre-PCI, n (%)			
0	106 (59,2)	85 (73,9)	0,010
1	7 (3,9)	7 (6,1)	0,538
2	32 (17,9)	13 (11,3)	0,127
3	34 (19)	10 (8,7)	0,016
TIMI post-PCI, n (%)			
0	0	5 (4,3)	0,001
1	0	2 (1,7)	0,077
2	3 (1,7)	23 (20)	0,000
3	176 (98,3)	85 (73,9)	0,000
Staining	0	51 (44,3)	0,000
Abciximab, µg/L	75 (41,8)	50 (43,5)	0,654

Data are presented as mean value ± SD or number (%) of patients in group

Table 15. Relationship Between MBG and CMR characteristics

CMR Characteristics	**MBG 2/3 (n=179)**	**MBG 0/1 (n=115)**	**P Value**
Location of myocardial infarction:			
Anterior, n (%)	72 (40,2)	76 (67)	0,000
Septal, n (%)	48 (26,8)	52 (45,2)	0,001
Lateral, n (%)	24 (13,5)	15 (13)	0,914
Inferior, n (%)	83 (46,6)	31 (27)	0,001
Mean number of TN segments	2,6 ± 2,4	5,3 ± 2,9	0,000
Infarct size index	0,82 ± 0,59	1,46 ± 0,6	0,000
TN per patients	82 (45,8)	99 (86,1)	0,000
Presence of SMD	8 (4,5)	39 (33,9)	0,000
SMD index	0,12 ± 0,34	0,62 ± 0,8	0,000

Data are presented as mean value ± SD, or number (%) of patients in group. SMD= Severe microvascular damage.

Table 16. CMR Characteristics according with the presence of Staining.

CMR Characteristics	MBG 0 without staining (n=52)	MBG 0 with staining (n=51)	P Value
Location of myocardial infarction:			
Anterior, n (%)	31 (59,6)	37 (72,5)	0,166
Septal, n (%)	21 (40)	26 (51)	0,000
Lateral, n (%)	6 (11,5)	6 (11,8)	0,591
Inferior, n (%)	17 (32,7)	12 (23,5)	0,301
Mean number of TN segments	4,7 ± 3,1	6,2 ± 2,3	0,008
Infarct size index	1,28± 0,64	1,63 ± 0,49	0,008
TN per patients	41 (78,8)	49 (96,1)	0,008
Presence of SMD	11 (21,2)	27 (52,9)	0,002
SMD index	0,21 ± 0,41	0,52 ± 0,5	0,001

Data are presented as mean value ± SD or number (%) of patients in group.

Figure 9:
A) late gadolinium CMR, basal short axis: inferior and inferolateral transmural infarct with midwall hypoenhanced core suggesting SMD (arrow).
B) frame from final RAO ventriculography before contrast medium injection: staining in the same region due to prior angiography (arrow)

A B

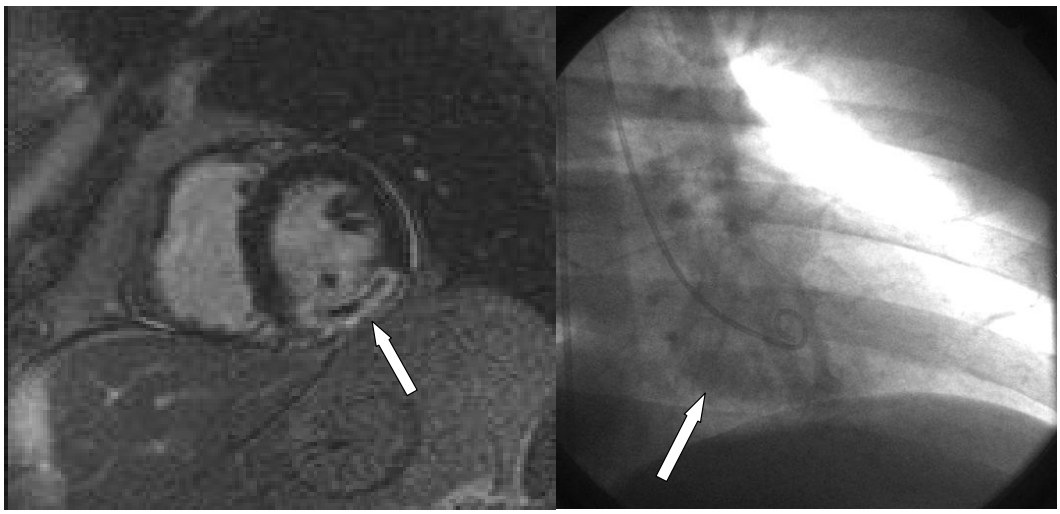

Figures 10:
A) late gadolinium CMR, 2 chambers view. Large transmural infarction with hypoenhanced core suggesting SMD in the middle and apical segments of the anterior wall.
B) Frame from lateral angiography. Diffuse staining phenomenon in the same segments (arrows).

A B

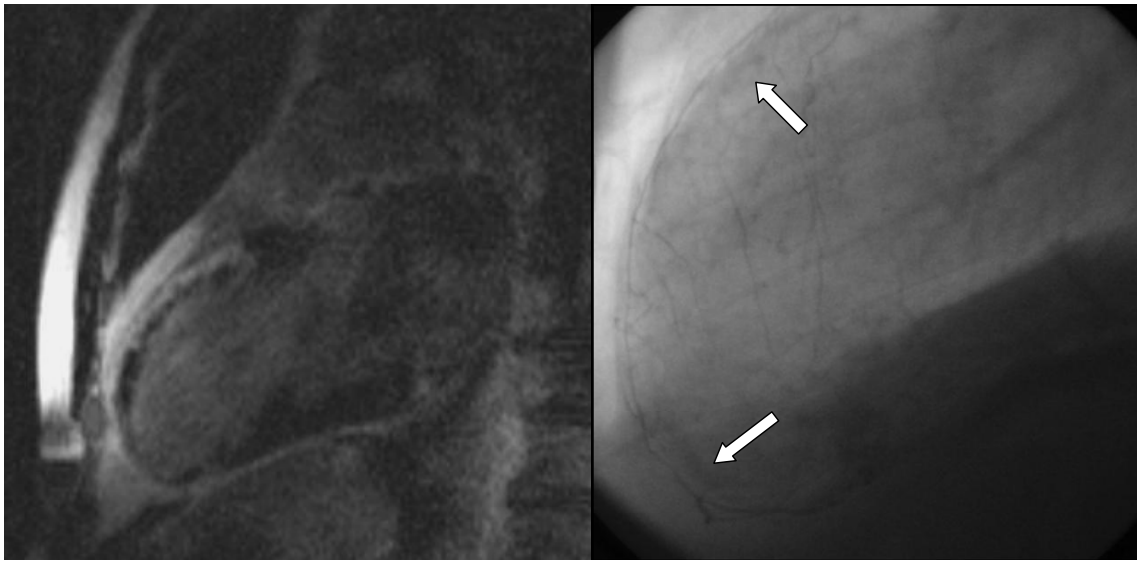

6. The investigation of the possibility to detect intramyocardial hemorrage after AMI, assessed by T2-weighted image on CMR, and the hemorrhagic findings role as a contributor, in humans, to the delayed hypoenhaced core traditionally referred only to microvascular obstruction.

Patient Population. Of the 116 patients who performed the entire CMR protocol, 8 (12,9%) were excluded for poor quality of T2-weighted images. Thus, a total of 108 patients partecipated in the final analysis. Enrolled patients were classified into two group according to the presence (32 patients) or absence (76 patients) of a dark area on T2-weighted images, assumed to indicate intramyocardial haemorrhage. In all cases the location of dark area on T2 images was in the mid portion of the myocardium, whitin the high signal intensity zone relate to risk area. Patients with T2 hypoenhancement were younger (54,9 ± 12,9 years versus 57,7 ± 8,5 years, p=0,032), and total enzimatic infarct size was greater as demonstrated by peak of troponin I (Table 17). Traditional risk factors did not statistically differ between group, also no difference were found about pain-to-balloon-time.

Angiographic Characteristics. Use of thrombolitic theraphy (Table 18) was associated with the presence of an hypoenhacement on T2-weighted images, (31,3% vs 3,9%, p=0,018); however, patients with PCI associated with thrombolitic agents had a longer duration of ischemia: pain-to-balloon-time was 367,1 ± 180,6 minutes in the first group, 238 ± 138,3 minutes in subject treated with primary PCI (p=0,018).

If compared to patients without haemorrage, those with CMR findings on T2 scans of hemorrhagic AMI showed more frequently the left anterior descending artery as culprit lesion (93,8% vs 59,2%, p=0,003). As far as traditional angiographic parameters of reperfusion were concerned (Table 19), patients without hemorrhagic AMI on T2 scans showed an higher post-procedural flow (TIMI 3 in 96% versus 65,6%, p=0,017) and MBG (grade 3 in 53,9% versus 9,4%, p<0,001): on the contrary, patients with radiological findings of myocardial haemorrahge showed in the majority a MBG 0 (84,4% versus 13,1%, p<0,001). No differences were noted neither in the pre-procedural profile, nor in the use of Abciximab. Collateral circulation (Rentrop 2 or 3) was present only in two patients, one for each group.

CMR Findings

Similarly to angiographic culprit lesion, anterior AMI on CMR was related with the presence of hypoenhancement on T2 images (90,6%, p=0,004); on the contrary, the inferior AMI was associated with lower number of T2 abnormalities (Table 20).

All the patients (32 pts) with mid dark area on T2 images showed SMD on post-contrast inversion recovery sequences: delayed hypoenhancement was topographically related to the segmental extent of hypointense signal on T2-weighted images (Figure 11, 12 and 13). Among seventy-six patients with AMI and no hypointense area on T2 scans, only 14 subjects (18,4% versus 100%, p<0,001) showed SMD; these hypointense areas were located in the subendocardial layers, not in the midmural portion.

Finally, patients with T2 hypoenhancement had a greater extent of myocardial necrosis as assessed by peak of troponin I and CMR extent of transmurality as identified by an higher precentage of number of segments with transmural necrosis (6,59 ± 1,94 vs 4,05 ± 2,8, p=0,007) and Infarct Size Index (1,7 ± 0,36 vs 0,59 ± 1,25, p=0,005).

Table 17. Clinical Characteristics

	Without T2 hypoenhancement (76 patients)	**With T2 hypoenhancement (32 patients)**	**p Value**
Age	57,7 ± 8,5	54,91 ± 12,9	0,032
Sex Male/Famale n (%)	60/16	29/3	0,90
Family history for CAD n (%)	62 (82)	16 (72,7)	0,262
Hypertension n (%)	45 (59,2)	13 (40,6)	0,268
Dyslipidemia n (%)	48 (63,1)	14 (43,8)	0,176
Diabetes Mellitus n (%)	3 (3,9)	8 (25)	0,067
Smoking n (%)	59 (77,6)	21 (65,6)	0,386
Previous angina n (%)	28 (36,8)	4 (12,5)	0,051
Pre-AMI angina n (%)	24 (31,5)	1 (3,1)	0,146
Previous PCI	10 (13,2)	0	0,062
Previous CABG	0	0	-
Pain-to-balloon-time, min	248,9 ± 202,6	284,57 ± 174,7	0,182
Tn I (μg/L)	112,3 ± 67,9	228,18 ± 147,8	0,020

Data are presented as mean value ± SD or number (%) of patients in group.

Table 18. Angiographic Findings

	Without T2 hypoenhancement (76 patients)	With T2 hypoenhancement (32 patients)	p Value
Primary PCI	73 (96)	22 (68,8)	0,008
Facilitated PCI/Rescue	3 (3,9)	10 (31,3)	0,018
One vessel disease n (%)	55 (72,3)	21 (65,6)	0,544
Two vessel disease n (%)	10 (13,1)	4 (12,5)	0,291
Three vessel disease n (%)	7 (9,2)	7 (21,9)	1
Infarct-related artery			
Anterior descending artery	45 (59,2)	30 (93,8)	0,003
Left circumflex artery	14 (18,4)	2 (6,3)	0,211
Right coronary artery	21 (27,6)	3 (9,4)	< 0,001
Ejection Fraction (%)	54,8 ± 12,1	50,03 ± 9,9	0,340
End-diastolic volume (ml/mq)	74,1 ± 20,6	65,7 ± 11,8	0,005
End-systolic volume (ml/mq)	33,9 ± 14,1	30,7 ± 11,9	0,198

Data are presented as mean value ± SD or number (%) of patients in group.

Table 19. Angiographic Findings

	Without T2 hypoenhancement (76 patients)	With T2 hypoenhancement (32 patients)	p Value
TIMI IN			
0	59 (77,6)	24 (75)	1
1	3 (3,9)	1 (3,1)	1
2	14 (18,4)	6 (18,8)	1
3	0	1 (3,1)	1
TIMI OUT			
0	0	1 (3,1)	1
1	0	1 (3,1)	1
2	3 (3,9)	9 (28,1)	0,036
3	73 (96)	21 (65,6)	0,017
MBG			
0	10 (13,1)	27 (84,4)	<0,001
1	7 (9,2)	0	0,161
2	17 (22,3)	2 (6,3)	0,107
3	41 (53,9)	3 (9,4)	<0,001
STAINING	10 (13,1)	21 (65,6)	<0,001
Abiciximab	45 (59,2)	13 (41,9)	0,153

Data are presented as number (%) of patients in group.

Table 20. CMR Findings

	Without T2 hypoenhancement (76 patients)	With T2 hypoenhancement (32 patients)	p Value
Location of AMI			
Anterior n (%)	45 (59,2)	29 (90,6)	0,004
Lateral n (%)	3 (3,9)	4 (12,5)	0,396
Inferior n (%)	28 (36,8)	2 (6,3)	0,010
Number of transmural segments	4,05 ± 2,80	6.59 ± 1,94	0,007
Infarct Size Index	0,59 ± 1,25	1,7 ± 0,36	0,005
Presence of SMD	14 (18,4)	32 (100)	<0,001
SMD Index	0,05 ± 0,12	1 ± 0,64	<0,001

Data are presented as mean value ± SD or number (%) of patients in group. SMD= Severe microvascular damage.

Figure 11. Topographic relationship between dark area on T2 images, suggesting myocardial hemorrhage, and delayed hypoenhancement due to severe microvascular damage.

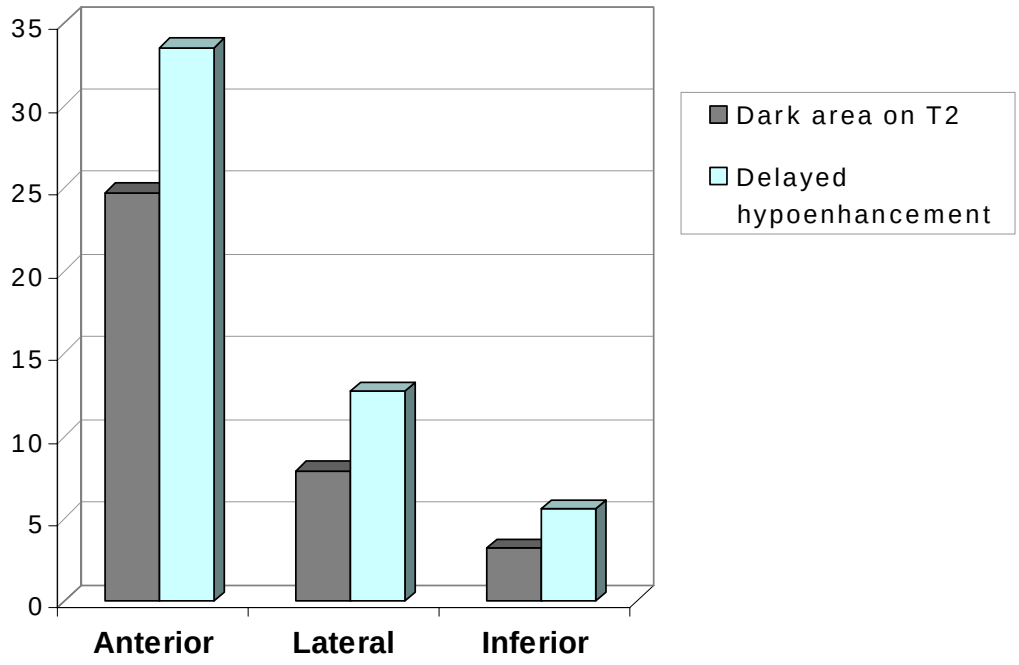

Figure 12. On the left (A) a T2-weighted CMR, 2-chamber view: a hypointense dark stria (asterisk) is clearly seen within the hyperintense edematous anterior wall. (B) Inversion recovery post contrast injection (IR DE CMR), the same location on 2-chamber view: in the same location of dark area on T2, can be detected an hypointese core in the infarction of infarcted anterior wall. Note the same susceptibility effect of the infarct core, with the two different sequences, of the thrombus.

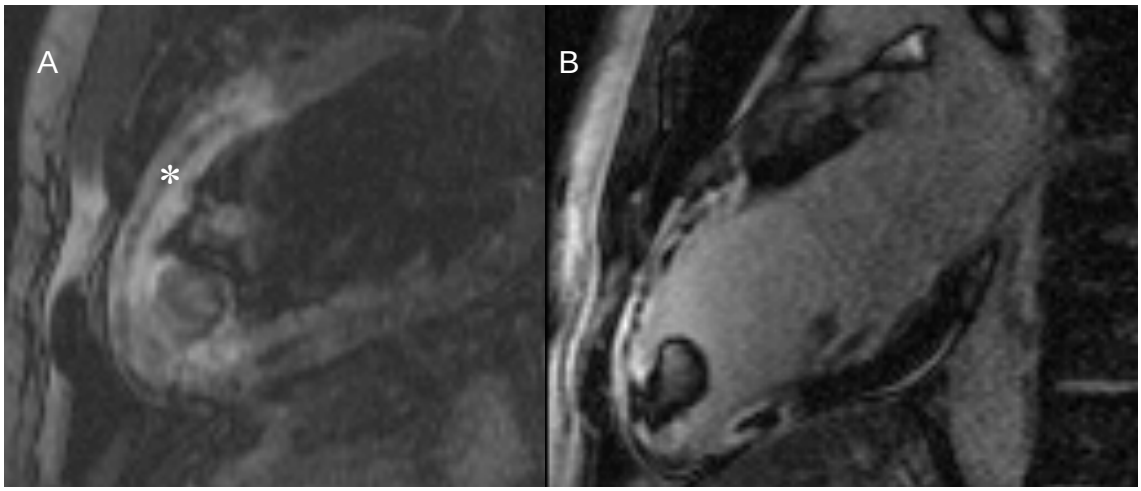

Figure 13. On the left (A) a T2-weighted CMR, 2-chamber view, without any abnormalities and an omogeneous high signal intesity due to edema of risk area. (B) Inversion recovery post contrast injection (IR DE CMR sequence), shows a transmural AMI without signs of SMD.

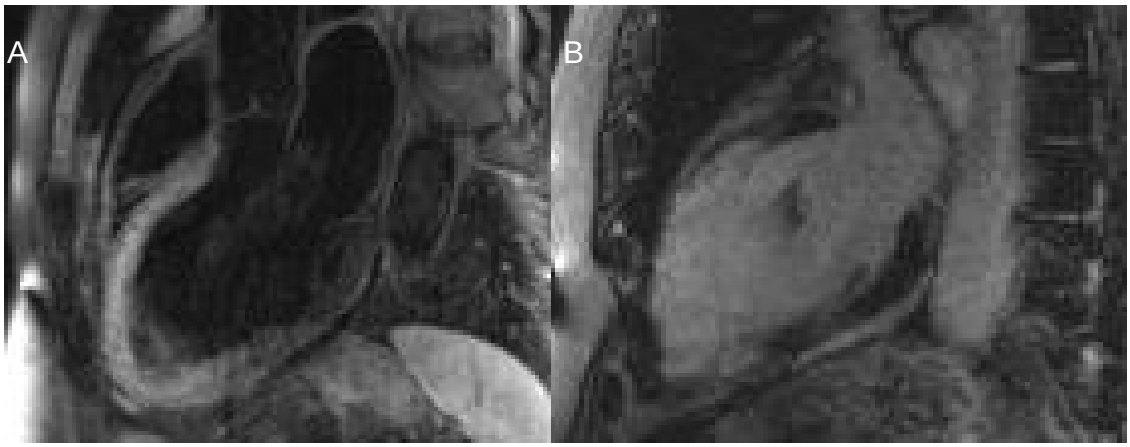

7. Comparision of the ex vivo cardiovascular magnetic resonance signals of pathologically proved hemorrhagic myocardial infarction and to correlate these with in vivo CMR findings.

Evaluating the two patients died during follow-up of whom we obtained autopsy, cardiogenic shock with acute pulmonary edema and peripheral congestion were found to be the cause of death at autopsy. Pathologic examination of the 2 hearts revealed hemorrhagic transmural septal and anterolateral AMI, in the setting of patent coronary artery stents (Figures 14 and 15). Hemorrhage was confined to the zone of necrosis and was massive at the core of AMI, with diffuse and confluent packed red blood cells, interspersed between myocytes with coagulation necrosis in patient 1, whereas an almost complete removal of dead myocytes was seen in patient 2.

Moving toward the periphery, hemorrhage was slight to moderate, with patchy distribution. In patient 2, at the border between the hemorrhagic core and the healing organizing tissue, patchy hemosiderin deposits were detected (Figure 16). In both instances, the total destruction of the microvasculature within the AMI core was evidenced. The AMI extent was 57 ± 30% and 44 ± 24% of the left ventricular area, with progressive increases from the base to the apex (ranges 29% to 88% and 16% to 68%, respectively). Hemorrhagic extent was 23 ± 13% and 19
± 8% of the left ventricular area, also showing progressive increases from the base to the apex (ranges 12% to 40% and 9% to 27%, respectively). T2-weighted images showed areas of signal hypointensity inside the hyperintense areas (Figures 14 and 15). The AMI extent and the area of hemorrhage (hypointense regions or “dark areas”) measured by ex vivo T2 CMR strongly correlated with the pathologic quantification (Figure 17). Using ex vivo DE CMR sequences, bright–signal intensity areas surrounded by dark rims, consistent with a magnetic susceptibility effect, were visible within the AMI regions. Compared with histopathologic findings, the bright signal and the dark border were found to correspond to areas of massive hemorrhage with red blood cell extravasation, with additional hemosiderin deposits at the periphery in patient 2 (Figure 16).

As expected, high-signal intensity on in vivo T2-weighted sequences was found in the MI area, reflecting tissue edema. However, low-signal areas were also detectable within the edematous myocardial wall and correlated well in location and extent

with the hemorrhage seen on the ex vivo T2 images and proved by histology (Figures1 to 3 and 5). On in vivo DE CMR images, a dark hypoenhanced core resembling persistent microvascular obstruction was present within the hyperenhanced AMI. However, on closer evaluation, a dark rim surrounding tiny central areas of higher signal intensity was visible, with susceptibility effects similar to those observed on ex vivo images (Figure 18).

Figure 14. Patient 1: transmural anteroseptal and lateral hemorrhagic AMI. Gross (A, B, C, D), histologic (E, F, G, H) (Heidenhain trichrome stain), and ex vivo T2 CMR (I, L, M, N) short-axis sections of the heart, from the base to the apex. Note the perfect overlap between the hemorrhage seen on pathologic examination and the low-signal intensity areas observed on ex vivo T2 CMR.

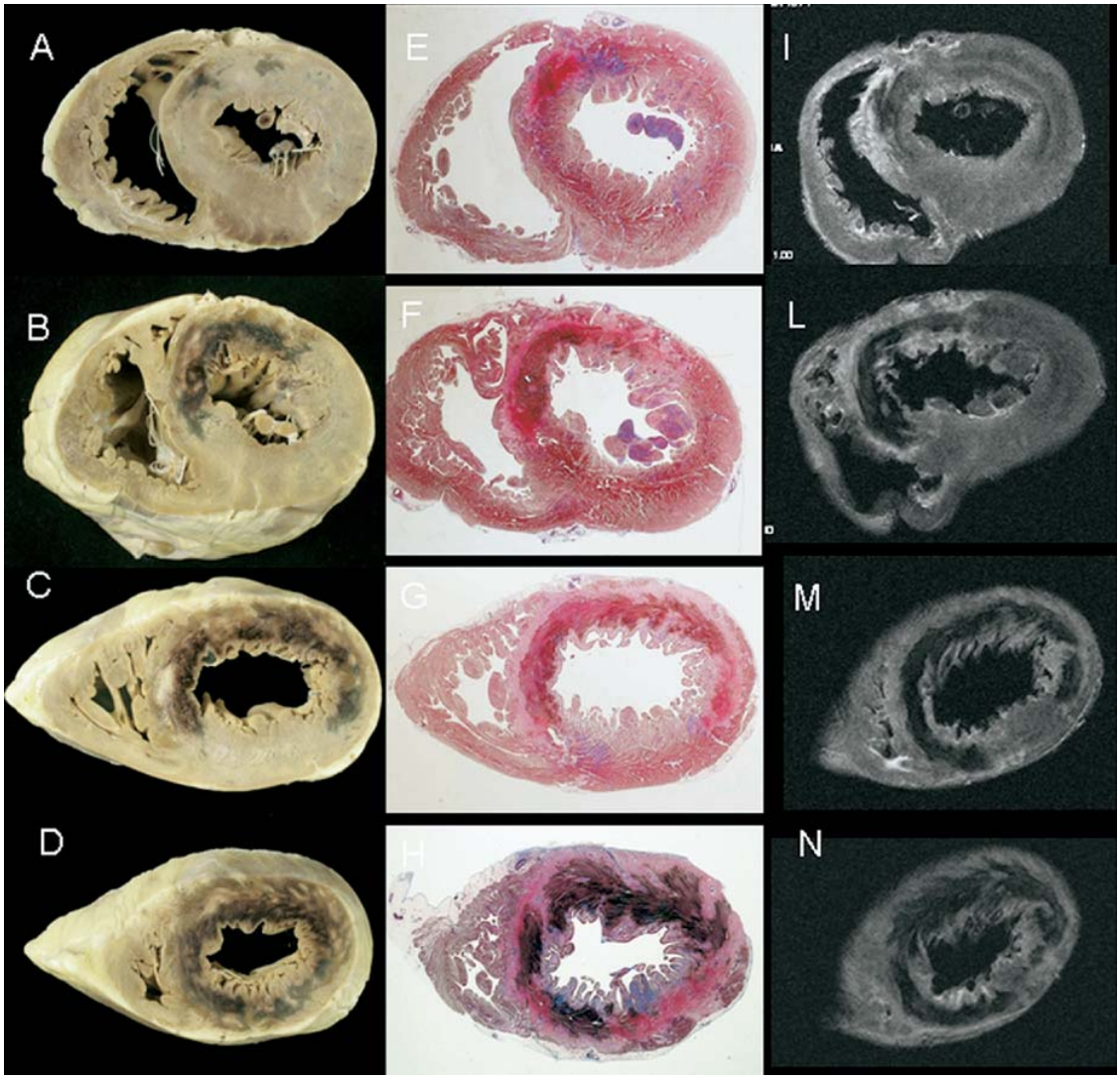

Figure 15. Patient 2: transmural anteroseptal and lateral hemorrhagic AMI. Gross (A, B, C, D), histologic (E, F, G, H) (Heidenhain trichrome stain), and ex vivo T2 CMR (I, L, M, N) short-axis sections of the heart, from the base to the apex. Note the perfect overlap between the hemorrhage seen on pathologic examination and the low-signal intensity areas observed on ex vivo T2 CMR.

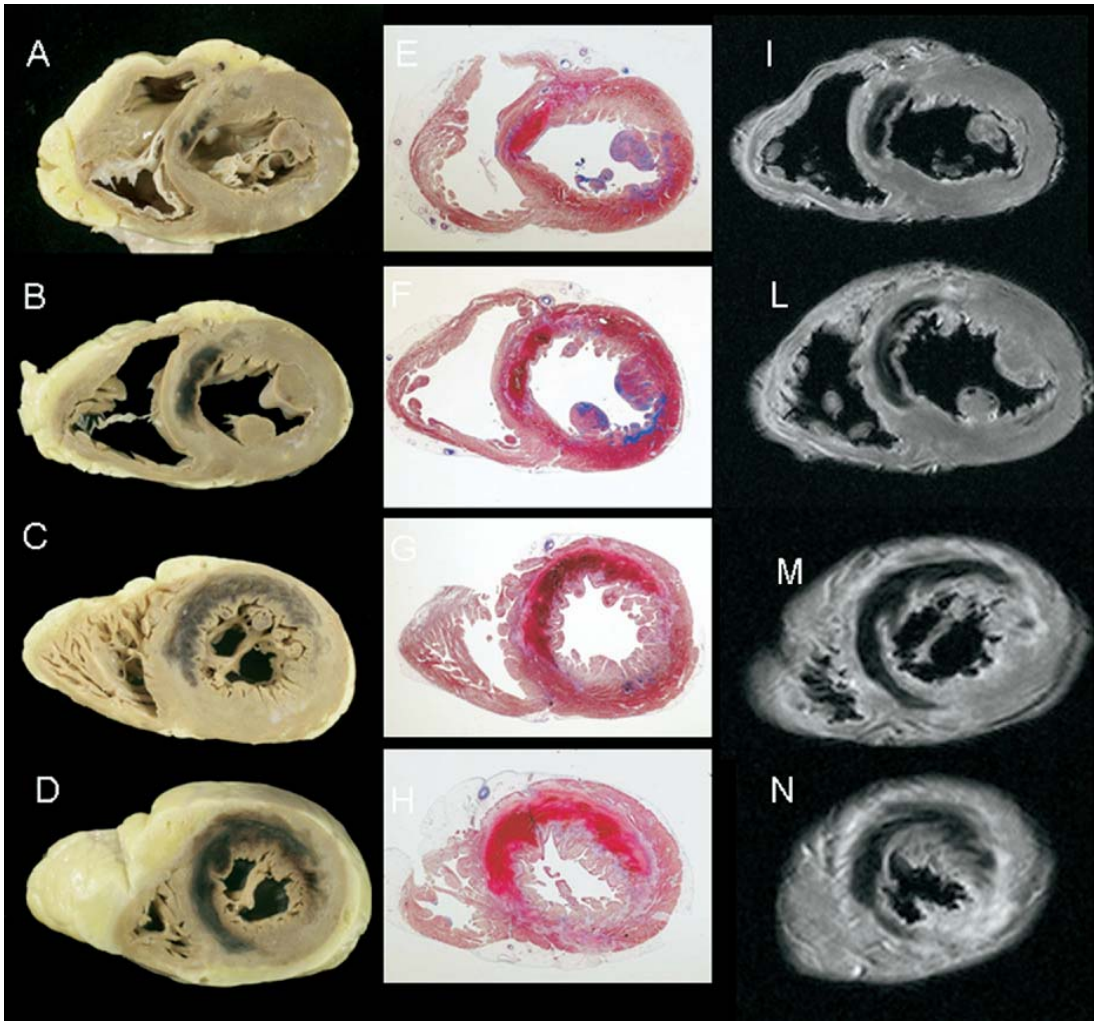

Figure 16. Patient 2: on ex vivo T2 (A) and IR DE (B) images, a perfect correspondence with histologic findings is visible (C), showing 2 areas of massive intramyocardial hemorrhage in the septum (hematoxylin-eosin x5); (D) close-up of the upper boxed area showing packed extravasated intact red blood cells (hematoxylin-eosin x31); (E) neovascularized organizing tissue with patchy hemosiderin deposits at the border close to hemorrhage (Perl's Prussian blue x31).

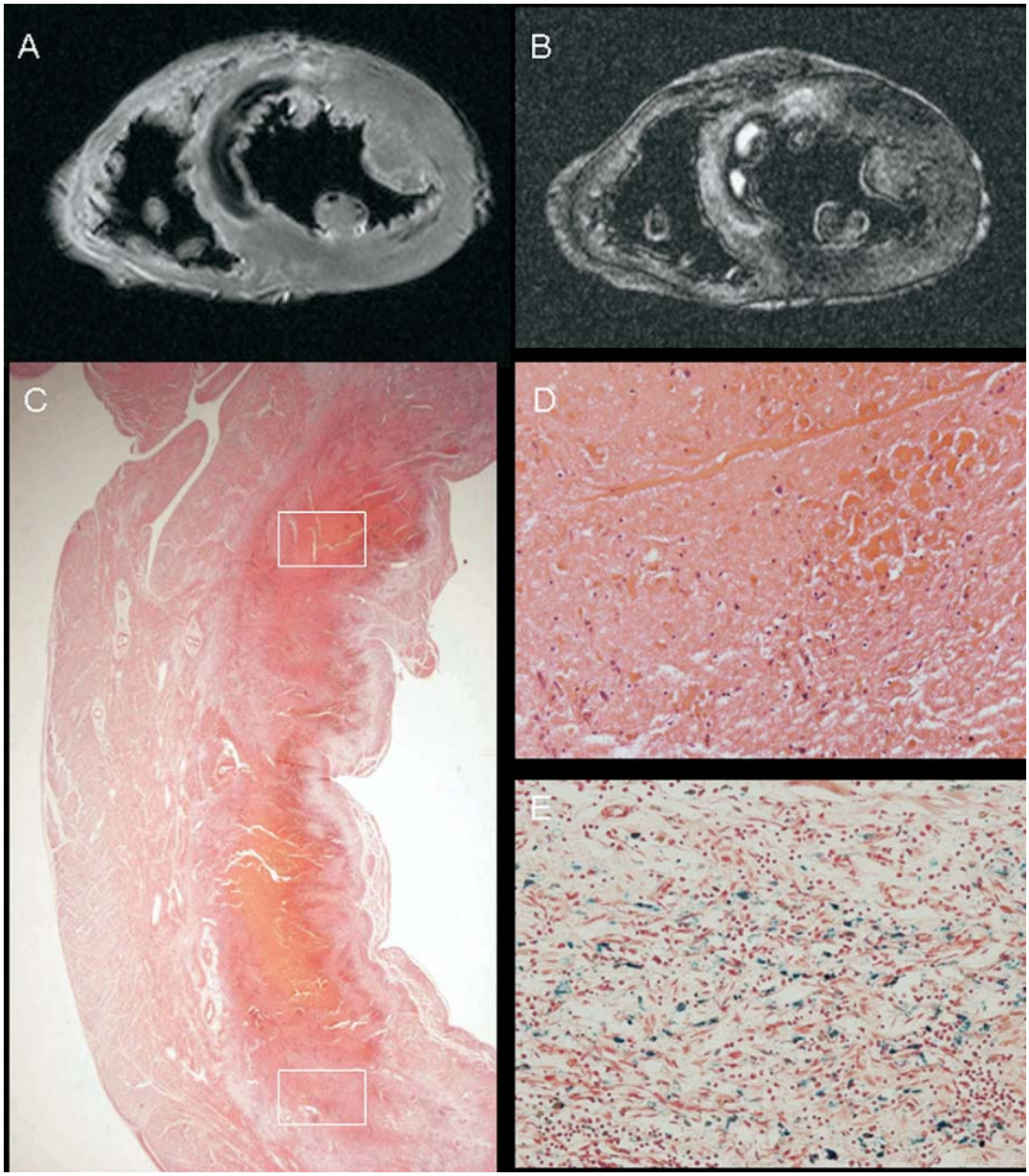

Figure 17. Comparison of CMR T2 sequences and pathology by linear regression analysis: AMI size (top) (R = 0.93, p = 0.0009) and hemorrhagic extent (bottom) (R = 0.93, p = 0.0007) showed a positive correlation. LV = left ventricular.

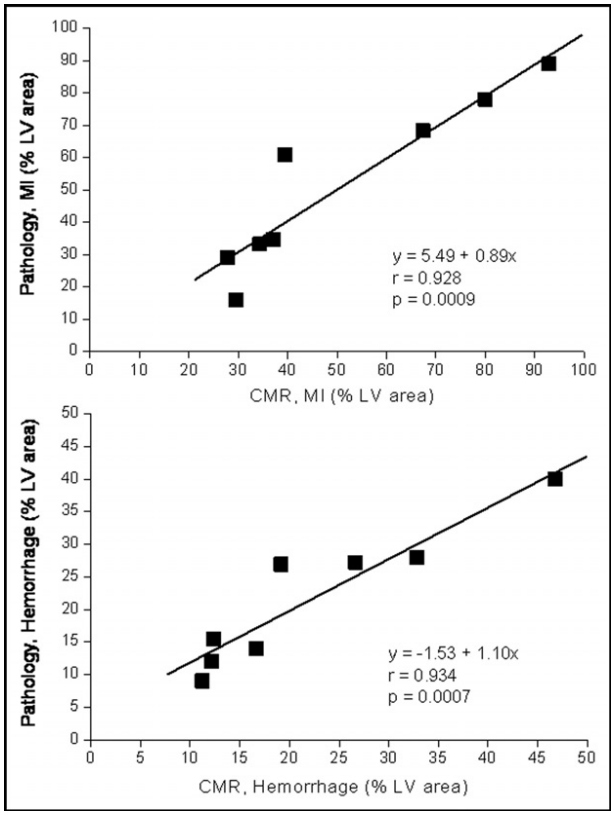

Figure 18. Patient 2: in vivo versus ex vivo CMR. (A) In vivo T2-weighted CMR, 4-chamber views: a hypointense rim (asterisk) is clearly seen within the hyperintense edematous septum. (B) In vivo IR DE sequence, long-axis view: a complex signal pattern is seen within the MI core of infarcted septum,with tiny bright areas surrounded by a dark rim (arrows), a feature typical of the susceptibility effect.(C) Ex vivo IR DE sequence, long-axis view: the same susceptibility effect as in (B) is clearly seen around the septal hemorrhage but is more evident because of the higher resolution of the image and the additional presence of hemosiderin, which normally occurs only at this stage of hemorrhage (i.e., 24 days after MI onset).

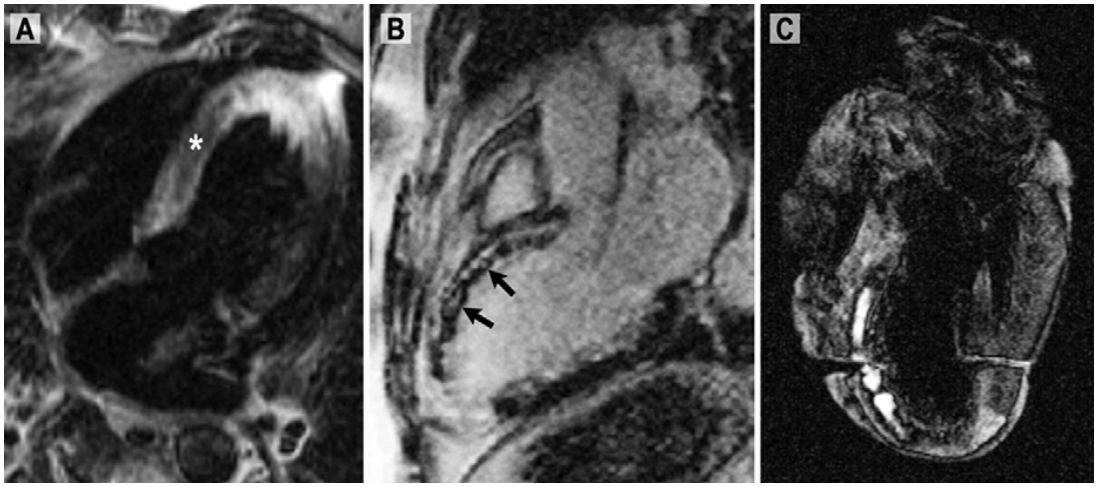

DISCUSSION

The major findings of this PhD thesis is the demonstration of the possibility to evaluate and explain the entire spectrum of myocardial damage, subsequently to ischemia by *in vivo* CMR. In this large prospective population study, we correlatet traditional clinical, electrocardiographic and angiographic parameters of reperfusion with *in vivo* myocardial and microvascular impairment, and we evaluated also the significance of current antiplatelet therapy in the acute phase and the CMR predictors, in terms of remodeling, on long-term follow-up.

Relevance of ischemic time in CMR findings of AMI

In animal models, the association between duration of the vessel occlusion and both TN (106) and no-reflow extent (107) has been well characterized. To the best of our knowledge, our study first shows a similar relationship in humans. After excluding patients with preprocedural TIMI flow grade 3 of infarct-related artery, in the remaining subjects the time from symptom onset to balloon inflation likely represents an indicator of total ischemic time. In this population, we found a continuous relationship among ischemic time and probability of TN and SMD, assessed by CMR. In fact, for each 30-min delay in treatment of patients undergoing successful primary PCI, the risk of TN or SMD increases by 37% and 21%, respectively. Although there was also a close correlation between presence of SMD and evidence of TN, it is noteworthy that for any time of reperfusion the probability of transmurality was higher than that of SMD (Fig. 2). In other words, SMD occurs later than TN, suggesting that, from a pathophysiologic point of view, SMD lags behind TN. These results are consistent with those of a recent experimental animal study, which has showed that both transmurality (106 8) and microvascular dysfunction depend on the duration of ischemia and that the extent of no reflow is driven by the extent of infarct size (107). In our study, we did not evaluate the infarct size; however, our results show that in patients with AMI undergoing successful primary PCI, TN and, more interestingly, SMD are strongly related to the length of ischemia. Similarly, the infarct size expressed as troponin I release (47) was progressively and significantly greater in patients with both TN and SMD compared with those with TN but not SMD and those with neither TN nor SMD.

Thus, it is not surprising that a longer duration of ischemia corresponds to a more pronounced impairment of myocardial perfusion (assessed by ST-segment resolution or myocardial blush) and, as a consequence, to a larger infarct size and a worse clinical outcome even when optimal mechanical reperfusion is applied (53, 108). In other words, restoration of TIMI flow grade 3 epicardial flow by PCI does not guarantee per se the normalization of myocardial perfusion (108). Therefore, although primary PCI, in comparison with thrombolysis, may guarantee a higher rate of recanalization in patients presenting late, it cannot prevent TN and SMD, which are strongly related, even after PCI, to the duration of occlusion. Interestingly, although infarct size is a major determinant of microvascular obstruction for any given delay in time to treatment, both experimental and clinical studies suggested that microvascular obstruction per se is a stronger predictor of worse left ventricular function and postinfarct complications compared with infarct size (53,70). On the other hand, TN seems to delineate viable and nonviable myocardium and predicts recovery of left ventricular function after AMI (47).

Predictors of LV remodeling: CMR findings and ECG correlation

Pronounced LV remodeling after AMI leads to heart failure and is an important predictor of mortality (49, 109). Compared to thrombolysis, the benefit of primary PCI has been ascribed, when performed timely, to the achievement of higher rate of vessel patency with a significant larger myocardial salvage and, consequently, reduced LV remodeling and an improved survival. However, LV remodeling also occurs despite successful primary PCI (49), and it has been also previously shown that restoration of TIMI grade 3 epicardial flow does not guarantee by itself myocardial salvage and the normalization of myocardial perfusion (71). In the present thesis, in the subgroup of patients in which we evaluated the LV remodeling by echocardiography, epicardial blood flow was restored in all patients within 7 hours from the symptom onset, mean infarct size index was 24%, 71% of the subjects presented TN at DE CMR and 36% SMD in at least one LV segment. In this group of patients, interestingly, we observed that ΔEnd-Diastolic volume index and ejection fraction variations are related to DE CMR-assessed infarct size index, SMD and TN as well as troponin I peak levels. Among all these parameters, however, only TN and troponin I peak level remain independent predictors of LV remodeling at follow-up at multiple linear regression.

Moreover, it is noteworthy that in a hierarchical model TN improves significantly the prediction of both ΔEnd-Diastolic volume index and ejection fraction changes at follow-up compared to troponin peak level alone and, when the analysis was restricted to patients with adverse remodeling (defined as an increase in ΔEnd-Diastolic volume index from baseline to follow-up of ≥ 20%), TN was the only predictor of LV dilatation and LV function worsening during follow-up.

Previous studies, using DE CMR to distinguish between scar and viable myocardium, have demonstrated that TN quantification across LV wall delineates viable and non-viable myocardium and predicts recovery of LV function after AMI (49,51). Other clinical studies using DE CMR early after AMI have confirmed that this tool is highly sensitive and reliable to detect morphological and functional sequelae of AMI and that DE imaging of TN appears to better predict functional outcome than traditional perfusion imaging (51,71). The majority of these studies using DE imaging reported an inverse relationship between the transmural extent of DE and the improvement of LV regional contractile function, with a minimal o no-improvement in dysfunctional segments with a DE transmural extent ≥75%. Our study shows that the (per patient) number of LV segments with TN is not only strongly related but has additional predictive value for early LVR and worse LV ejection fraction, independently of SMD and infarct size (determined either by infarct size index or by troponin peak level). By ROC, we found that 4 LV segments with TN are the better predictor of adverse LV remodeling (defined as LV ΔEnd-Diastolic volume index change ≥ 20%) after primary PCI, while Troponin peak level remains an independent predictor of early LV remodeling in case of milder amount of TN. Interestingly, these findings parallel the results of studies showing, by means of dobutamine stress echocardiography, that LV viable segments ≥ 4 is the best cut off in predicting LV ejection fraction improvement in ischemic cardiomyopathy after revascularization (109). This cut off represents approximately 25% of total LV segments: when refers to “non viable” segments, this cut off identifies patients who will show adverse LV remodeling; when expresses “viable” segments, it means that ongoing LV remodeling may be prevented in ischemic cardiomyopathy by revascularization. Our data also parallel those of Bolognese et al. that found that the extent of infarct zone viability detected by echo was the most powerful independent predictor of LV remodeling after first AMI (110) and those of Nijland et al. who

showed that the presence of viability, as assessed by dobutamine echocardiography, early after AMI was associated with preservation of LV size (111).

The importance of no-reflow evaluated by perfusion imaging as predictor of remodeling and outcome has been previously shown (51, 89, 1l2, 113). Here, our intention was to report on severe form of microvascular obstruction. SMD with persistent contrast filling defects, has recently been reported to be related to a worse LV remodeling and outcome, but its value has not been clearly weighted and reported versus TN and infarct size (71). By contrast, according to our data obtained by hierarchical multivariate analyses, SMD did not remain as independent predictor of ΔEnd-Diastolic volume index and LV ejection fraction changes when TN was included in the model.

Among the new concept about imaging predictors of LV remodeling detected both by echocardiography and CMR, ECG has been traditionally used to predict presence of impaired reperfusion and presence of LV aneurysm. In fact, persistence of ST-segment elevation lasting for a long time after the development of necrosis has been traditionally ascribed to the development of left ventricular aneurysm (114-117). However, this correlation is one of the most controversial in electrocardiography, since previous studies failed to demonstrate a close relationship between this electrocardiographic pattern and left ventricular aneurysm (118-120). Furthermore, the explanation of the underlying mechanism of persistent ST-segment elevation and its pathological correlates are still unclear (48,53,100). Interestingly, previous studies provided evidence for a significant relationship between ST-segment elevation persistence and the amount of creatine kinase release and extent of Q-waves after myocardial infarction (116,118). Recently, Tibrewala et al. in a small series of patients with anterior myocardial infarction found that persistent ST-segment elevation was associated with larger myocardial scars, as detected by CMR (121). However, this study did not find any difference in left ventricular function and did not provide data about the presence of wall motion abnormalities or aneurysm, thus failing to clarify the mechanism of ST-segment elevation persistence. The results of our subgroup study performed in first AMI patietnts treated with primary PCI, are in agreement with the previous findings; nevertheless they suggest that the persistence of ST-segment elevation indicates not only a larger extent of myocardial necrosis, but also, and more interestingly, the presence of persistent microvascular damage. In fact, although patients with ST-segment

elevation showed larger infarct size and greater extent of transmural necrosis than patients without ST-segment elevation, the former group differed from the latter mainly for the presence and the extent of persistent microvascular damage, as indicated by multivariate analysis. Moreover, in our experience, patients exhibiting persistent ST-segment elevation showed left ventricular aneurysm more frequently, even though this difference did not achieve a statistical significance. Taking into account the findings of previous studies (114-120), this result is not surprising and highlights the low positive predicting value of persistent ST-segment elevation in detecting left ventricular aneurysm, leading to the criticism about wall motion abnormalities as mechanism of electrocardiographic alterations.

Recently, Li et al provided direct evidence in animals that the opening of sarcolemmal K_{ATP} channels underlies ST-segment elevation during ischemia (122). It has been also demonstrated in a swine model that mechanical stimuli can induce marked ST-segment elevation, by producing the stretching activation of K_{ATP} channels (123). On this basis, it has been hypothesized that the outward bulging of myocardial necrotic wall, producing an abnormal stretch on the adjacent tissue, may alter cellular activity, generating injury currents at this level, responsible for the ST-segment elevation (124). In our study, patients exhibiting persistence of ST-segment elevation had not only larger myocardial necrosis, but also severe damage of the myocardial microvasculature within it, accounting for a profound alteration of myocardial skeletal. In animal studies, regions of delayed hypoenhancement are characterized by profound microvascular damage at the infarct core, with microvascular obstruction by red blood cells and necrotic debris (81). This severe damage in the context of a necrotic core may account for diffuse alterations in myocardial skeletal, favouring myocardial bulging and mechanical activation of K_{ATP} channels in the adjacent tissue, even if a macroscopic aneurysm is not or not yet evident. Other authors have suggested that persistent ST-segment elevation, in the setting of reperfused infarction, may be ascribed to residual ischemia arising from areas of viable myocardium at the boundary of necrotic regions (107). However, in our study this explanation seems to be unlikely, since patients with STE showed transmural necrosis in about 90% of cases, making the presence of viable myocardium in this setting highly unlikely .

In this thesis, the observed larger myocardial necrosis in patients with persistent ST-segment elevation may be largely ascribed to the more severe ischemic

insult suffered by patients in the ST-segment elevation persistence group, since they had longer ischemic time and a larger extent of the risk area, as expressed by the greater ST-segment elevation at baseline. In conlusion, finding a persistent ST-elevation after an acute myocardial infarction should not be surely addressed to left ventricular aneurysm formation but it should be considered as the possible expression of microvascular damage occurrence.

CMR and the impact of current antiplatelet therapy on SMD detected

Evidence of the superiority of Abciximab over placebo in primary PCI is well known (125). Nevertheless, data from meta-analyses showed that the advantage of the administration of Abciximab in terms of epicardial patency (TIMI flow before and not after PCI) and myocardial reperfusion is mainly limited to patients who received Abciximab early (126) . The authors also found a promising trend in favor of early Abciximab administration in terms of death, new myocardial infarction, or urgent revascularization rate. Recently, two randomized and controlled trials have confirmed that early Abciximab administration resulted in more frequent infarct-related artery patency before PCI, better myocardial perfusion after PCI, smaller enzymatic infarct size and lower degree of LV remodeling (127,128). By contrast, the effects of periprocedural administration of Abciximab in terms of myocardial reperfusion and microvascular damage are poorly characterized.

In this thesis, evaluating the subgroup of patient treated with a full dose of antiGP IIb/IIIa, SMD assessed by CMR was not influenced by intravenous Abciximab (per itself) if it is administered late in the catheterization laboratory, before mechanical recanalization of the occluded infarct-related artery. Our data confirmed that SMD is related to the extent of TN which is the result of total ischemic time,ischemic preconditioning, collateral flow and the level of oxygen demand (129). Therefore, the earlier the abciximab administration, the higher the probability to improve preprocedural flow of the infarct-related artery (7 Tarantini Cardiology), to reduce the ‘true’ ischemic time and to increase the extent of myocardial salvage (130) (see fig. 8). To this regard, other authors showed that an early opening, by pharmacological treatment, of the epicardial artery in AMI patients before delayed primary PCI gives a broader time window for PCI

intervention (131,132) and preserves LV size and function. Our results may appear in conflict with those of others (133-136). However, both studies by Petronio et al. (133) and Sciagrà et al. (134) did not restrict analyses to STEMI patients with occluded infarct-related artery and without angiographic evidence of collateral circulation (i.e. patients with open infarct-related artery were not excluded from the study). This is an important limitation because the effect of abciximab on microvasculature could be biased by the presence of patent infarct-related artery, as observed also the in ADMIRAL trial (135). Similarly, Neumann et al. (136) included into their analysis also patients without ST elevation who by definition presented with patency of infarct-related artery. Moreover, all these studies used surrogate indices of microvascular damage such as TIMI frame count, TIMI flow, flow velocity, and single photon emission computed tomography. Indeed, these indices show a lower sensitivity compared to DE, in detecting SMD (137). On the other hand, a recent subanalysis of the CADILLAC trial failed to find a clear impact of abciximab on microvasculature in STEMI patients treated with primary PCI, a result consistent with our data (138).

Therefore, our analysis appears important from a pathophysiological point of view for two reasons. First, the most accurate methodology to investigate severe and clinical relevant microvascular obstruction was utilized. Second, we found a relationship between TN and the probability of SMD as illustrated in figure 8. that confirms the importance to obtain early and optimal restoration of anterograde flow, in order to prevent myocardial and microvascular damage. In conclusion, although larger trials are required, the current study suggests that if abciximab is given at all, it should be given as early as possible to reduce ischemic time and therefore TN and microvascular obstruction.

Angiographic and CMR findings: relationship between staining phenomenon and SMD

The main result of this thesis is the angiographic data and CMR correlations in a large study population of 294 enrolled patients. From this data, we were able to understand the mechanism underlyng lower MBG, with evidence that grades 0/1 reflect a SMD as demonstrated by CMR. The presence of delayed hypoenhancement in the core of infarct area detected by CMR is strongly associated (53,71) with poor

prognosis, as well as with impaired MBG on follow-up (37). Furthermore, we demonstrated for the first time that the detection of a staining phenomenon in acute phase of AMI suggests the presence of SMD.

In the clinical setting, the assessment of the efficacy of reperfusion can be achieved by using simple methods such as an early ST-segment resolution (22) and by myocardial contrast echocardiography (139), or single photon computed tomography (140). However, during PCI, the assessment of microvascular status after recanalization can be routinely performed either by visual evaluation of the contrast density in the infarcted myocardium (MBG) (37) or by the filling and the clearance of dye in the infarcted tissue (TIMI Myocardial Perfusion Grade (TMPG) (36). Definite grades of myocardial perfusion impairment have been established, with the most severe vascular damage characterized by the total absence of dye within the infarcted myocardium and/or its persistent extravasation, suggesting vascular rupture and intramyocardial hemorrhage (6,24,25 lavoro staining).

CMR is a well-established technique to evaluate AMI because it provides not only information about extent of necrosis and function, but it can also assess myocardium perfusion after PCI, with important long term prognostic implications (53,70). Visualization of perfusion defects reflecting microvascular impairment can be accomplished by CMR immediately after gadolinium injection during first pass of contrast medium or, in the late phase, by demonstration of persistent hypoenhanced zones within enhanced infarction (69). Although a definite agreement about the best method of visualizing the vascular impairment has not been reached, a good correlation between these methods has been demonstrated in previous study (38). In addition, areas of persistent hypoenhancement within late enhanced infarction are commonly considered as the result of a particularly severe microvascular damage in the infarct core (69).

CMR and Angiographic parameters of myocardial perfusion: two faces of the same coin

Although angiographic and CMR signs of microvascular damage after epicardial recanalization are presumably related to the same underlying pathological substrate, their relationship has not been fully elucidated yet. In a recent study by Appelbaum et al (141) in a group of 21 patients who underwent successful primary

PCI and CMR, evidence of impaired perfusion at first pass was present in 90% of cases with abnormal post-PCI Myocardial Perfusion Grade (0/1/2), but only in 18,2% of patients with normal Myocardial Perfusion Grade. In another study Porto et al. (142) analysed 27 patients with acute AMI and found a linear correlation between decreasing MBG grades and CMR signs of vascular obstruction, thus confirming the relationship between post PCI perfusion index and CMR measures of microvascular impairment.

As far as our results are concerned, the following main findings have to be highlighted.

First, SMD at CMR was significantly less frequent in patients with preprocedural TIMI 3 flow and was associated with an overall worse postprocedural TIMI flow. These findings suggest that the relation between TIMI and SMD might be similar to that previously demonstrated between TIMI and MBG (37); impaired capillary patency in the infarct zone, as depicted by SMD, might affect the corresponding epicardial flow and result in lower TIMI grades. However, although this relation may be hypothesized, a substantial number of patients show impaired myocardial perfusion (MBG 0/1) in association with epicardial TIMI 3 flow and this has been related to the presence of collateral circulation allowing the clearance of dye from infarcted tissue and thus resulting in preserved epicardial TIMI flow (71.96).

Secondly, severely impaired post PCI myocardial perfusion, as demonstrated by MBG 0/1 patients, was strongly associated with presence of SMD. These data are in agreement with the above mentioned studies by Appelbaum et al. (141) and Porto et al. (142) and confirm on an higher number of cases the relationship between SMD and MBG. Moreover, the occurrence of SMD only in transmural infarcts observed in our population, in association with higher troponin I release and infarct size, further supports this relationship, given the likelihood to microvascular damage in such more severe cases, as proven both in experimental (86) and clinical studies (71).

Thirdly, and interestingly, MBG-0-staining was associated with an higher occurrence of SMD. Relationship between staining and SMD has not been previously reported in the literature and this is the first study approaching this particular aspect. Since the first experience (97), staining phenomenon was supposed to be the result of postreperfusion extravasation of contrast into the myocardium (96) and considered as an useful angiographic sign of hemorrhagic AMI (97). In the

subsequent classifications of myocardial perfusion after recanalization, the persistence of myocardial blush ("staining"), suggesting leakage of the contrast medium into the extravascular space, was included in the worst postprocedural perfusion grades, (MBG 0, Myocardial Perfusion Grade 1), and the presence for lower grades value, including staining, of a negative predictive in terms of long term mortality was demonstrated (71,96). The linear correlation that we observed in our patients between SMD and staining phenomenon further confirms the previously reported value of SMD as a strong negative prognostic marker (53,71), and raises also some questions about its pathological substrate. In fact, in the literature the term of "severe / persistent microvascular obstruction" has been widely used to indicate persistent zones of hypoenhancement surrounded by late enhanced infarcted myocardium. Previous studies indicated that these dark regions, surrounded by hyperenhanced infarcted myocardium correspond to experimentally produced no-reflow regions (69). Experimental studies proved that if the coronary occlusion is prolonged, the anatomic integrity of the microvasculature can be damaged thus leading to the extravasation of blood in the myocardium and persistence of dye in the interstitial space at the time of coronary reopening (25,137) . During angiography, staining is very likely the result of this phenomenon. In such cases and experimental study (86), the loss of signal in the infarct core on late gadolinium CMR could be correlated to the extravasated blood, leading to susceptibility effects due to paramagnetic breakdown products of hemoglobine (76,143).

Although a correlation between SMD and staining was demonstrated in our patients, in a small number of cases (21%) SMD at CMR was not associated with MBG-0-staining at acute angiography (see Table 16). It can be speculated that this discrepancy may be due to a smaller staining extension and/or to our definition of SMD. An additional explanation could be related to the healing process, leading to removal of hemorrhagic leakage and making SMD not detectable on the CMR performed 7±3 days after coronary recanalization.

In the majority of our patients SMD occurred in the territory of LAD artery, while it was uncommon in inferior infarcts. In this respect our data match closely those of Iwakura et al. (144) and Galiuto et al (145), who independently found similar evidence of microvascular damage during myocardial contrast echocardiography. However, in our series SMD was observed only in 16% of AMI, a percentage which is inferior to that reported in other studies (71,72). This

difference can be explained considering the inclusion criteria of our study (i.e. patients with SMD extending in at least two adjacent ventricular segments). Since our aim was to qualitatively evaluate the relationship between angiographic and CMR signs of postreperfusion microvascular damage, patients with minor SMD involving only one segment were excluded. This allows comparison between unquestionable SMD and the corresponding angiographic features, thus avoiding potential false negative angiographic results that could be found in presence of minimal SMD.

Role of CMR in differential diagnosis between microvascular obstruction and intramyocardial hemorrhage

Intramyocardial haemorrhage is caused by vascular cell damage with blood leakage of the injured vessels. Experimental studies showed that vessels injury represents a late event in the course of the mycardial cells damage during reperfusion injury, expanding gradually after reperfusion itself (146). In contrast with intracranial haemorrhage, very few studies have been performed to evaluate the presence of the haemorragic area by using CMR after reperfusion therapy. In fact CMR can characterize the tissue on the basis of the changes in relaxation times T1 and T2, reflecting changes in image signal intensity (147). By assessing the paramagnetic susceptibility effects of deoxyhemoglobin, we were able to confirm previous experimental observations (148) in which dark areas on post-contrast IR sequences were the expression not only of microvascular ostruction, but also of areas of intramyocardial haemorrhage.

In fact the hearts of 2 patients who died from cardiogenic shock after AMI who had undergone coronary recanalization and in vivo CMR, were examined by T2 and T1 late enhancement sequences as well as by gross and histologic investigation. Pathological examination revealed hemorrhagic AMI in both and the low-signal intensity areas observed by ex vivo T2 CMR strongly correlated with the hemorrhage quantified on histology ($R=0.93$, $p=0.0007$). Using ex vivo late gadolinium sequences, bright areas surrounded by thin dark rims, consistent with magnetic susceptibility effects, were detected, corresponding with hemorrhage. On in vivo CMR images, low-signal intensity and hyperintense areas with peripheral susceptibility artifacts were observed within the MI core on T2 and late gadolinium

sequences, respectively. Thus, by clinicopathologic study we provided evidence that hemorrhagic AMI accounts for CMR late gadolinium hypoenhancement associated with magnetic susceptibility effects and hypointense T2 signal, casting some doubt on the belief that low-signal intensity areas surrounded by bright zones on late enhancement CMR always represent no-reflow zones.

According with these clinoco-pathologic findings we performed a CMR T2 in vivo study which represents the first clinical experience, demontrating, in patient succesfully treated by PCI, the presence of an intramyocardial haemorrhage and revealing its contribute to the dark zones after gadolinium injection. Our observations confirm previous experimental studies (148,149) who compared T2 scans to delayed hypoenhancement. In particular, in a clinical population, our CMR findings confirm the presence of a low signal intensity area within the risk area, detected by gradient-echo scans and corresponding in all cases to an hypoenhanced area within a high-signal intensity zone, the latter detected by gadolinium-enhanced spin-echo CMR. Post-mortem pathologic specimen, as described before, showed an overlap between the hypointense zone and myocardial haemorrhage: so the presence of an hypointense core on T2-weighted images can be used, as a marker of a worst microvascular damage resulting in hemorrhage. On the basis of our results, the incidence of hemorrhagic AMI detected with T2-images in our series (29.6%) is similar to other studies (33%) (150). However, the incidence of SMD is greater (37%) than hypoenhancement on T2 (29.6%), and also is not possible to correlate this results with other studies for lack of a complete protocol in other series. This lack of overlapping (between microvascular damage detected by T2 scans and post-contrast inversion recovery) could be explain by different histopatholical features in the contest of the same delayed hypoenhancement. The identification of T2-hypoenhanced areas could reveal the contribute of intramyocardial haemorrhage to SMD.

Moreover, our observations confirm both experimental and post-mortem reports regarding the location of myocardial haemorrhage, i.e. the mid-mural portion of the transmural necrosis. The peculiar location of the haemorrhage has been well established by Garcia-Dorado (39) who demonstrated that red blood cell counts were maximal in the mid portion, hypothezying that the distribution does not correspond to the usual susceptibility of myocardial cell to ischemia and can be alternalively explained by a physical reason. In fact, the suffusion of blood could be

influenced by the combined effects of transmural shear stress distribution and orientation of the muscle fibers. Moreover, the passive diffusion of oxygen from the surrounding tissues and from the thebesian venous system could explain the relative protection on behalf of the subendocardial layers. Our data confirm that when dealing with more severe infarcts (evaluating by mean number of transmural segments, Infarct Size Index and also peak of troponin I), there is a grater occurence of intramyocardial haemorrhage.

In our popolation, CMR findings for intramyocardial haemorrhage were related to the descending coronary artery, as culprit lesion and consequent anterior location of AMI. This is not surprising since anterior AMI is the most common location of the no-reflow phenomenon. The explanation can be due to epidemiological reasons because of the more frequent involvement of the descending coronary artery which acts like the culprit lesion; the same preferential anterior location of the haemorrhage and the free wall rupture suggests the same pathogenetic pathway; the anterior infarction has significantly been related to the lower myocardial blush grade both after primary PCI (95), and after thrombolysis (36). The same location for AMI, is strongly associated with impaired perfusion after a successful first reperfused AMI when taking into consideration myocardial contrast echocardiography (145). All the above mentioned data were confirmed by our experience: in fact patients with T2- hypoenhancement and dark zones on T1 IR sequences showed a worse angiographic reperfusion profile in terms of post-procedural TIMI flow 3 (65,6% vs 95,5%) and MBG 3 (9,4% vs 54,5%). Interestingly, haemorrhagic infarcts showed an even higher frequency of MBG 0 (84,4% vs 13,6%) with a prevalence of staining phenomenon (65,6% vs 13,6%), suggesting leakage of the contrast medium in the extravascular space (97): the present data confirms and broaden previous studies by showing that the worse prognostic significance of dark areas and MBG may be related to a common pathway represented by intramyocardial hemorrhage. These findings are in line with the unfavourable mechanical consequences of intramyocardial haemorrhage, comprising increased myocardial stiffness, propensity to rupture, a delayed healing process or a negative LV remodeling also associated with lower MBG. In fact, summarizing the traditional risk factors for the left ventricular wall rupture, the anterior location of the AMI and presence of a haemorrhage are traditionally considered. In particular, regarding the role of haemorrhagic infarcts in myocardial

ruptures, there is evidence that thrombolysis appears to accelerate the rupture event. This paradoxical effect of thrombolysis could comprise the extension of the myocardial haemorrhage, the weakening and the dissection of the necrotizing zone (151), and the diminishing of the myocardial collagens content (152), and the digestion of collagen by collagens and plasmin (153,154). In the present thesis it seems that PCI with thrombolysis increased the risk to develop an hemorrhagic AMI. Since there was only a small number of our patients treated with facilitated/rescue PCI, we cannot reach a definite conclusion. However so far, studies demonstrating the impact of these procedures for hemorrhagic infarcts are not yet present in large population studies. Furthermore regarding past studies evaluating thrombolysis alone, there is evidence to suggest that, contrary to the data provided by previous reports and post-hoc analysis of pivotal trials (155,156), neither thrombolysis itself nor the delay to thrombolitic treatment actually seem to increase the absolute risk of a left ventricle rupture (151). Future randomized studies may clarify the role of PCI and the contribution of thrombolysis to the development of intramyocardial haemorrhage detected *in vivo* by CMR.

The present study has just demonstrated that hemorrhagic AMI could be detected and its recognization results associated to traditional index of worse prognosis (lower post-TIMI, MBG, the anterior AMI location).

CONCLUSION

The results of this PhD study focusing on CMR assessment of AMI suggest firstly that in patients with ST-segment elevation AMI undergoing primary PCI, all efforts should be made to shorten the time from symptom onset and reperfusion, because even small differences in time delay result in a significant increase in TN and SMD.

When evaluating the clinical significance of these CMR findings, the amount of TN as assessed by CMR was found to be a major determinant of LV remodeling and function, with significant additional predictive value to infarct size and SMD.

When considering the ECG finding related to CMR, a persistent ST-elevation after an AMI should not be directly ascribed to left ventricular aneurysm formation, but it should be considered as the possible expression of microvascular damage occurrence.

As far as the influence of current antiplatelet therapy is concerned, although larger trials are required, the current experience suggests that (when indicated) Abciximab should be given as early as possible to reduce ischemic time and therefore TN and SMD.

In addition, we demonstrated that signs of post PCI microvascular impairment detected with angiography and CMR show a good correlation in AMI patients. In particular, we also demonstrated a clear relationship between lower MBG and SMD. In fact, MGB 0-staining are determined by the presence of a greater extent of TN and just of SMD on delayed hypoenhancement.

Staining detection allows the identification of a subset of patients with an even more severe structural intramyocardial microvascular alterations and, hence, very likely a more severe clinical outcome. On the basis of these considerations, angiographic assessment of myocardial perfusion during acute phase of AMI represents an extremely reliable tool that not only allows the identification of patients with poor perfusion after recanalization, but also of those (among the not-reperfused cases) with even more severe impairment (MBG with staining). Further studies aimed at identifying the functional and clinical impact of different pattern of severe MBG with or without staining are needed for a better understanding of the clinical significance of such angiographic findings.

Finally, our experience indicates that a complete CMR protocol performing also T2-images allows both in vivo and ex vivo the detection of intramyocardial hemorrhage. Our results show that signs of hemorrhagic infarcts such as T2 hypoenhancement are correlated to the hypoenhanced areas in the infarct core at CMR after gadolinium, usually referred to severe microvascular obstruction, and so related in the majority of cases to intramyocardial haemorrhage. The presence of both T2-hypoenhancement and delayed dark zones reflects AMI with a more severely injured microvascular damage, as confirmed by worst perfusion profile. Whether myocardial haemorrhage occurs spontaneously after prolonged ischemia or may be related to reperfusion therapy is still debated, as well as its relevance in the clinical outcome.

Future study will address the prognostic significance of hemorrhagic AMI also to define the role of current therapy in the acute phase of myocardial infarction and if hemorrhagic occurrence really represents an increased risk of rupture or unfavourable remodelling or whether it is just a cosmetic effect of the reperfusion era.

REFERENCES

1. Phibbs B, Marcus F, Marriott HJC, et al. Q-wave versus non-Q-wave myocardial infarction: A meaningless distinction. J Am Coll Cardiol 1999, 33:576–582.
2. Braunwald E, Antman EM, Beasley JW, et al. ACC-AHA Guidelines for the management of patients with unstable angina. J Am Coll Cardiol 2000; 36: 970.
3. Boersma E, Mercado N, Poldermans D, et al. Acute myocardial infarction. Lancet 2003; 361: 847.
4. Braunwald E, Antman EM, Beasley JW, et al: ACC-AHA 2002 Guideline update for the management of patients with unstable angina and non-ST segment elevation myocardial infarction-summary article. J Am Coll Cardiol 2002; 40:1366.
5. Zipes, Libby, Bonow, Brounwald: Braunwald's Heart Disease, A Text Book of Cardiovascular Medicine, 7° edition, Elsevier Saunders, 2005.
6. Reimer KA, Lowe JE, Rasmussen MM, et al. The wavefront phenomenon of ischemic cell death. 1. Myocardial infarct size vs duration of coronary occlusion in dogs. Circulation 1977; 56:788–94.
7. Reimer KA, Jennings RB. The ‘‘wavefront phenomenon’’ of myocardial ischemic cell death: II. Transmural progression of necrosis within the framework of ischemic bed size (myocardium at risk) and collateral flow. Lab Invest 1979; 40:633–44.
8. DeWood MA, Spores J, Notske RN, et al. Prevalence of total coronary artery occlusion during the early hours of transmural myocardial infarction. N Engl J Med 1980; 303: 897–902.
9. Fujita M, Nakae I, Kihara Y, et al. Determinants of collateral development in patients with acute myocardial infarction. Clin Cardiol 1999; 22: 595–599.
10. Davies MJ. The pathophysiology of acute coronary syndromes. Heart 2000; 83:361–6.
11. Vargas SO, Sampson BA, Schoen FJ. Pathologic detection of early myocardial infarction: A critical review of the evolution and usefulness of modern techniques. Mod Pathol 1999; 12: 635–645.
12. Braunwald E, Kloner RA. Myocardial reperfusion: a double-edged sword? J Clin Invest 1985; 76:1713–9.

13. Maxwell SRJ, Lip GYH. Reperfusion injury: a review of the pathophysiology,clinical manifestations and therapeutic options. Int J Cardiol 1997; 58: 95–117.
14. Kloner R. Does reperfusion injury exist in humans? J Am Coll Cardiol 1993; 21: 537.
15. Basso C, Thiene G. The pathophysiology of myocardial reperfusion: a pathologist's perspective. Heart 2006; 92: 1559–1562.
16. Ambrosio G, Tritto I. Reperfusion injury: experimental evidence and clinicalimplications. Am Heart J 1999; 138: S69–75.
17. Baroldi G. Different types of myocardial necrosis in coronary heart disease: a pathophysiologic review of their functional significance. Am Heart J 1975; 89: 742–52.
18. Buja LM. Myocardial ischemia and reperfusion injury. Cardiovasc Pathol 2005; 14:170–5.
19. Kloner RA, Ganote CE, Jennings RB. The ‘‘no-reflow’’ phenomenon after temporary coronary occlusion in the dog. Clin Invest 1974; 54:1496–1508.
20. Kloner RA, Ellis SG, Lange R, et al: Studies of experimental coronary artery reperfusion: Effects on infarct size, myocardial function, biochemistry, ultrastructure and microvascular damage. Circulation 1983; 68: 15–18.
21. Reffelmann T, Kloner RA. Microvascular alterations after temporary coronary artery occlusion: The no-reflow phenomenon. J Cardiovasc Pharmacol Ther 2004; 9: 163–172.
22. Dignan RJ, Kadletz M, Dyke CM, Lutz HA, Yeh T Jr, Wechsler AS. Microvascular dysfunction after myocardial ischemia. J Thorac Cardiovasc Surg 1995; 109: 892–897.
23. Carlson RE, Aisen AM, Buda AJ. Effect of reduction in myocardial edema on myocardial blood flow and ventricular function after coronary reperfusion. Am J Physiol 1992; 262: H641–H648.
24. Manciet LH, Poole DC, McDonagh PF, Copeland JG, Mathieu-Costello O. Microvascular compression during myocardial ischemia: Mechanistic basis for no-reflow phenomenon. Am J Physiol 1994; 266: H1541–H1550.
25. Reffelmann T, Kloner RA. Microvascular reperfusion injury: Rapid expansion of anatomic no-reflow during reperfusion in the rabbit. Am J Physiol Heart Circ Physiol 2002; 283: H1099–H1107.

26. Reffelmann T, Kloner RA. The no-reflow phenomenon: A basic mechanism of myocardial ischemia and reperfusion. Basic Res Cardiol 2006; 101: 359–372.
27. Stone GW, Webb J, Cox DA, et al for the Enhanced Myocardial Efficacy and Recovery by Aspiration of Liberated Debris (EMERALD) Investigators. Distal microcirculatory protection during percutaneous coronary intervention inacute ST-segment elevation myocardial infarction: a randomized controlled trial. JAMA 2005; 293: 1063–72.
28. Basso C, Bacchion F, Ramondo A, et al. A postmortem investigation of distal coronary microembolization in acute coronary syndromes. Lab Invest 2006; 86(suppl 1): 46A.
29. Xu Y, Huo Y, Toufektsian MC et al. Activated platelets contribute importantly to myocardial reperfusion injury. Am J Phisiol Heart Circ Physiol 2006; 290: H692-H699.
30. Heindl B, Zahler S, Welsch U, Becker BF. Disparate effects of adhesion and degranulation of platelets on myocardial and coronary function in postischaemic hearts. Cardiovasc Res 1998; 38: 383-394.
31. Niccoli G, Giubilato S, Russo E et al. Plasma levels tromboxane A2 on admission are associated with no-reflow after primary percutaneous coronary intervention. Eur Heart J 2008; 29: 1843-1850.
32. Okamura A, Ito H, Iwakura K, Kawano S, Inoue K, Yamamoto K, Ogihara T, Fujii K. Usefulness of a new grading system based on coronary flow velocity pattern in predicting outcome in patients with acute myocardial infarction having percutaneous coronary intervention. Am J Cardiol 2005; 96: 927–932.
33. Iwakura K, Ito H, Nishikawa N, Hiraoka K, Sugimoto K, Higashino Y, Masuyama T, Hori M, Fujii K, Minamino T. Early temporal changes in coronary flow velocity patterns in patients with acute myocardial infarction demonstrating the ‘‘no-reflow’’ phenomenon. Am J Cardiol 1999; 84: 415–419.
34. Agostini F, Iannone MA, Mazzucco R, Cionini F, Baccaglioni N, Lettieri C et al.. Coronary flow velocity pattern assessed by transthoracic Doppler echocardiography predicts adverse clinical events and myocardial recovery after successful primary angioplasty. J Cardiovasc Med (Hagerstown) 2006; 7: 753–760.
35. Albert TSE, Kim RJ, Judd RM. Assessment of no-reflow regions using cardiac MRI. Basic Res Cardiol 2006; 101: 383–390.

36. Gibson CM, Murphy SA, Rizzo JM, et al. Relationship between TIMI frame count and clinical outcomes after trombolytic administration. Thrombolysis In Myocardial Infarction (TIMI) Study Group. Circulation 1990; 99: 1945-50.
37. van't Hof AWJ, Liem A, Suryapranata H, Hoorntje JCA, de Boer MJ, Zijlstra F. Angiographic assessment of myocardial reperfusion in patients treated with primary angioplasty for acute myocardial infarction. Myocardial Blush Grade, Circulation 1998; 97: 2302-6.
38. Fishbein MC, Rit J, Lando U, et al. The relationship of vascular injury and myocardial hemorrhage to necrosis after reperfusion. Circulation 1980; 62:1274–9.
39. Garcia-Dorado D, Theroux P, Solares J, et al. Determinants of hemorrhagic infarcts. Histologic observations from experiments involving coronary occlusion, coronary reperfusion, and reocclusion. Am J Pathol 1990; 137: 301–11.
40. Tennant R, Wiggers CJ: The effect of coronary occlusion on myocardial contractions. Am J Physiol 1935; 112: 351.
41. Heyndrickx GR, Millard RW, McRitchie RJ, et al: Regional myocardial functional and electrophysiological alterations after brief coronary artery occlusion in conscious dogs. J Clin Invest 1975; 56: 978–985.
42. Kloner RA, Bolli R, Marban E, et al: Medical and cellular implications of stunning, hibernation, and preconditioning: An NHLBI workshop. Circulation 1998; 97:1848–1867.
43. Bolli R, Marban E: Molecular and cellular mechanisms of myocardial stunning. Physiol Rev 1999; 79: 609–634.
44. Bolli R: Basic and clinical aspects of myocardial stunning. Prog Cardiovasc Dis 1998; 40:477–516.
45. Majidi M, Kosinski AS, Al-Khatib SM. Reperfusion ventricular arrhythmia 'bursts' in TIMI 3 flow restoration with primary angioplasty for anterior ST-elevation myocardial infarction: a more precise definition of reperfusion arrhythmias. Europace 2008 Aug; 10(8):988-97.
46. Vera Z, Pride HP, Zipes DP. Reperfusion arrhythmias: role of early afterdepolarizations studied by monophasic action potential recordings in the intact canine heart during autonomically denervated and stimulated states. J Cardiovasc Electrophysiol 1995 Jul; 6(7):532-43.

47. Gibbons RJ , Valeti US, Araoz PA, Jaffe AS. The quantification of infarct size. J Am Coll Cardiol 2004; 44: 1533– 42.
48. Wu E, Judd RM, Vargas JD, Klocke FJ, Bonow RO and Kim RJ. Visualisation of presence, location, and transmural extent of healed Q-wave and non–Q-wave myocardial infarction. Lancet 2001; 357: 21–28.
49. Choi KM, Kim RJ, Gubernikoff G, Vargas JD, Parker M and Judd RM. Transmural extent of acute myocardial infarction predicts long-term improvement in contractile function. Circulation 2001; 104: 1101–1107.
50. Petersen SE, Horstick G, Voigtlander T et al. Diagnostic value of routine clinical parameters in acute myocardial infarction: a comparison to delayed contrast enhanced magnetic resonance imaging: Delayed enhancement and routine clinical parameters after myocardial infarction. Int J Cardiovasc Imaging 2003; 19: 409–416.
51. Gerber BL, Garot J, Bluemke DA, Wu KC and Lima JA. Accuracy of contrast-enhanced magnetic resonance imaging in predicting improvement of regional myocardial function in patients after acute myocardial infarction. Circulation 2002; 106: 1083–1089.
52. Kim RJ, Wu E, Rafael A et al. The use of contrast-enhanced magnetic resonance imaging to identify reversible myocardial dysfunction. N Engl J Med 2000; 343: 1445–1453.
53. Wu KC, Zerhouni EA, Judd RM, et al. Prognostic significance of microvascular obstruction by magnetic resonance imaging in patients with acute myocardial infarction. Circulation 1998; 97: 765-72.
54. Thygesen K, Alpert JS, White HD. Joint ESC/ACCF/AHA/WHF Task Force for the Redefinition of Myocardial InfarctionUniversal definition of myocardial infarction. Eur Heart J. 2007 Oct; 28(20): 2525-38.
55. Kim RJ, Albert TS, Wible JH et al. Performance of delayed-enhancement magnetic resonance imaging with with gadoversetamide contrast for the detection and assessment of myocardial infarction: an international, multicenter, double-blinded, randomized trial. Circulation 2008; 117: 629 –37.
56. Lombardi M, Bartolozzi C. Risonanza Magnetica del cuore e dei vasi, Ed. Springer 2006.
57. Selvanayagam JB, Robson MD, Francis JM & Neubauer S. Cardiac CT, PET and MR. Chapter 2. Ed. Blackwell Futura 2006.

58. Simonetti OP, Kim RJ, Fieno DS et al. An improved MR imaging technique for the visualization of myocardial infarction. Radiology 2001; 218: 215–223.
59. Bucciarelli-Ducci C, Wu E, Lee DC, Holly TA, Klocke FJ, Bonow RO. Contrast-enhanced cardiac magnetic resonance in the evaluation of myocardial infarction and myocardial viability in patients with ischemic heart disease. Curr Probl Cardiol. 2006 Feb; 31(2): 128-68.
60. Grobner T. Gadolinium-a specific trigger for the development of nephrogenic fibrosing dermopathy and nephrogenic systemic fibrosis? Nephrol Dial Transplant 2006; 21: 1104–8.
61. Singh M, Davenport A, Clatworthy I, et al. A follow-up of four cases of nephrogenic systemic fibrosis: is gadolinium the specific trigger? Br J Dermatol 2008; 158: 1358–62.
62. Swaminathan S, High WA, Ranville J, et al. Cardiac and vascular metal deposition with high mortality in nephrogenic systemic fibrosis. Kidney Int 2008; 73: 1413– 8.
63. Schroeder JA, Weingart C, Coras B, et al. Ultrastructural evidence of dermal gadolinium deposits in a patient with nephrogenic systemic fibrosis and end-stage renal disease. Clin J Am Soc Nephrol 2008; 3: 968–75.
64. Thomsen HS. ESUR guideline: gadolinium-based contrast media and nephrogenic systemic fibrosis. Eur Radiol 2007; 17: 2692–6.
65. Kaandorp TA, Lamb HJ, Bax JJ, van der Wall EE, de Roos A. Magnetic resonance imaging of coronary arteries, the ischemic cascade, and the myocardial infarction. Am J Cardiol 2005; 149: 200-8.
66. Gould KL, Lipscomb K. Effects of coronary stenosis on the coronary flow reserve and resistance. Am J Cardiol 1974; 34: 48-55.
67. Chiu CW, So NM, Lam WW et al. Combined first-pass perfusion and viability study at MR imaging in patients with non-ST segment elevation acute coronary syndromes: feasibility study. Radiology 2003; 226: 717-22.
68. Rogers WJ Jr, Kramer CM, Geskin G, et al. Early contrast-enhanced MRI predicts late functional recovery after reperfused myocardial infarction. Circulation. 1999; 99: 744-50.
69. Rochitte CE, Lima JA, Bluemke DA, et al. Magnitude and time course of microvascular obstruction and tissue injury after myocardial infarction. Circulation 1998; 98: 1006-14.

70. Gerber BL, Rochitte CE, Melin JA, McVeigh ER, Bluemke DA, Wu KC et al. Microvascular obstruction and left ventricular remodeling early after acute myocardial infarction. Circulation 2000; 101(23): 2734-41.
71. Hombach V, Grebe O, Merkle N, et al. Sequelae of acute myocardial infarction regarding cardiac structure and function and their prognostic significance as assessed by magnetic resonance imaging. Eur Heart J. 2005; 26: 549-57.
72. Lund GK, Stork A, Saeed M, et al. Acute Myocardial Infarction: Evaluation with First-Pass Enhancement and Delayed Enhancement MR Imaging Compared with 201Tl SPECT Imaging. Radiology 2004; 232: 49-57.
73. Abdel-Aty H, Zagrosek A, Schulz-Menger J, et al. Delayed enhancement and T2-weighted cardiovascular magnetic resonance imaging differentiate acute from chronic myocardial infarction. Circulation 2004; 109: 2411–6.
74. Natanzon A, Aletras AH, Hsu L, Arai AE. Determininig canine myocardial area at risk with manganese-enhanced MR imaging. Radiology 2005; 236: 859-866.
75. Friedrich MG. There is more than shape and function size J Am Coll Cardiol 2008; 51: 1581-7.
76. van den Bos EJ, Baks T, Moelker AD,et al. Magnetic resonance imaging of haemorrhage within reperfused myocardial infarcts: possible interference with iron oxide-labelled cell tracking? Eur Heart J 2006; 27: 1620-1626.
77. Rehwald W, Fieno DS, Chen EL, et al. Myocardial magnetic resonance imaging contrast agent concentration after reversible and irreversible ischemic injury. Circulation 2002; 105: 224-9.
78. Kim RJ, Choi KM, Judd RM.Assessment of myocardial viability by contrast enhancement. In: Higgins CB, De Roos A, editors. Cardiovascular MRI and MRA. Philadelphia, PA: Lippincott Williams & Wilkins, 2003: p. 209-37
79. Brasch RC, Weinmann HJ, Wesbey GE. Contrast-enhanced NMR imaging: animal studies using gadolinium-DTPA complex. AJR Am J Roentgenol 1984;142: 625-30.
80. Saeed M, Lund G, Wendland MF, et al. Magnetic resonance characterization of the peri-infarction zone of reperfused myocardial infarction with necrosis-specific and extracellular nonspecific contrast media. Circulation 2001; 103: 871-6.

81. Kim RJ, Chen EL, Lima JAC, et al. Myocardial Gd-DTPA kinetics determine MRI contrast enhancement and reflect the extent and severity of myocardial injury after acute reperfused infarction. Circulation 1996; 94: 3318-26.
82. Oshinski JN, Yang Z, Jones JR, et al. Imaging time after Gd-DTPA injection is critical in using delayed enhancement to determine infarct size accurately with magnetic resonance imaging. Circulation 2001; 104: 2838-42.
83. Ingkanisorn WP, Rhoads KL, Aletras AH, Kellman P, Arai AE. Gadolinium delayed enhancement cardiovascular magnetic resonance correlates with clinical measures of myocardial infarction.J Am Coll Cardiol 2004; 43: 2253-9.
84. Hillenbrand HB, Kim RJ, Parker MA, et al. Early assessment of myocardial salvage by contrast-enhanced magnetic resonance imaging. Circulation 2000; 102: 1678-83.
85. Selvanayagam JB, Kardos A, Francis JM, et al. Value of delayed-enhancement cardiovascular magnetic resonance imaging in predicting myocardial viability after surgical revascularization. Circulation 2004; 110: 1535-41.
86. Judd RM, Lugo-Olivieri CH, Arai M, et al. Physiological basis of myocardial contrast enhancement in fast magnetic resonance images of a 2-day-old reperfused canine infarcts. Circulation 1995; 92: 1902-10.
87. Schlegel JU. Demonstration of blood vessels and lymphatics with a fluorescent dye in ultraviolet light. Anat Rec 1949; 105: 433-53.
88. Rochitte CE, Kim RJ, Hillebrand HB, et al. Microvascular integrity and the time course of myocardial sodium accumulation after acute infarction. Circ Res 2000; 87: 648-55.
89. Ito H, Maruyama A, Iwakura K, et al. Clinical implication of the 'no-reflow' phenomenon: a predictor of complications and left ventricular remodeling in reperfused anterior wall myocardial infarction. Circulation 1996; 93: 223-8.
90. Wu E, Tejedor P, Lee DC, et al. No reflow detected by delayed contrast enhancment predicts remodeling following an ST-segment myocardial infarction. Circulation 2004; 110: III-444 [abstract].
91. Azevedo CF, Amado LC, Kraitchman DL et al. The effect of intraaortic balloon counterpulsation on left ventricular functional recovery early after acute myocardial inarction: a randomized experimental magnetic resonance imaging study. Eur Heart J 2005; 26 (12): 1235-41.

92. Amado LC, Kraitchman DL, Gerber BL, et al. Reduction of “no-reflow” phenomenon by intra-aortic balloon conuterpulsation in a randomized magnetic resonance imaging experimental study. J Am Coll Cardiol 2004; 43: 1291-8.
93. Rentrop KP, Cohen M, Blanke H, Phillips RA. Changes in the collateral channel filling immediately after controlled coronary artery occlusion by an angioplasty balloon in human subject. J Am Coll Cardiol 1985; 5: 587–592.
94. Cohen M, Rentrop KP. Limitation of myocardial ischemia by collateral circulation during sudden controlled coronary artery occlusion in human subjects: a prospective study. Circulation. 1986; 74(3): 469-76.
95. C. M. Gibson and A. Schomig Coronary and Myocardial Angiography: Angiographic Assessment of Both Epicardial and Myocardial Perfusion Circulation 2004; 109(25): 3096–3105.
96. Henriques JPS, Zijlstra F, van’t Hof AWJ, Menko-jan de Boer, Jan-Henk E Dambrink, Gosselink M, et al. Angiographic assessment of reperfusion in acute myocardial infarction by myocardial blush grade. Circulation 2003; 107:2115-19.
97. Little WC, Rogers EW. Angiographic evidence of hemorrhagic myocardial infarction after intracoronary thrombolysis with streptokinase. Am J Cardiol 1983 Mar 1; 51(5): 906-8.
98. Tarantini G, Ramondo A, Napodano M et al. Myocardial perfusion grade and survival after percutaneous transluminal coronary angioplasty in patients with cardiogenic shock. Am J Cardiol 2004; 93: 1081–1085.
99. Cerqueira MD, Weissman NJ, Dilsizian V, et al. Standardized myocardial segmentation and nomenclature for tomographic imaging of the heart: a statement for healthcare professional from the Cardiac Imaging Committee of the Council on Clinical Cardiology of the American Heart Association. Circulation 2002; 105: 539-42.
100. Lima JA, Judd RM, Bazille A, et al. Regional heterogeneity of human myocardial infarcts demonstrated by contrast-enhanced MRI. Circulation 1995; 92: 1117–25.
101. Beek AM, Kuhl HP, Bondarenko O, et al. Delayed contrast-enhanced magnetic resonance imaging for the prediction of regional functional improvement after acute myocardial infarction. J Am Coll Cardiol 2003; 42: 895–901.

102. Tibrewala AV, Asch F, Shah S, Fuisz A, Lindsay J Jr. Association of size of myocardial scar and persistence of ST-segment elevation after healing of anterior wall myocardial infarction. Am J Cardiol 2007; 99: 1106-8.
103. Mollet NR, Dymarkowski S, Volders W, Wathiong J, Herbots L, Rademakers FE et al. Visualization of ventricular thrombi with contrast-enhanced magnetic resonance imaging in patients with ischemic heart disease. Circulation. 2002; 106(23): 2873-6.
104. Schiller NB, Shah PM, Crawford M, DeMaria A, Devereux R, Feigenbaum H, et al. Recommendations for quantitation of the left ventricle by two-dimensional echocardiography. American Society of Echocardiography Committee on Standards, Subcommitee on Quantitation of Two-Dimensional Echocardiograms. J Am Soc Echocardiogr 1989; 2: 358-67.
105. Konen E, Merchant N, Gutierrez C, Provost Y, Mickleborough L, Paul NS, et al. True versus false left ventricular aneurysm: differentiation with MR imaging-initial experience. Radiology 2005; 236: 65-75.
106. Reimer KA, Heide RSV, Richard VJ. Reperfusion in acute myocardial infarction: effect of timing and modulating factors in experimental models. Am J Cardiol 1993; 72: 13G–21G.
107. Reffelmann T, Hale SL, Li G, Kloner RA. Relationship between no reflow and infarct size as influenced by the duration of ischemia and reperfusion. Am J Physiol 2002; 282: H766–72.
108. De Luca G, Suryapranata H, Ottervanger JP, Antman EM. Time delay to treatment and mortality in primary angioplasty for acute myocardial infarction: every minute of delay count. Circulation 2004; 109:1223–5
109. Rizzello V, Poldermans D, Boersma E, Biagini E, Schinkel AFL, Krenning B et al. Opposite patterns of left ventricular remodeling after coronary revascularization in patients with ischemic cardiomyopathy. Role of myocardial viability. Circulation 2004; 110: 2383–2388.
110. Bologense L, Cerisano G, Buonamici P, Santini A, Santoro GM, Antoniucci D et al. Influence of infarct-zone viabilità on left ventricular remodeling after acute myocardial infarction. Circulation 1997; 96: 3353-3359.
111. Nijland F, Kamp O, Verhorst PMJ, WG de Voogt, Bosh HG, Visser CA. Myocardial viability: impact on left ventricular dilatation after acute myocardial infarction. Heart 2002; 87: 17-22.

112. Bolognese L, Neskovic AN, Parodi G, Cerisano G, Buonamici P, Santoro GM et al. Left ventricular remodeling after primary coronary angioplasty. Patterns of left ventricular dilation and long-term prognostic inplications. Circulation 2002; 106: 2351-57.
113. Morton J. Kern Patterns of Left Ventricular Dilatation With an Opened Artery After Acute Myocardial Infarction Circulation. Circulation 2002;106: 2294-2295.
114. Mills RM Jr, Young E, Gorlin R, Lesch M. Natural history of ST-segment elevation after acute myocardial infarction. Am J Cardiol 1975; 35: 609-614.
115. Chon K, Dymnicka S, Forlini FJ Jr. Use of electrocardiogram as an aid in screening for left ventricular aneurysm. J Electrocardiol 1976; 9: 53-58.
116. Arvan S, Varat MA. Persistent ST-segment elevation and left ventricular wall abnormalities: a 2-dimensional echocardiographic study. Am J Cardiol 1984; 53: 1542-46.
117. Herman MV, Heinle RA, Klein MD, Gorlin R. Localized disorders in myocardial contraction. Asynergy and its role in congestive heart failure. N Engl J Med 1967; 277: 222-232.
118. Bar FW, Brugada P, Dassen WR, van der Werf T, Wellens HJ. Prognostic value of Q waves, R/S ratio, loss of R wave voltage, ST-T segment abnormalities, electrical axis, low voltage and notching: correlation of electrocardiogram and left ventriculogram. J Am Coll Cardiol 1984; 4:17-27.
119. Lindsay J Jr, Dewey RC, Talesnick BS, Nolan NG. Relation of ST-segment elevation after healing of acute myocardial infarction to the presence of left ventricular aneurysm. Am J Cardiol 1984; 54: 84-6.
120. Bhatnagar SK. Observations of the relationship between left ventricular aneurysm and ST segment elevation in patients with a first acute anterior Q wave myocardial infarction. Eur Heart J 1994; 15: 1500-1504.
121. Tibrewala AV, Asch F, Shah S, Fuisz A, Lindsay J Jr. Association of size of myocardial scar and persistence of ST-segment elevation after healing of anterior wall myocardial infarction. Am J Cardiol 2007; 99: 1106-8.
122. Li RA, Reppo M, Miki T, Seino S, Marbàn E. Molecular basis of electrocardiographic ST-segment elevation. Circ Res 2000; 87: 837-39.
123. Link MS, Wang PJ, VanderBrink BA, Avelar E, Pandian NG, Maron BJ, et al. Selective activation of the K_{ATP} channel is a mechanism by which sudden death

is produced by low-energy chest-wall impact (commotio cordis). Circulation 1999; 100: 413-18.

124. Gussak I, Wright RS, Kopecky SL, Hammil SC. Exercise-induced ST segment elevation in Q wave leads in postinfarction patients: defining its meaning and utility in today's practice. Cardiology 2000; 93: 205-209.
125. De Luca G, Suryapranata H, Stone G, et al. Abciximab as adjunctive therapy to reperfusion in acute ST-segment elevation myocardial infarction. JAMA 2005; 293: 1759–1765.
126. Godicke J, Flather M, Noc M, et al. Early versus periprocedural administration of abciximab for primary angioplasy: a pooled analysis of 6 studies. Am Heart J 2005; 150: 1015e11–1015e17
127. Maioli M, Bellandi F, Leoncini M, Toso A, Dabizi RP. Randomized early versus late abciximab in acute myocardial infarction treated with primary coronary intervention (RELAx-AMI trial). J Am Coll Cardiol 2007; 49: 1517–1524
128. Rakowski T, Zalewski J, Legutko J, et al. Early abciximab administration before primary percutaneous coronary intervention improves infarct-related artery patency and left ventricular function in high risk patients with anterior wall myocardial infarction: a randomized study. Am Heart J 2007; 153: 360–365.
129. Reimer KA, Jennings RB, Cobb FR, et al. Animal models for protection ischemic myocardium: results of the NHLBI Cooperative Study. Comparison of unconscious and conscious dog models. Circ Res 1985; 56: 651– 665
130. De Luca G, Ernst N, Zijlstra F, et al. Preprocedural TIMI flow and mortality in patients with acute myocardial infarction treated by primary angioplasty. J Am Coll Cardiol 2004; 43: 1363–1367.
131. Fernandez-Avilés F, Alonso JJ, Pena G, et al. Primary optimal percutaneous coronary intervention versus facilitated intervention (tenecteplase plus stenting) in patients with ST-elevated acute myocardial infarction (GRACIA-2). Eur Heart J 2007, E-pub ahead of print.
132. Ross AM, Coyne KS, Reiner JS, et al. A randomized trial comparing primary angioplasty with a strategy of short-acting thrombolysis and immediate planned rescue angioplasty in acute myocardial infarction: the PACT trial.

PACT investigators. Plasminogen- activator Angioplasty Compatibility Trial. J Am Coll Cardiol 1999; 34: 1954– 1962.

133. Petronio AS, Rovai D, Musumeci G, et al. Effects of abciximab on microvascular integrity and left ventricular functional recovery in patients with acute infarction treated by primary coronary angioplasty. Eur Heart J 2003; 24: 67–76.
134. Sciagrà R, Parodi G, Pupi A, et al. Gated SPECT evaluation of outcome after abciximab- supported primary infarct artery stenting for acute myocardial infarction: the scintigraphic data of the abciximab and carbostent evaluation (ACE) randomized trial. J Nucl Med 2005; 46: 722–27.
135. Montalescot G, Barragan P, Wittenberg O, et al. Platelet glycoprotein IIb/IIIa inhibition with coronary stenting for acute myocardial infarction. N Engl J Med 2001; 344: 1895–1903.
136. Neumann FJ, Blasini R, Schmitt C, et al. Effect of glycoprotein IIb/IIIa receptor blockade on recovery of coronary flow and left ventricular function after the placement of coronary-artery stents in acute myocardial infarction. Circulation 1998; 98: 2695–2701.
137. Reffelman T, Kloner RA. The 'no-reflow' phenomenon: basic science and clinical correlates.Heart 2002; 87: 162–168.
138. Costantini CO, Stone GW, Mehran R, et al: Frequency, correlates, and clinical implications of myocardial perfusion after primary angioplasty and stenting, with and without glycoprotein IIb/IIIa inhibition, in acute myocardial infarction. J Am Coll Cardiol 2004; 44: 305–312.
139. Iliceto S, Marangelli V, Marchese A, et al. Myocardial contrast echocardiography in acute myocardial infarction: pathophysiological background and clinical applications. Eur Heart J 1996; 17: 344-353.
140. Dong J, Ndrepepa G, Schmitt C, Mehilli J, Schmieder S, Schwaiger M, et al. Early resolution of ST-segment elevation correlates with myocardial salvage assessed by Tc-99m sestamibi scintigraphy in patients with acute myocardial infarction after mechanical or thromolytic reperfusion therapy. Circulation 2002; 105: 2946-2949.
141. Appelbaum E, Ajay J Kirtane Alica Clark, et al. Association of TIMI Myocardial Perfusion Grade and ST-segment resolution with cardiovascular magnetic resonance measures of microvascular obstruction and infarct size

following ST-segment elevation myocardial infarction. J Thromb Thrombolysis. 2008 Feb 2. Epub ahead of print

142. Porto I, Burzotta F, Brancati M, Trani C, et al. Realtionship of myocardial blush grade to microvascular perfusion and myocardial infarct size after primary or rescue percutaneous coronary intervention. Am J Cardiol 2007; 99:1671-1673.
143. Thulborn KR, Biochemical basis of the MRI appearance of cerebral hemorrhage. In:Edelman RR, Hesslink JR, Zlatkin MB, Crues JV, eds. Clinical Magnetic Resonance Imaging. 3rd ed. Philadelphia, PA: Saunders, 2006:174-186.
144. Iwakura K, Ito H, Kawano S, et al. Predictive factors for development of the no-reflow phenomenon in patients with reperfused anterior wall acute myocardial infarction. J Am Coll Cardiol 2001; 38: 472-478.
145. Galiuto L, Garramone B, Scarà A, Rebuzzi AG, Crea F, La Torre G, et al AMICI Investigators. The extent of microvascular damage during myocardial contrast echocardiography is superior to other known indexes of post-infarct reperfusion in predicting left ventricular remodeling: results of the multicenter AMICI study. J Am Coll Cardiol. 2008 Feb 5;51(5):552-9.
146. Shishido T, Beppu S, Matsuda H, Miyatake K. Progression of intramural hemorrhage in the reperfused area: an experimental study assessed by myocardial contrast echocardiography. Circulation. 1993; 88(suppl I):I-402.
147. de Roos A, van Rossum AC, van der Wall E, Postema S, et al. Reperfused and nonreperfused myocardial infarction: diagnostic potential of Gd-DTPA-enhanced MR imaging. Radiology 1989; 172: 717-720.
148. Ewout J. van den Bos, Baks T, Moelker AD, Kerver W, van geuns RJ, van der Giessen WJ et al. Magnetic resonance imaging of haemorrhage within reperfused myocardial infarcts: possible interference with iron oxide-labelled cell tracking? European Heart Journal 2006; 27: 1620-1626.
149. Asanuma T, Tanabe K, Ochiai K, Yoshitomi H, Nakamura K, Murakami Y, et al. Relationship between progressive microvascular damage and intramyocardial hemorrhage in patients with reperfused anterior myocardial infarction. Circulation 1997; 96: 448-53.
150. Ochiai K, Shimada T, Murami Y, Ishibashi Y, Sano K, Kitamura J, et al. Hemorrhagic myocardial infarction after coronary reperfusion detected in vivo

by magnetic resonance imaging in humans: prevalence and clinical implications. J cardiovasc Magn Resonan 1999; 1: 247-256.

151. Becker RC, Charlesworth A, Wilcox RG. Cardiac rupture associated with thrombolytic therapy: impact of time to treatment in the Late Assessment of Thrombolytic Efficacy (LATE) study.J Am Coll Cardiol 1995; 25: 1063-1068.
152. Factor SM, Robinson TF, Dominitz R, Cho SH. Alterations of the myocardial skeletal framework in acute myocardial infarction with and without ventricular rupture. A preliminary report. Am J Cardiovascular Pathol 1987; 1: 91-7.
153. Charney RH, Takahashi S, Zhao M, Sonnenblick EH, Eng C. Collagen loss in the stunned myocardium Circulation 1992; 85: 2123-34.
154. Peuhkurinen KJ, Risteli L, Melkko JT ey al.Thrombolytic therapy with streptokinase stimulates collagen breakdown Circulation 1991; 83: 1969-75.
155. Maggioni AP et al., GISSI-2. Age-Related Increase in Mortality among Patients with First Myocardial Infarctions Treated with Thrombolysis NEJM 1993; 329: 1442-48.
156. Honan MB, Harrell FE Jr, Reimer KA, Califf RM, Mark DB, Pryor DB, and MA Hlatky Cardiac rupture, mortality and the timing of thrombolytic therapy: a meta-analysis J Am Coll Cardiol 1990; 16: 359-367.